

TRAIL-Receptor 2 as a novel regulator of tumor suppressor protein p53

Dissertation

zur Erlangung des Doktorgrades
der Mathematisch-Naturwissenschaftlichen Fakultät
der Christian-Albrechts-Universität zu Kiel
vorgelegt von

Anna Willms

Kiel, 2021

First Reviewer: Prof. Dr. rer. nat. Anna Trauzold

Second Reviewer: Prof. Dr. rer. nat. Thomas Roeder

Disputation: 13.04.2021

Parts of this dissertation have been already published in

Wilms, A., Schitteck, H., Rahn, S., Sosna, J., Mert, U., Adam, D., & Trauzold, A. (2019). Impact of p53 status on TRAIL-mediated apoptotic and non-apoptotic signaling in cancer cells. PLoS One.

or have been submitted for publication

Wilms, A., Schupp, H., Poelker, M., Hartwig, T., Krichel, T., Fritsch, J., Singh, S., Walczak, H., von Karstedt, S., Schäfer, H., Trauzold, A. TRAIL-Receptor 2 - a novel negative regulator of p53.

I. Zusammenfassung

TRAIL (Tumor necrosis factor-related apoptosis-inducing ligand) Rezeptor 2 (TRAIL-R2) kann nach der Bindung seines Liganden TRAIL den Zelltod präferentiell in Tumorzellen auslösen. Allerdings kann TRAIL-R2 neben dem Zelltod auch diverse pro-inflammatorische Signaltransduktionswege induzieren, was in Apoptose resistenten malignen Zellen Proliferation, Invasion und Migration fördern kann. Darüber hinaus wurde ein vermehrtes intrazelluläres Vorkommen von TRAIL-R2 in verschiedensten Tumoren beschrieben. Tatsächlich konnte gezeigt werden, dass TRAIL-R2 im Zellkern eine tumorfördernde Funktion ausübt, indem es die Reifung von microRNAs (miRNAs) reguliert. Übereinstimmend, korreliert ein hohes intrazelluläres Vorkommen von TRAIL-R2 mit einer schlechten Patientenprognose. In der vorliegenden Studie wurde ein neuartiger Mechanismus aufgedeckt, wie nukleärer TRAIL-R2 (nTRAIL-R2) im Zellkern die Tumorprogression fördert.

Es konnte gezeigt werden, dass nTRAIL-R2 mit dem Tumorsuppressorprotein p53 interagiert. Die Herunterregulation von TRAIL-R2 in wildtyp p53 exprimierenden HCT116 und A549 Zellen erhöhte das p53 Proteinlevel, sowie die Expression von seinen Zielgenen p21, BAX (Bcl-2 associated x protein) und MDM2 (mouse double minute 2 homolog). *Vice versa* führte die exogene Überexpression von beiden TRAIL-R2 Isoformen zu einer Herunterregulation sowohl von p53, als auch von p21 und MDM2 in A549 Zellen. Dabei agiert TRAIL-R2 unabhängig von TRAIL und seiner Funktion als Induktor von Caspasen. Genexpressions- und Proteinhalbwertszeit Analysen deuteten darauf hin, dass TRAIL-R2 nicht die Transkription von p53, sondern dessen Proteinstabilität beeinflusst. Dieser Effekt ist abhängig vom Ubiquitin-Proteasom-System, welches für den Abbau von p53 verantwortlich ist. Durch die Blockierung des proteasomalen Abbaus über die Inhibition des 26S Proteasoms mittels MG132, sowie die Blockierung der MDM2-vermittelten Ubiquitinierung von p53 über Nutlin 3a, konnte die TRAIL-R2-vermittelte Destabilisierung von p53 aufgehoben werden. Diese Ergebnisse weisen darauf hin, dass TRAIL-R2 die MDM2-vermittelte Ubiquitinierung von p53 fördert. Immunpräzipitationsexperimente zeigten keine Interaktion zwischen TRAIL-R2 und MDM2. Jedoch deuteten Immunfluoreszenzfärbungen darauf hin, dass TRAIL-R2 in Proteinkomplexen zusammen mit p53 und MDM2 vorkommt. Dabei assoziierten p53 und MDM2 unabhängig vom TRAIL-R2 Status der Zellen, was die Vermutung nahelegt, dass neben MDM2 ein weiterer Ko-Faktor an der TRAIL-R2-p53-Regulationsachse beteiligt ist, der die Stabilität von p53 beeinflusst. Auf der Suche nach potenziellen Mitspielern konnte der Einfluss von Ubiquitin Peptidasen, insbesondere USP10 (Ubiquitin Peptidase 10), sowie HMGA2 (high mobility group AT-hook 2), welches die MDM2-vermittelte Ubiquitinierung von p53 in Kolorektalen Tumoren fördern kann, ausgeschlossen werden. Interessanterweise konnte TRAIL-R2 als ein neuer potenzieller Interaktionspartner von PML (promyelocytic leukemia) identifiziert werden. Zudem konnte gezeigt werden, dass der Knockdown von PML

das p53 Proteinlevel in wildtyp Zellen auf ein vergleichbares Level zu TRAIL-R2 Knockout Zellen erhöht, während der PML Knockdown keinen Effekt in TRAIL-R2 Knockout Zellen hatte. PML ist ein Schlüsselorganisator von PML Kernkörpern, die Partnerproteine sequestrieren, modifizieren oder abbauen können, einschließlich p53 und MDM2. Folglich, könnte PML TRAIL-R2 bei der Destabilisierung von p53 assistieren.

Zusammenfassend konnte in der vorliegenden Arbeit eine neue potenzielle Rückkopplungsschleife zwischen nTRAIL-R2 und p53 in wildtyp p53 exprimierenden Krebszellen identifiziert werden. Aktiviertes p53 kann TRAIL-R2 auf transkriptioneller Ebene hochregulieren, *vice versa* destabilisiert nTRAIL-R2 p53 und inhibiert dabei die Transkription von p53 Zielgenen. Die detaillierte Aufklärung des hier zugrundeliegenden Mechanismus wird Teil weiterer Studien sein.

II. Summary

TRAIL (Tumor necrosis factor-related apoptosis-inducing ligand) receptor 2 (TRAIL-R2) has been shown to induce cell death preferentially in tumor cells upon binding of its ligand TRAIL. Nevertheless, TRAIL-R2 can also induce various pro-inflammatory pathways which promote invasion, migration and proliferation of apoptosis resistant malignant cells. Moreover, high intracellular levels of TRAIL-R2 are a characteristic feature for various tumors, suggesting a pro-tumoral function. Indeed, nuclear TRAIL-R2 (nTRAIL-R2) was shown to execute tumor promoting functions by regulating the maturation of microRNAs (miRNAs). Consistently, a high intracellular abundance of TRAIL-R2 was correlated with worse patient prognosis. In the present study a novel mechanism was uncovered how nTRAIL-R2 promotes tumor progression.

TRAIL-R2 co-localizes and interacts with tumor suppressor protein p53 in the nucleus. Silencing of TRAIL-R2 in wild type p53 expressing HCT116 and A549 cells, elevates the protein level of p53 as well as the expression of its targets p21, BAX (Bcl-2 associated x protein) and MDM2 (mouse double minute 2 homolog). *Vice versa* exogenous overexpression of TRAIL-R2 isoforms decreased the protein levels of p53, p21 and MDM2 in A549 cells. Thereby, TRAIL-R2 acts independent of TRAIL and its death inducing function as an activator of caspases. Gene expression and protein half-life analyses indicated that TRAIL-R2 does not impact p53 transcription, but destabilizes p53 protein. Furthermore, this effect is dependent on the conventional p53 degradation pathway by the ubiquitin-proteasome-system. Blocking of the proteasomal degradation pathway by inhibition of the 26S proteasome via MG132 as well as blocking MDM2-mediated p53 ubiquitination by Nutlin 3a, abolished the TRAIL-R2-mediated destabilization of p53. Consequently, TRAIL-R2 might promote MDM2-mediated p53 ubiquitination. Immunoprecipitation experiments revealed no TRAIL-R2-MDM2 interaction, but immunofluorescence stainings indicated a presence of TRAIL-R2 in protein complexes with both p53 and MDM2. Thereby, p53 and MDM2 associate independent of the TRAIL-R2 status in A549 cells. Therefore, besides MDM2, a co-factor might participate in the TRAIL-R2-p53 regulatory axis to modulate p53 protein stability. On the track of identifying potential co-players, an involvement of ubiquitin peptidases, especially USP10 (ubiquitin specific peptidase 10), as well as HMGA2 (high mobility group AT-hook 2), which was shown to promote MDM2-mediated p53 ubiquitination in colorectal cancer, was excluded. Interestingly, TRAIL-R2 was identified as a novel potential interaction partner of promyelocytic leukemia (PML) protein. Moreover, PML knockdown led to an increased p53 protein level in TRAIL-R2-expressing cells to similar extent as the knockout of TRAIL-R2 itself, whereas no alteration of p53 level was seen by PML knockdown in TRAIL-R2 knockout cells. PML is the key organizer of PML nuclear bodies that can sequester, modify, or degrade partner proteins including p53 and MDM2. Accordingly, PML might assist TRAIL-R2 in destabilizing p53.

In summary, in the present study a potential regulatory feedback signaling loop between nTRAIL-R2 and p53 was identified in wild type p53 expressing cancer cells. Activated p53 transcriptionally upregulates TRAIL-R2 expression, *vice versa* nTRAIL-R2 destabilizes p53 and thereby inhibits its transcriptional output. The detailed mechanism how TRAIL-R2 impacts p53 stability will be examined in future studies.

III. List of Abbreviations

°C	degree Celsius
μ	micro
μg	microgram
μg	microgram
μl	microliter
μm	micrometer
5-FU	5-Fluorouracil
A	ampere
AGO2	Argonaute 2
APAF-1	apoptotic protease-activating factor 1
ARF-BP1	ADP-ribosylation factor-binding protein 1
ATM	ataxia-telangiectasia mutated
ATR	ataxia telangiectasia and Rad3 related
Bak	Bcl-2 homologous antagonist killer
BAX	Bcl-2 associated X protein
Bcl-XL	B-cell lymphoma-extra-large
Bid	Bcl-2-homology domain 3 (BH3) interacting domain death agonist
BMK1	big MAP kinase 1
BSA	bovine serum albumin
CBP	CREB-binding protein
CDK	cyclin-dependent kinase
CDKN1A	cyclin Dependent Kinase Inhibitor 1A
cDNA	complementary desoxyribonucleic acid
c-FLIP	cellular FADD-like IL-1β-converting enzyme (FLICE)-inhibitory protein
ChIP	chromatin immunoprecipitation
Chk1	checkpoint kinase 1
Chk2	checkpoint kinase 2
ciAP1	cellular inhibitor of apoptosis protein 1
ciAP2	cellular inhibitor of apoptosis protein 2
CIP	CDK interacting protein
c-Myc	Avian myelocytomatosis virus oncogene cellular homolog
COP1	coat protein complex I
CRISPR	clustered regularly interspaced short palindromic repeats
Ct	cycle threshold
C-terminus	carboxyl terminus
DcR	decoy receptor

DD	death domain
ddH ₂ O	double distilled water
DDX5	DEAD-box helicase 5
DED	death-effector domain
DGCR8	DiGeorge syndrome critical region 8
DISC	death inducing signaling complex
DNA	deoxyribonucleic acid
DNA-PK	DNA-dependent protein kinase
DUB	deubiquitinating enzyme
ECL	enhanced chemiluminescence
EMT	epithelial-mesenchymal transition
ER	endoplasmic reticulum
ERK	extracellular signal-regulated kinase
FADD	FAS-associated protein with death domain
FCS	fetal calf serum
FLIP	FLICE-inhibitory protein
g	gram
Gadd45a	growth arrest and DNA damage inducible 45 alpha
GPI	glycosylphosphatidylinositol
h	hour(s)
HAT	histone acetyl transferases
HAUSP	herpesvirus associated USP
HIPK2	homeodomain-interacting protein kinase 2
HMGA2	high mobility group AT-hook 2
hnRNPA1	heterogeneous nuclear ribonucleoprotein A1
HRP	horseradish peroxidase
IAPs	inhibitors of apoptosis
ICAD	inhibitor of caspase-activated DNase
IKK	NF- κ B essential modifier (NEMO)/inhibitor of κ B (I κ B) kinase
JNK	JUN N-terminal kinase
kDa	kilo Dalton
KIP	kinase inhibitory protein
l	liter
let-7	lethal-7
Lin28B	Lin-28 Homolog B
LUBAC	linear ubiquitin chain assembly complex
mA	milli ampere
Mad1	mitotic arrest deficient 1

MAPK	mitogen-activated protein kinase
Mcl-1	induced myeloid leukemia cell differentiation protein
MDM2	mouse double minute 2 homolog
min	minute(s)
miRNA	microRNA
ml	milliliter
MLKL	mixed lineage kinase domain like pseudokinase
mM	millimolar
MOMP	mitochondrial outer membrane permeabilization
MPD	membrane-proximal domain
MRE11	meiotic recombination 11 homolog 1
MRN	Mre11–Rad50–Nbs1 complex
NBS1	Nijmegen breakage syndrome protein 1
NEMO	NF- κ B essential modifier
NES	nuclear export sequence
NF45	nuclear factor 45
NF- κ B	nuclear factor kappa B-cells
ng	nanogram
NK	natural killer
NLS	nuclear localization sequence
N-terminus	amino terminus
nTRAIL-R2	nuclear TRAIL-Receptor 2
OPG	osteoprotegerin
PBS	phosphate-buffered saline
PBSE	phosphate-buffered saline supplemented with EDTA
PCAP	p300/CBP associated factor
PFA	paraformaldehyde
PHLDB3	pleckstrin homology domain-containing protein
PI	propidium iodide
PI3K	phosphoinositide 3-kinase
Pirh2	p53-induced RING-H2 protein
PML	promyelocytic leukemia
PPI	protein-protein interaction
pRb	retinoblastoma tumor suppressor protein
PUMA	p53-upregulated modulator of apoptosis
PVDF	polyvinylidene fluoride
qPCR	quantitative real-time polymerase chain reaction
Rac1	rat sarcoma (Ras)-related C3 botulinum toxin substrate 1

Ras	rat sarcoma
RBM38	RNA-binding-motif protein 38
rcf	relative centrifugal force
RIPK1	receptor-interacting protein kinase 1
RISC	RNA-induced silencing complex
RNA	ribonucleic acid
ROS	reactive oxygen species
RT	room temperature
SD	standard deviation
SDS-PAGE	Sodium dodecyl sulfate polyacrylamide gel electrophoresis
SEM	standard error of the mean
SIM	SUMO-interacting motif
SIRT1	Sirtuin-1
Smac/DIABLO	second mitochondrial activator of caspases/direct inhibitor of apoptosis-binding protein with low pI
SRC	Rous sarcoma oncogene cellular homolog
STAT3	signal transducer and activator of transcription 3
SUMO	small ubiquitin-related modifier
TAPE domain	threonine, alanine, proline, glutamine domain
tBid	truncated Bid
TBS	Tris-buffered saline
TBS-T	Tris-buffered saline supplemented with Tween 20
TNF	tumor necrosis factor
TRAF2	TNF receptor-associated factor 2
TRAIL	TNF-related apoptosis-inducing ligand
UBE4B	ubiquitination factor E4B
UPR	unfolded protein response
UPS	ubiquitin-proteasome-system
USP	ubiquitin-specific protease
USP10	ubiquitin specific peptidase 10
USP28	ubiquitin specific peptidase 28
UTR	untranslated region
V	volt
v/v	volume per volume
w/v	weight per volume
XIAP	X-linked inhibitor of apoptosis
XPE	Xeroderma pigmentosum complementation group E protein
YY1	Yin Yang 1

IV. Table of contents

I. Zusammenfassung	I
II. Summary	III
III. List of Abbreviations	V
IV. Table of contents	IX
1. Introduction	1
1.1 The TRAIL-TRAIL-Receptor System	1
1.1.1 TRAIL-mediated death signaling.....	3
1.1.2 TRAIL-induced non-canonical signaling.....	6
1.1.3 Intracellular TRAIL-Receptors.....	8
1.1.4 TRAIL based therapy.....	9
1.2 Tumor suppressor protein p53	10
1.2.1 p53 functions.....	11
1.2.2 Regulation of p53.....	12
1.2.3 p53 in cancer.....	15
1.3 Aims of the study	17
2. Material	18
2.1 Chemicals and Reagents	18
2.2 Buffers	20
2.3 Cell culture material	22
2.3.1 Cell lines.....	22
2.3.2 Culture media.....	22
2.3.3 Plasmids.....	22
2.3.4 Short interfering RNAs.....	23
2.4 Molecular biological material	23
2.4.1 Oligonucleotides.....	23
2.4.2 Antibodies.....	24
2.4.3 Consumables.....	26

2.4.4	Kit systems	27
2.4.5	Software	27
2.4.6	Laboratory Devices	28
3.	Methods	31
3.1	Cell biology methods.....	31
3.1.1	Cell culture	31
3.1.2	Determination of the cell number	31
3.1.3	Cell stimulation	31
3.1.4	Long-term storage of cells in liquid nitrogen.....	32
3.1.5	Small RNA interference.....	32
3.1.6	Overexpression of TRAIL-R2 isoforms	32
3.2	Biochemical methods.....	33
3.2.1	Preparation of whole cell lysates.....	33
3.2.2	Preparation of whole cell lysates for immunoprecipitation.....	33
3.2.3	Preparation of nuclear fractions for immunoprecipitation.....	33
3.2.4	Preparation of cytosolic, nuclear and chromatin fractions.....	33
3.2.5	Protein quantification using Bicinchoninic acid assay.....	34
3.2.6	Protein quantification using Lowry assay.....	34
3.2.7	Protein quantification using Bradford assay.....	35
3.2.8	SDS-Polyacrylamide-gel electrophoresis (SDS-PAGE).....	35
3.2.9	Western blotting.....	35
3.2.10	Cell cycle analysis by propidium iodide (PI) staining	36
3.2.11	DNA-fragmentation assay.....	36
3.3	Immunological methods.....	36
3.3.1	Immunofluorescence.....	36
3.3.2	Flow cytometric analyses of cell surface expression of TRAIL receptors.....	37
3.3.3	Immunoprecipitation analysis of whole cell lysates.....	37
3.3.4	Immunoprecipitation analysis of nuclear fractions.....	37
3.3.5	Chromatin immunoprecipitation	38

3.4	Molecular biology methods	39
3.4.1	Preparation and quantification of RNA	39
3.4.2	Complementary DNA synthesis	39
3.4.3	Quantitative real-time polymerase chain reaction.....	39
3.5	Statistical analysis	40
4.	Results	41
4.1	Determination of TRAIL-receptor levels in A549 and HCT116 wild type and TRAIL-R2 silenced cells	41
4.2	Activation of p53 upregulates TRAIL-R2 in A549 cells	43
4.3	TRAIL-R2 interacts with p53	43
4.4	Impact of TRAIL-R2 status on p53 and its targets	45
4.4.1	Silencing TRAIL-R2 increases the cellular level of p53 and the expression of its transcriptional targets.....	45
4.4.2	Overexpression of TRAIL-R2 decreases the cellular p53 level	47
4.4.3	TRAIL-R2's impact on p53 levels and its transcriptional output does not depend on the activity of caspases	48
4.4.4	TRAIL-R2 affects p53 independent of TRAIL.....	49
4.5	Analysis of the regulatory mechanism by which TRAIL-R2 affects the protein level of p53	51
4.5.1	TRAIL-R2 affects p53 protein stability	51
4.5.2	TRAIL-R2-mediated p53 degradation depends on the ubiquitin-proteasome-system.....	53
4.5.3	TRAIL-R2 co-localizes with MDM2 in the nucleus.....	55
4.5.4	TRAIL-R2 does not affect the deubiquitination activity of USP10 towards p53 58	
4.5.5	Deubiquitinases are not involved in TRAIL-R2-mediated destabilization of p53 63	
4.5.6	TRAIL-R2 affects p53 protein level independent of HMGA2	64
4.5.7	TRAIL-R2 co-localizes with PML protein in distinct nuclear domains.....	66
5.	Discussion	69
5.1	Interrelationship between TRAIL-R2 and p53	69

5.2	TRAIL-R2 destabilizes p53 protein.....	72
5.3	TRAIL-R2 destabilizes p53 independent of deubiquitinases	73
5.4	TRAIL-R2 impacts p53 independent of HMGA2	74
5.5	TRAIL-R2 interacts with PML	75
6.	Conclusion	77
7.	References.....	79
	List of Figures.....	94
	List of Tables	96
	Supplementary Data.....	97
	Declaration on oath.....	98
	Acknowledgements.....	99

1. Introduction

1.1 The TRAIL-TRAIL-Receptor System

Tumor necrosis factor (TNF)-related apoptosis-inducing ligand (TRAIL/ Apo2L) belongs to the TNF-superfamily and was discovered in 1995 [1]. TRAIL is a type II transmembrane protein and proteolytic shedding leads to the release of the 24 kDa extracellular portion from the cell surface. The proteases that are involved in TRAIL shedding have not been conclusively identified even though a role of ADAM33 and cathepsin E have been suggested [2,3]. TRAIL is active as a trimer and can induce apoptosis via binding to the death receptors TRAIL-R1 (DR4, APO-2) and TRAIL-R2 (DR5, KILLER, TRICK2) (Fig. 1) [4–6]. Besides TRAIL-R1 and TRAIL-R2, three other receptors are known, namely TRAIL-R3 (DcR3, DcR1, TRID, LIT), TRAIL-R4 (DcR2, TNFRSF10D, TRUNDD) and the soluble receptor osteoprotegerin (OPG) [7,8]. While only TRAIL-R1 and TRAIL-R2 can induce apoptosis via their cytoplasmic death domain (DD) [5,9] (Fig. 1), TRAIL-R3 and TRAIL-R4 lack a functional intracellular DD, thus they are not able to induce cell death. TRAIL-R3, anchored in the plasma membrane via glycosylphosphatidylinositol (GPI), contains neither a transmembrane nor a cytoplasmic domain. Accordingly, TRAIL-R3 cannot transmit TRAIL-induced signaling. The cytoplasmic domain of TRAIL-R4 can induce several non-apoptotic signal transduction pathways but contains a truncated, non-functional DD. Therefore, TRAIL-R3 and TRAIL-R4 are designated as decoy receptors (DcR) and are proposed to negatively regulate TRAIL-induced apoptosis via ligand competition and/ or direct interaction with the pro-apoptotic receptors TRAIL-R1/ R2 [10–12]. The affinity of TRAIL to OPG is weaker compared to the membrane-bound receptors. Therefore, a rather subordinate role of this receptor in TRAIL signaling is suggested [13,14]. The binding preference of TRAIL to its receptors depends on its concentration, its membrane bound or soluble form and the availability of the different TRAIL-Rs. This varies between cell populations and tissue types. Since one TRAIL trimer binds three TRAIL-Rs, the composition of this complex largely determines downstream signal transduction.

In contrast to humans, mice express only one death receptor that shares high homology with both, human TRAIL-R1 and TRAIL-R2 [15]. Despite intensive research, it is still unknown why humans developed two death receptors. In addition, two distinct splice variants of TRAIL-R2 exist, a short and a long isoform, respectively (Fig. 1). While TRAIL-R2 short isoform harbors one TAPE (threonine, alanine, proline and glutamine) domain, TRAIL-R2 long isoform contains a second TAPE region present in the extracellular portion. Both forms are ubiquitously expressed in human tissues and cell lines. In general, TRAIL-R2 long isoform predominates, but the proportion of the two variants differs between tissue types [16]. TRAIL is expressed by various cells of the immune systems including T-cells, neutrophils, dendritic cells, plasmacytoid dendritic cells, innate lymphocytes, natural killer (NK)- and NK T-cells upon activation by type

I and type II interferons, but it is also expressed by tumor cells. TRAIL and its receptors were shown to play an important role in the immune regulation, immune response and in immune surveillance [17–20].

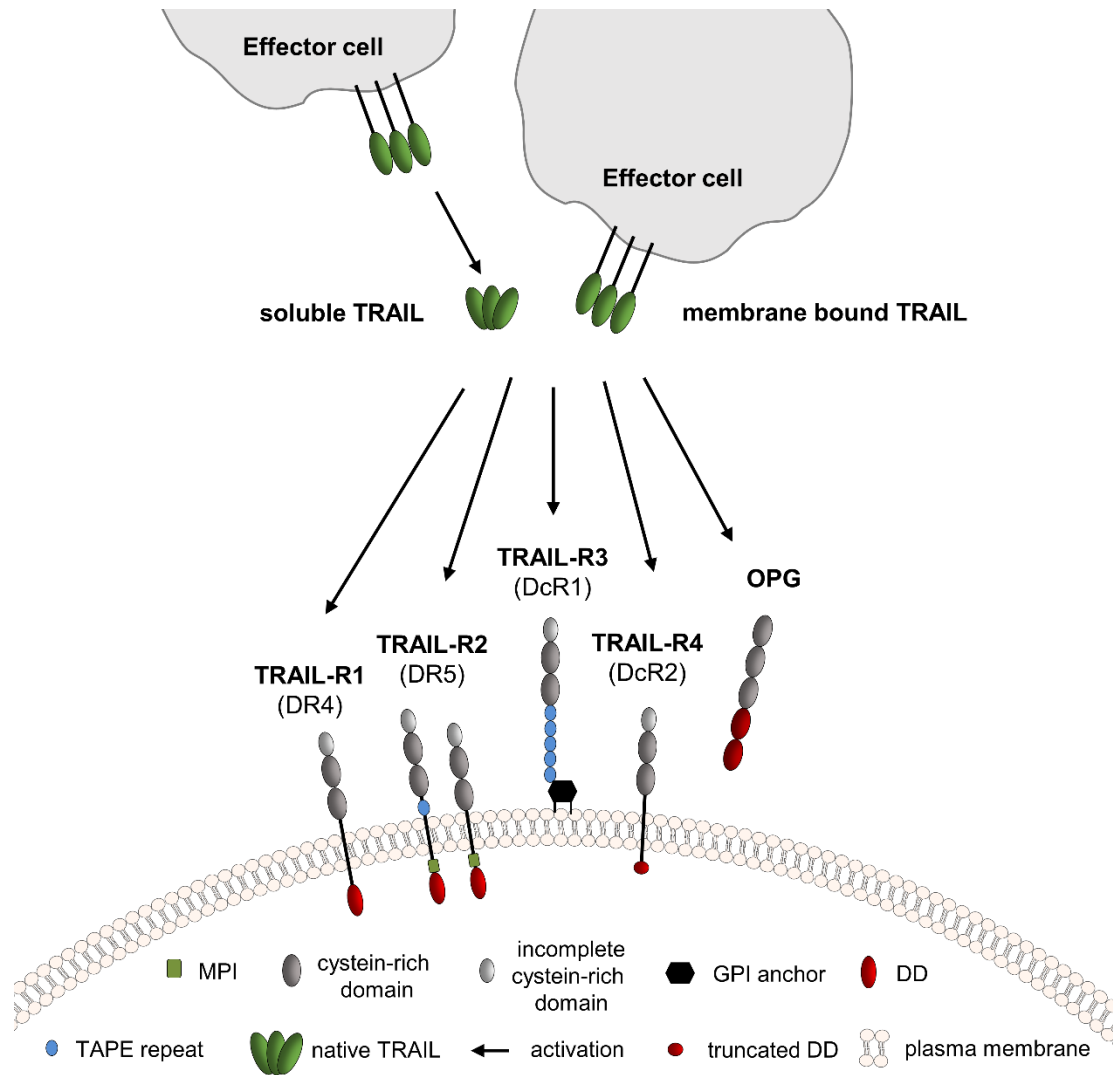


Figure 1: The TRAIL-TRAIL-Receptor System.

Human tumor-necrosis-factor-related apoptosis-inducing ligand (TRAIL) is expressed as a transmembrane protein and can be released from the cell surface by shedding (soluble TRAIL). TRAIL binds to four membrane-bound TRAIL receptors (TRAIL-Rs) and one soluble receptor. TRAIL-R1 and TRAIL-R2 can mediate apoptotic signals via their intracellular death domain (DD). TRAIL-R2 is expressed as a long and a short isoform differing in the presence or absence of a TAPE (threonine, alanine, proline and glutamine) domain. TRAIL-R3 contains five TAPE domains, is anchored to the plasma membrane via glycosylphosphatidylinositol (GPI) and lacks an intracellular domain. TRAIL-R4 contains a truncated DD, unable to mediate death signaling. TRAIL-R3 and TRAIL-R4 serve as decoys that negatively regulate apoptosis. The cysteine-rich domains of the receptors are essential for ligand binding. Osteoprotegerin (OPG) represents a soluble receptor with a low affinity to TRAIL. MPI, membrane proximal domain. Adapted from [21].

1.1.1 TRAIL-mediated death signaling

Apoptosis, a form of programmed cell death was first described in 1972 [22]. The program is responsible for the elimination of various cell types during normal development as well as elimination of aberrantly functioning, irreparably damaged or infected cells. The apoptotic pathway is induced by either an extrinsic or an intrinsic initial signal. The intrinsic apoptotic program is triggered by signals that originate from within the cell including genomic damage, anoxia, imbalanced cell growth signals and cytotoxic stress. Whereas the extrinsic apoptotic signaling is mediated via death ligand binding to a death receptor. Both apoptotic signaling pathways cause profound morphological transformations of the dying cell like nuclear condensation and shrinkage, DNA fragmentation, cell shrinkage and formation of apoptotic bodies. These characteristic changes are orchestrated by caspases.

The TRAIL-TRAIL-R system can induce extrinsic apoptotic signaling (Fig. 2). Following TRAIL-ligation to TRAIL-R1 and/ or TRAIL-R2 the death-inducing signaling-complex (DISC) is assembled at the DD of the receptors. The DISC is composed of FAS-associated protein with death domain (FADD) and pro-caspases-8/-10 [23]. Thereby, one FADD molecule is recruited by three TRAIL-R1/ R2 DD's. FADD in turn recruits several pro-caspase-8 molecules via homotypic interactions of their death-effector domains (DED) forming a growing chain of caspases [24]. DISC triggers the proximity induced self-cleavage of pro-caspases leading to their activation, dissociation from the protein complex and initiation of a caspase cascade. The execution of extrinsic apoptotic-signaling can be inhibited by the caspase-8 homologue cellular FADD-like IL-1 β -converting enzyme (FLICE)-inhibitory protein (c-FLIP), which associates with FADD and caspase-8 thereby interfering with the elongation of caspase-8 chains and blocking the autocatalytic activation of caspase-8 [25]. In so called type I cells, the extrinsic apoptotic signal and DISC formation is sufficient to activate downstream executioner caspases-3/ -6/ -7. In contrast, in so called type II cells, amplification of the initial extrinsic apoptotic signal via a mitochondrial activation loop is required to induce cell death (Fig. 2). This is necessary to effectively activate effector caspases-3/ -6/ -7 [26]. In type II cells activated caspase-8 cleaves Bcl-2-homology domain 3 (BH3) interacting domain death agonist (Bid) to its truncated form tBid. Activated tBid translocates to the mitochondria where it initiates mitochondrial outer membrane permeabilization (MOMP) via Bcl-2 associated X protein (BAX) and Bcl-2 homologous antagonist killer (Bak) [27,28]. This in turn leads to the release of pro-apoptotic mitochondrial proteins such as cytochrome c and second mitochondrial activator of caspases/ direct inhibitor of apoptosis-binding protein with low pI (Smac/ DIABLO). In the cytosol, cytochrome c, the apoptotic protease-activating factor 1 (APAF-1) and pro-caspase-9 form a multiprotein platform, called apoptosome, which is crucial for the activation of the initiator caspase-9 [29]. Caspase-9 in turn can activate effector caspases-3/ -6/ -7 to trigger apoptosis. The effector caspases cleave multiple substrates, among them inhibitor of caspase-activated DNase (ICAD), lamin, actin and vimentin, responsible for the apoptotic phenotype.

Multiple anti-apoptotic proteins may interfere with the mitochondrial apoptotic pathway by inactivating effector caspases-3/ -6/ -7. So called inhibitors of apoptosis proteins (IAPs), like X-linked inhibitor of apoptosis (XIAP), can attach to caspases leading to their inactivation or marking them for ubiquitination and proteasomal degradation [30]. This blocking mechanism is antagonized by the mitochondrial protein Smac/ DIABLO which associates with XIAP. Moreover, members of Bcl-2 protein family including Bcl-2, B-cell lymphoma-extra-large (Bcl-XL) and induced myeloid leukemia cell differentiation protein (Mcl-1) can bind to and convert BAX and Bak to their inactive form preventing MOMP. Consequently, the relative levels of pro- and anti-apoptotic proteins determine the life and death of a cell [26].

Besides the induction of apoptosis, TRAIL/ TRAIL-Rs can initiate an alternative cell death pathway called necroptosis which is induced by receptor-interacting protein kinase 1 and 3 (RIPK1, RIPK3) and executed by mixed lineage kinase domain like pseudokinase (MLKL). In case of inhibited caspase activation, apoptosis is prevented and the formation of the necrosome is induced by the interaction of RIPK1 and RIPK3 (Fig. 3) [31].

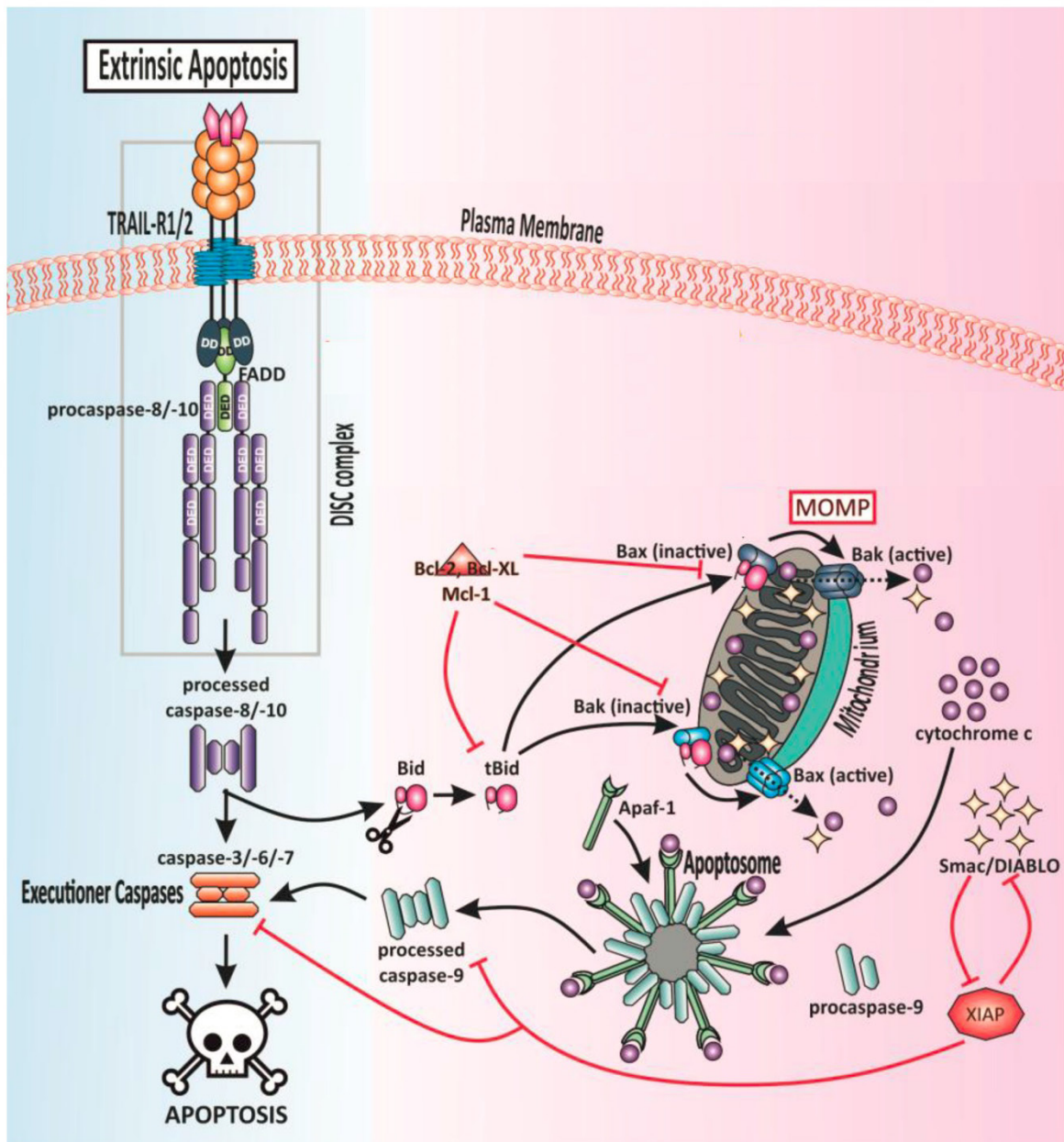


Figure 2: TRAIL-mediated apoptotic signaling.

TRAIL-induced extrinsic apoptosis. TRAIL binding to TRAIL-R1 and/ or TRAIL-R2 initiates the assembly of the death inducing signaling complex (DISC) leading to autocatalytic activation of caspase-8/-10. In type I cells, DISC signal is sufficient to activate a downstream caspase cascade leading to apoptosis induction. In type II cells the DISC signal needs amplification via a mitochondrial activation loop. Caspase-8 cleaves Bid to its truncated form tBid, which induces BAX/ Bak-mediated mitochondrial outer membrane permeabilization (MOMP) and release of the pro-apoptotic mitochondrial proteins cytochrome c and Smac/ DIABLO. In the cytosol, cytochrome c, the apoptotic protease-activating factor 1 (APAF-1) and pro-caspase-9 form the apoptosome initiating the activation of caspase-9, which in turn activates effector caspases-3/-6/-7. MOMP neutralizes the caspase inhibitor X-linked inhibitor of apoptosis (XIAP) protein, which is antagonized by the mitochondrial protein Smac/ DIABLO. Other apoptosis inhibition mechanisms include cellular FADD-like IL-1 β -converting enzyme (FLICE)-inhibitory protein (c-FLIP), which competes with caspase-8 for binding to FADD, hindering caspase-8 activation. Bcl-2, B-cell lymphoma-extra-large (Bcl-XL) and induced myeloid leukemia cell differentiation protein (Mcl-1) can bind to and convert BAX and Bak to their inactive form preventing MOMP. Bid, Bcl-2-homology domain 3 (BH3) interacting domain death agonist; BAX, Bcl-2 associated X protein; Bak, Bcl-2 homologous antagonist killer. Adapted from [32].

1.1.2 TRAIL-induced non-canonical signaling

Besides death signaling TRAIL-Rs are able to activate various pro-inflammatory signal transduction pathways such as nuclear factor kappa-light-chain-enhancer of activated B-cells (NF- κ B), mitogen-activated protein kinase (MAPK), tyrosine kinase Rous sarcoma oncogene cellular homolog (SRC), phosphoinositide 3-kinase (PI3K) pathways and protein kinase B (AKT) signaling, which can promote proliferation, migration, invasion and metastasis of apoptosis resistant malignant cells [33–40]. TRAIL-mediated induction of these pathways is supposed to be transmitted via a TRAIL-R-associated plasma membrane located complex I or a TRAIL-R-devoid cytosolic complex II (Fig. 3). Both complexes are dependent on TRAIL and act as death-inducing and gene-activatory signaling platforms [41]. Like complex I, complex II consists of DISC components FADD and caspase-8, but in addition RIPK1, TNF receptor-associated factor 2 (TRAF2), NF- κ B essential modifier (NEMO) and inhibitor of κ B (I κ B) kinase (IKK) are recruited. TRAF2 is crucial for the assembly of cellular inhibitor of apoptosis protein 1/2 (cIAP1/2), which in turn induces the ubiquitination of RIPK1 with linked poly-ubiquitin chains [42]. Ubiquitin modified RIPK1 forms a platform for the recruitment of the linear ubiquitin chain assembly complex (LUBAC). LUBAC is a ubiquitin E3 ligase complex adding linear poly-ubiquitin chains on RIPK1. LUBAC in turn facilitates caspase-8 activation and the recruitment of the IKK complex leading to NF- κ B activation, which is one of the main drivers of pro-inflammatory cytokine production [41].

RIPK1 is mandatory for the activation of SRC and signal transducer and activator of transcription 3 (STAT3) promoting cell migration and invasion. Complex I and complex II trigger NF- κ B, p38 mitogen-activated protein kinase (p38 MAPK), JUN N-terminal kinase (JNK) as well as extracellular signal-regulated kinase (ERK) signaling.

Independent of FADD and complex I and II, the membrane-proximal domain of TRAIL-R2 is able to activate Rat sarcoma (Ras)-related C3 botulinum toxin substrate 1 (Rac1)/PI3K pathway promoting tumor growth, migration, invasion and metastasis [39]. Furthermore, TRAIL can induce a cancer secretome in a FADD- and caspase-8-dependent manner that promotes a tumor-supportive microenvironment [43].

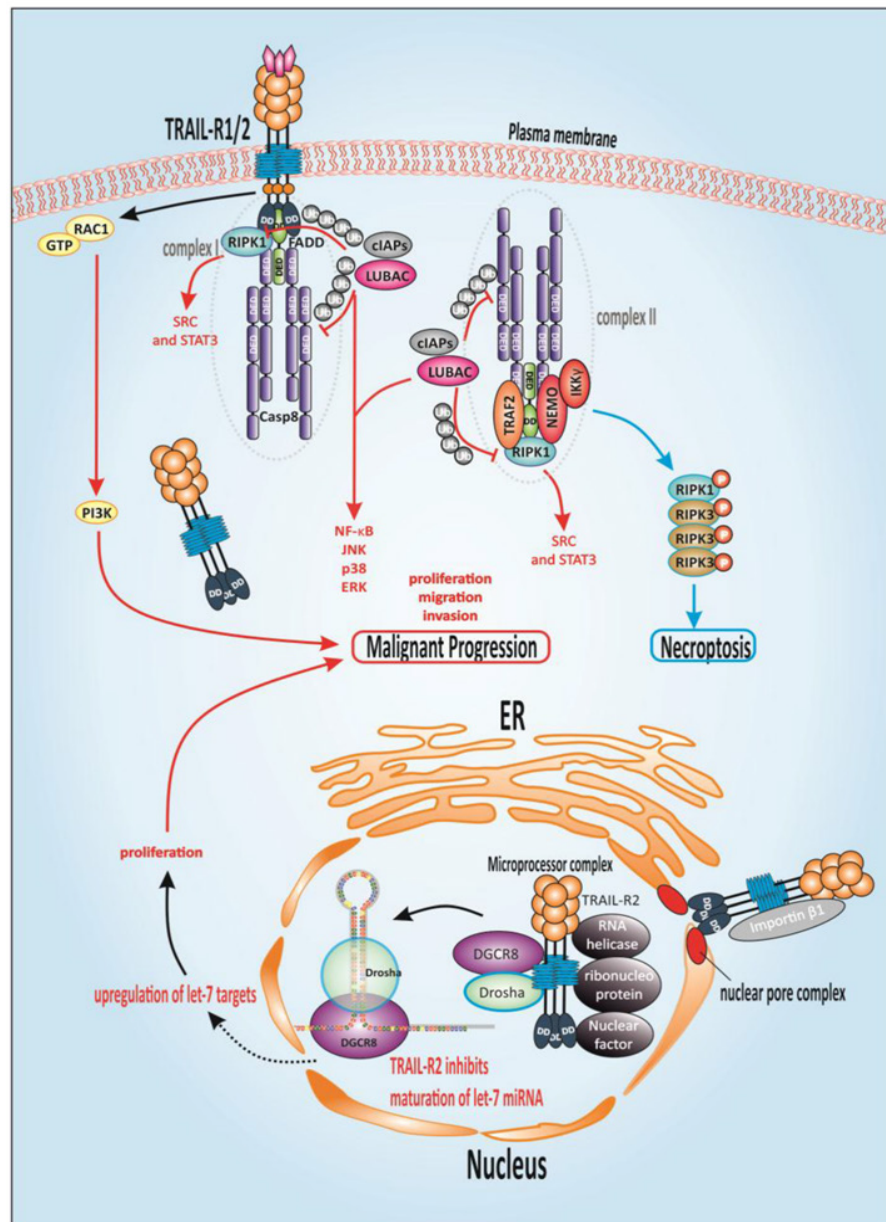


Figure 3: TRAIL-induced non-canonical signaling and functions of nuclear TRAIL-R2.

Binding of TRAIL to TRAIL-R1/ R2 induces the formation of the TRAIL-R-associated complex I or TRAIL-R-devoid cytosolic complex II. In complex I, downstream of FADD, caspase-8, RIPK1, TRAF2 and NEMO are recruited. TRAF2 recruits cIAP1/ 2, that executes ubiquitination of RIPK1 leading in turn to the recruitment of LUBAC. LUBAC modifies RIPK1 with linear ubiquitin chains. The composition of complex II is similar to that of complex I. In both complexes LUBAC facilitates caspase-8 activation and the recruitment of the IKK complex leading to NF-κB activation. In case of inhibition of caspase activation necroptosis is induced by the interaction of RIPK1 and RIPK3 building the necrosome. TRAIL-R2 is also present in the nucleus and interacts with the core components of the microprocessor complex Drosha/ DGCR8 and the accessory proteins RNA helicase p68, ribonucleoprotein hnRNPA1 and nuclear factor NF45 attributed to the maturation of microRNAs (miRNAs). Nuclear TRAIL-R2 inhibits the maturation of let-7 miRNAs thereby enhances the expression of its targets HMGA2 and Lin28B and promotes proliferation and malignant progression. FADD, FAS-associated protein with death domain; RIPK1, receptor-interacting protein kinase 1, TRAF2, tumor necrosis factor (TNF) receptor-associated factor 2; NEMO, nuclear factor kappa light chain enhancer of activated B cells (NF-κB) essential modifier; LUBAC, linear ubiquitin chain-assembly complex; ER, endoplasmic reticulum; DGCR8, DiGeorge critical region 8; let-7, lethal-7; hnRNPA1, heterogeneous nuclear ribonucleoprotein A1; HMGA2, High Mobility Group AT-Hook 2; Lin28B, Lin-28 Homolog B. Ub, Ubiquitin; P, phosphorylated. [32].

1.1.3 Intracellular TRAIL-Receptors

The aforementioned TRAIL-R functions are linked to their location at the plasma membrane. Interestingly, TRAIL-R1 and TRAIL-R2 are commonly expressed at high levels in cancer cells but mainly located intracellularly in the cytoplasm and/ or nucleus. Intracellular localization was declared as a mechanism of cancer cells to escape TRAIL-mediated apoptosis [44,45]. Correspondingly, a high intracellular abundance, especially of TRAIL-R2, was correlated with poor patient prognosis [46].

Whether the intracellular soluble TRAIL-Rs originate from a plasma membrane or a non-membranous soluble cytoplasmic pool, as well as the mode of their nuclear translocation, was completely unknown for a long time. A recent study unraveled that nuclear TRAIL-Rs originate from the plasma membrane. Moreover, their translocation to the nucleus is TRAIL-mediated and requires clathrin-dependent endocytosis [47]. TRAIL-R2 contains two nuclear localization sequences (NLS) mediating cytosolic-nuclear shuttling of TRAIL-R2 via nuclear importer protein Importin- β 1 [44]. The reverse transport of nuclear TRAIL-R2 (nTRAIL-R2) to the cytosol is facilitated by the nucleo-cytoplasmic shuttle protein Exportin-1/ CRM-1 that recognizes the nuclear export sequence (NES) in TRAIL-R2 [47]. The nuclear functions of TRAIL-Rs are still not completely understood. However, a direct link between nTRAIL-R2 and the maturation of microRNAs (miRNAs) was reported (Fig. 3). Thus, it has been shown that nTRAIL-R2 interacts with the core components of the microprocessor complex Drosha and DiGeorge critical region 8 (DGCR8) as well as with its accessory proteins p68, nuclear factor 45 (NF45) and heterogeneous nuclear ribonucleoprotein A1 (hnRNPA1). Thereby, nTRAIL-R2 negatively regulates the maturation of microRNAs (miRNAs) of the lethal-7 (let-7) family that interact with and inhibit mRNAs of several regulators of mitogenic pathways including rat sarcoma (Ras) and avian myelocytomatosis virus oncogene cellular homolog (c-Myc) [48]. Let-7 plays a central role in differentiation processes during embryonic development. Accordingly, loss or reduction of its expression results in dedifferentiation, epithelial-mesenchymal transition (EMT) and promotes malignant transformation [49]. TRAIL-R2-mediated let-7 inhibition particularly results in increased expression of the let-7 targets high mobility group AT-Hook 2 (HMGA2) and Lin-28 homolog B (Lin28B) which promote cell proliferation [48]. HMGA family proteins are transcriptional regulators that play an important role in DNA repair, chromatin remodeling and DNA processing. Thereby, HMGA proteins alter several cellular pathways including cell cycle, cell differentiation, senescence and neoplastic transformation [50].

In addition to their nuclear localization, it has been shown that TRAIL-R1 and TRAIL-R2 associate with chromatin suggesting their role in the regulation of gene expression [47].

Regarding their cytoplasmic functions, it has been shown that both TRAIL-R1 and TRAIL-R2 are involved in the unfolded protein response (UPR) where they contribute to unresolved endoplasmic reticulum (ER) stress-induced cell death in a TRAIL-independent manner [51,52].

Recently Lam *et al.* showed that misfolded proteins can act as ligands to activate TRAIL-R2 intracellularly leading to assemble of pro-apoptotic caspase 8-activating complexes [53].

1.1.4 TRAIL based therapy

In 1999 two preclinical *in vivo* studies by two independent groups revealed tumor regression after systemic treatment with recombinant variants of human TRAIL [54,55]. TRAIL's ability to selectively eliminate tumor cells, while sparing healthy cells made it a promising molecule for cancer treatment. Based on these findings the development of clinical TRAIL-R agonists, including recombinant forms of human TRAIL or agonistic antibodies targeting TRAIL-R1/ R2 started. As a result, one recombinant form of human TRAIL (Dulanermin) as well as several agonistic TRAIL-R-specific antibodies (e.g. Mapatumumab, Conatumumab, Lexatumumab, Tigatuzumab) entered clinical trials. Although these TRAIL-R agonists revealed promising anti-tumoral activity in pre-clinical studies, no clinical benefit could be demonstrated in cancer patients [21,56,57]. This outcome was not only attributed to an insufficient activity and stability of the molecules, but rather to an intrinsic or acquired resistance of cancer cells to TRAIL-induced apoptotic signaling. To date it is known that the sensitivity to TRAIL-induced cell death can be modulated at multiple steps, such as the level of TRAIL-Rs at the cell surface, FLIP, caspases or the expression of proteins belonging to the Bcl-2 family. Consequently, a better understanding of the TRAIL-TRAIL-R system led to the concept of a combination therapy of TRAIL and other compounds such as genotoxic drugs, kinase inhibitors and proteasome inhibitors, directing to sensitize TRAIL-resistant cancer cells to TRAIL apoptotic signaling. Nevertheless, TRAIL not only induces cell death signaling, but also stimulates several non-canonical pathways that promote malignant progression, proliferation, invasion and migration [37,38,40]. Moreover, it has been shown that the TRAIL-TRAIL-R system plays a tumor-supportive immune-modulatory role via induction of cytokine secretion that in turn promote the accumulation of tumor-supportive immune cells in the cancer microenvironment [43]. These latest aspects led to new ideas for TRAIL-R based cancer therapy that harness TRAIL's apoptosis-inducing activity and inhibit undesired pro-tumorigenic effects [32,58].

1.2 Tumor suppressor protein p53

P53 was discovered in 1979 as a 53 to 54 kDa protein associated with the large T protein of the SV40 virus [59]. By the discovery that wild type p53 is able to suppress cell proliferation and the demonstration of inactivating mutations in human cancers [60–62], p53 gene was categorized as a tumor suppressor gene. Due to its emerging role as a main regulator in the cellular response to DNA damage p53 was named “the guardian of the genome” [63]. Biochemical and structural analyses of the p53 protein revealed that p53 is a nuclear protein existing as a homotetramer in the cell. This p53 protein complex is assembled by four identical polypeptides composed of 393 amino acids that are complexed of different functional subunits (Fig. 4). Near the amino terminus (N-terminus) two small transactivation domains are located (amino acids 1-40 and 40-61 respectively). The transactivation domains mediate the interaction with various transcriptional co-factors, thereby enhancing the expression of p53 target genes. The nearby proline rich domain (amino acids 64-92) is proposed to facilitate protein-protein interactions important for p53 pro-apoptotic activity [64], but a structural role was suggested to be the main function [65]. The sequence-specific DNA binding domain is located in the protein center (amino acids 100-300). This domain is crucial for sequence-specific binding to p53 responsive elements of target genes. Several arginine and lysine residues as well as a zinc atom mediate the recognition and binding of p53 to DNA sequences [66,67]. Since 80 % of p53 mutations in human tumors are localized in the sequence specific DNA binding domain, apparently this domain is crucial for p53 tumor suppression and inhibition of p53-induced transcription represents a crucial event in tumorigenesis. At the p53 carboxyl terminus (C-terminus) a tetramerization domain (amino acids 323-355), the NLS and the regulatory domain are located. The tetramerization domain facilitates the oligomerization of p53 molecules. The regulatory domain binds DNA in a non-sequence-specific manner enabling p53 to bind to its responsive elements. Moreover, the regulatory domain includes a lysine-rich domain, which provides a platform for post-translational modifications that enhance p53 stability and facilitate sequence specific binding [68].

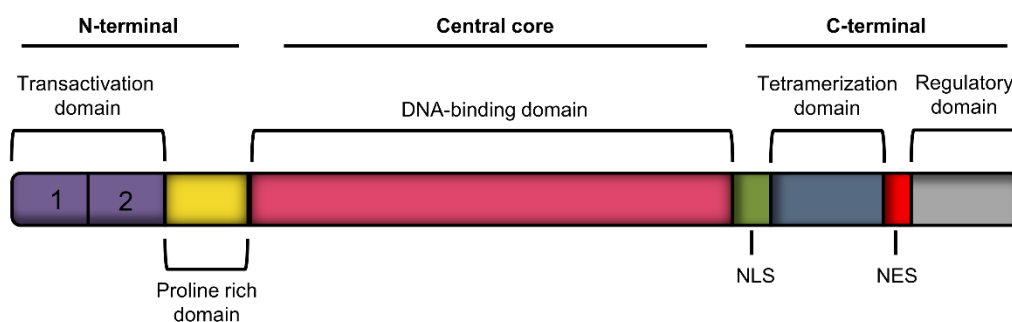


Figure 4: The domain organization of p53.

P53 is composed of two amino-terminal transactivation domains, a proline-rich domain, a central DNA-binding domain, a carboxyl-terminal tetramerization domain and a regulatory domain.

1.2.1 p53 functions

A variety of agents and cellular stress factors including X-rays, ultraviolet radiation, chemotherapeutic drugs that damage DNA, inhibitors of DNA or RNA synthesis, agents that disrupt microtubule components of the cytoskeleton, hypoxia, nutrient deprivation, oncogene signaling, oxidative stress, ribosomal dysfunction, telomere attrition and nucleotide depletion are capable of inducing rapid increases in p53 protein levels [69]. Moreover, various sensors are responsible for monitoring the integrity and functions of the cellular system as well as transmitting signals to p53 in case of detecting a discrepancy. In response to stress p53 protein undergoes post-translational modifications that activate p53's ability to initiate cellular responses such as cell cycle inhibition, senescence, apoptosis and DNA repair (Fig. 5). Moreover, p53 modulates cellular pathways that prevent tumor development like oncogenic metabolic reprogramming, inhibits the enrichment of reactive oxygen species (ROS), initiates autophagy, mediates tumor microenvironment communication, stops self-renewal and reprogramming of differentiated cells to stem cells and thereby blocks tumor invasion and metastasis [70]. The fact that p53 regulates such a great variety of cellular processes is mediated by its ability to essentially control the expression of around 500 genes. Well known p53 targets are growth arrest and DNA damage inducible protein 45a (Gadd45a) and Xeroderma pigmentosum complementation group E protein (XPE) which are both involved in DNA damage response. The p53 target gene *CDKN1A* (cyclin dependent kinase inhibitor 1A) encodes the protein p21, which is an important regulator of reversible and irreversible cell cycle arrest. P21, also termed p21^{waf1/cip1} belongs to the CIP/ KIP (CDK interacting protein/ kinase inhibitory protein) family of cyclin-dependent kinase (CDK) inhibitors. By inhibiting CDK4, 6/ cyclin-D and CDK2/ cyclin-E, p21 can arrest the cell cycle progression in G1/ S and G2/ M transition, respectively [71]. Moreover, p21 disrupts the interaction of retinoblastoma tumor suppressor protein (pRb) and CDK-Cyclins through inhibiting the phosphorylation of the pRb [72].

P53 also participates in cell death signaling by activating the intrinsic apoptosis pathway in response to intracellular stresses including DNA damage, hypoxia and oncogenes. Upon stress, p53 is activated and induces the expression of BH3 only proteins (BAX/ Bak) leading to MOMP and repressing of anti-apoptotic Bcl2 proteins and cellular inhibitor of apoptosis proteins 1/ 2 (cIAP1/ 2). Moreover, p53 induces the expression of other pro-apoptotic proteins like NOXA and PUMA (p53-upregulated modulator of apoptosis) [73]. In addition, p53 can transcriptionally modulate the protein level of TRAIL-R1/ R2 as well as their ligand TRAIL and participates thereby also in the extrinsic apoptotic pathway [74,75].

In addition, to the regulation of protein-coding target genes as a transcription factor, p53 is also engaged in the modulation of cellular miRNA levels. Thereby, p53 can regulate the expression of miRNAs at different levels. On the one hand, p53 can directly regulate their transcription. On the other hand, p53 impacts on miRNA levels via different mechanisms. Thus, it regulates

the activity of the microprocessor complex via interaction with the DEAD-box RNA helicase p68 (also termed DDX5, DEAD-box helicase 5). Thereby, p53 affects the processing of primary miRNAs to precursor miRNAs [76]. Furthermore, p53 regulates the target selection of miRNAs by inducing the RNA-binding-motif protein 38 (RBM38), which determines target selectivity by binding to 3'UTRs (untranslated regions) of miRNA target sequences. Thus, RBM38 selectively blocks the action of miRNA on several p53-induced messenger RNAs (mRNAs) supporting an efficient p53-mediated cellular stress response [77]. Moreover, p53 regulates the association between miRNAs and the RNA-induced silencing complex (RISC) by interacting with RISC component AGO2 (Argonaute RISC Catalytic Component 2) to modulate AGO2's association to multiple miRNAs, including let-7 family members [78]. P53's ability to modulate the cellular level of multiple miRNAs contributes to its role as a regulator of several cellular processes including cell cycle regulation, cell proliferation and survival, senescence and apoptosis, as well as inhibition of EMT, metastasis, angiogenesis and glycolysis [79].

1.2.2 Regulation of p53

P53 is an exceedingly unstable protein that is degraded by proteolysis approximately 20 min after its synthesis. This keeps p53 at low steady state levels under unstressed conditions and enables a rapid adaptation of p53 protein levels by blocking its degradation. Consequently, cells can double p53 concentration within 20 min allowing a dynamic response to certain physiological signals. P53 protein stability and activity is regulated by protein folding, localization [81,82] and posttranslational modifications such as phosphorylation, acetylation and ubiquitination [83].

P53 is phosphorylated at multiple serine and threonine sites across the whole protein, especially within the transactivation domain. Various kinases can phosphorylate p53 including ATM (ataxia-telangiectasia mutated), ATR (Ataxia telangiectasia and Rad3 related), DNA-dependent protein kinase (DNA-PK), checkpoint kinase 1 and 2 (Chk1 and Chk2). P53 phosphorylation can result in conformational changes that promote its intrinsic activity and sequence-specific DNA binding. In addition, phosphorylation regulates p53 mitochondrial translocation and transcription-independent apoptosis as well as protects p53 from proteasomal degradation by inhibiting its ubiquitination and blocking the interaction with its major negative regulator mouse double minute 2 homolog (MDM2) [83–85].

Acetylation takes place at specific p53 lysine residues by histone acetyl transferases (HATs) including CREB binding protein (CBP) and p300, as well as p300/ CBP associated

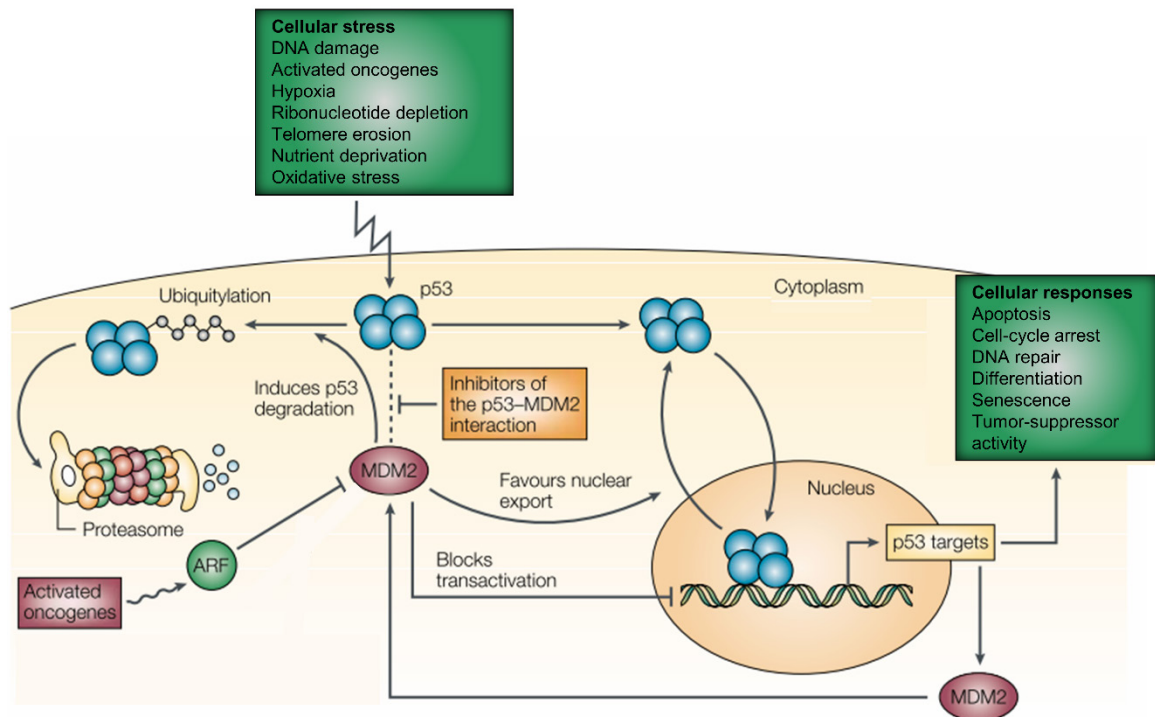


Figure 5: The p53-mediated cellular responses and its regulation by MDM2.

Under cellular stress p53 accumulates in the cell, binds to p53-responsive elements and induces the transcription of various genes that are involved in cell-cycle control, apoptosis, DNA repair, differentiation, senescence and tumor suppression. In the nucleus, p53 transcriptionally activates MDM2. MDM2 in turn associates with and inhibits p53 forming an p53-MDM2 auto-regulatory feedback loop. MDM2 blocks p53 activity via inhibition of its transcriptional activity, favours its nuclear export and degradation by ubiquitination. Upon stress, like DNA damage, MDM2 and p53 are conjugated with post-translational modifications that disrupt the interaction of both proteins preventing p53 from MDM2-mediated ubiquitination and degradation. In addition, the expression of oncogenes activates ADP-ribosylation factor (ARF), which in turn promotes MDM2 degradation. MDM2, mouse double minute 2 homolog. Adapted from [80].

factor (PCAP) [86,87]. P53 acetylation induces conformational changes resulting in sequence-specific DNA-binding activity, enhanced stability by blocking ubiquitination and altered protein-protein interactions between p53 and transcriptional co-activators [86,88–90]. Therefore, the p53 acetylation level correlates with its activity and stability [84,91].

P53 is, as many other proteins, degraded by the ubiquitin-proteasome-system (UPS) [92,93]. Numerous E3 Ubiquitin-ligases including coat protein complex I (COP1), p53-induced RING-H2 protein (Pirh2), ADP-ribosylation factor-binding protein 1 (ARF-BP1) and MDM2 were identified to be involved in p53 regulation by ubiquitination [94]. MDM2 represents the key negative regulator of p53 [92,93]. Low cellular levels of MDM2 lead to mono-ubiquitination and nuclear export of p53, while high levels of MDM2 mediate poly-ubiquitination of p53 and nuclear degradation (Fig. 5) [95]. MDM2 is not only responsible for the stability of p53, but also inhibits its transcriptional activity by binding to p53's transactivation domain and thereby hinders the recruitment of components crucial for transcription. Importantly, p53 assists its own maintenance by transcriptionally activating the gene expression of *mdm2* in a negative feedback loop (Fig. 5) [96]. In response to cellular stress signals p53 is activated via inhibition

of MDM2. MDM2 blocking can be achieved by different mechanisms. For example, posttranslational modifications of MDM2 and p53 can disrupt the interaction of both proteins or the activation of oncogenes can induce ADP-ribosylation factor (ARF), which in turn promotes MDM2 degradation (Fig. 5) [97]. Moreover, nucleolar-stress induces the binding of ribosomal proteins to MDM2 inhibiting MDM2-mediated ubiquitination of p53 [98,99]. Thus, due to its importance in the regulation of p53, it is not surprising that tumors bearing a wild type p53 allele commonly overexpress MDM2 [100].

Ubiquitination of p53 can be reversed by a process termed deubiquitination, which is catalyzed by deubiquitinating enzymes (DUBs). Several DUBs from the ubiquitin-specific proteases (USP) family were identified as regulators of the p53-MDM2-loop. Well known p53 DUBs are USP7, also called herpesvirus associated ubiquitin specific peptidase (HAUSP) and ubiquitin specific peptidase 10 (USP10). While HAUSP deubiquitinates p53 as well as MDM2, USP10 is a specific DUB for p53 (Fig. 6) [103,104]. HAUSP is mainly localized in the nucleus, but a small fraction was also found in the cytoplasm and mitochondria [101,102]. In contrast, USP10 is mainly located in the cytoplasm, where it counteracts p53's nuclear export and cytoplasmic degradation by reversing MDM2-mediated ubiquitination of p53. Nevertheless, upon DNA damage a fraction of USP10 translocates into the nucleus to deubiquitinate and activate p53 (Fig. 6). Interestingly, USP10 itself is regulated by posttranslational modifications that are generated by the same enzymes, which target p53. Thus, ATM phosphorylates USP10 at

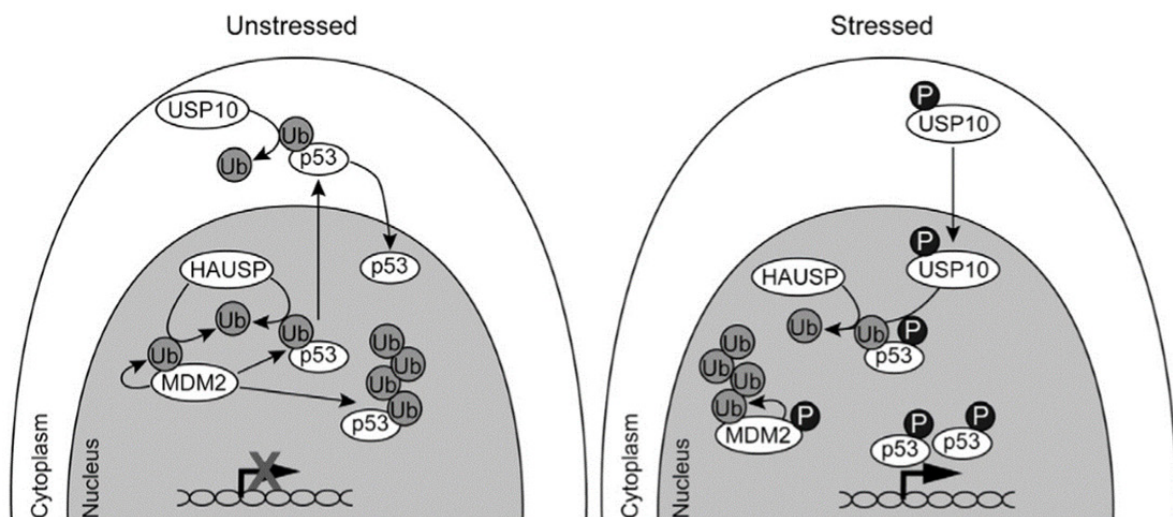


Figure 6: Regulation of p53 by MDM2, HAUSP and USP10.

In unstressed cells (left), p53 is maintained at low levels by MDM2. HAUSP removes ubiquitin from p53 and MDM2 leading to their stabilization. Mono-ubiquitinated p53 translocates to from the nucleus to the cytosol. USP10 deubiquitinates p53 in the cytosol. Poly-ubiquitinated p53 undergoes proteasomal degradation. Upon stress (right), both p53 and MDM2 are phosphorylated by various stress induced kinases, inhibiting the interaction between MDM2 and p53. MDM2 auto-ubiquitinates itself and undergoes proteasomal degradation. Induced by phosphorylation, a portion of USP10 translocates to the nucleus where it assists HAUSP to further stabilize p53 [105]. MDM2, mouse double minute 2 homolog; HAUSP, herpesvirus associated USP; USP10, ubiquitin specific peptidase 10; Ub, ubiquitin; p, phosphorylation.

Threonine 42 and Serine 337 leading to its stabilization and promoting its translocation to the nucleus [104].

Another protein that was described to play a key role in the regulation of p53 stability, especially under cellular stress conditions, is Promyelocytic leukemia protein (PML). PML is the core organizer of membraneless sub-nuclear organelles called PML nuclear bodies (NBs) that can sequester, modify or degrade partner proteins such as p53. By the assembly of various p53 regulators including ATM, ATR, Chk2, Sirtuin-1 (SIRT1), Homeodomain-interacting protein kinase 2 (HIPK2), HAUSP and MDM2, PML regulates p53 turnover [106–111].

In summary, p53 is regulated by a complex network of stress-responsive enzymes that modify p53 post-transcriptionally. While some p53 sites are constitutively modified in unstressed cells, most modifications are induced upon stress responses. Variations of these posttranslational modifications represent a diverse code, regulating p53 localization, stability and activity [84].

1.2.3 p53 in cancer

Based on its essential role in the maintenance of genome integrity and regulating of the cell cycle as well as apoptosis, *TP53* is mutated in around 50 % and inactive or low expressed in around 80 % of human tumors. Inactivation of p53 by post-translational mechanisms is prevalent in almost 50 % of tumors expressing wild type p53. Nevertheless, some tumors express functional p53 and treatment with chemo- or radiotherapy intends to activate a p53-mediated stress response.

In the majority of cancers *TP53* mutations represent missense mutations localized in the sequence-specific DNA binding domain, suggesting that this domain is crucial for p53 tumor suppression. These mutations result mostly in the expression of full-length mutant proteins that have lost their ability to activate p53 target genes and are therefore termed loss of function mutations. Interestingly, several mutant p53 variants are commonly accumulated in malignant cells. On the one hand, mutant p53 can form heterotetramers with wild type p53, leading to its inactivation (dominant-negative effect). On the other hand, some mutant p53 variants acquire new oncogenic capacities that are independent of wild type p53, known as gain-of-function properties. These mutant forms of p53 can increase tumor aggressiveness and metastatic potential by the acquisition of novel transcriptional activities [112–115]. For example, point mutations in p53 that affect the protein conformation, such as R175H, can interact with p63 and p73 and interfere with their activity, although wild type p53 is neither able to bind to p63 nor p73 [116–118].

Since, they are commonly overexpressed in tumors, p53 mutants represent alternative targets for anti-tumor therapy. These therapeutic implementations include the destabilization or inactivation of mutant p53, as well as the reactivation of wild type p53 functions. For example,

heat shock proteins were targeted through histone deacetylases to restore MDM2-dependent degradation of mutant p53 [119]. In order to inactivate mutant p53 functions, synthetic molecules were generated that prevent its interaction with other transcription factors like p73 [120]. Notably, synthetic molecules were also used to force the folding of mutant p53 to wild type conformation [121,122].

Interestingly, a substantial proportion of human tumors retain a wild type *TP53* allele, but the functions of the wild type p53 protein are inhibited by a variety of mechanisms including the overexpression of negative regulators such as MDM2. Therefore, the disruption of MDM2-p53 interaction represent a promising therapeutic approach and lead to the development of small molecule protein-protein interaction (PPI) inhibitors. These molecules mimic three to four residues of p53's transactivation domain which are crucial for the interaction with MDM2 [123]. One of the first discovered potent PPI inhibitor of MDM2 was Nutlin 3a, an enantiomer consisting of a 4,5-dihydroimidazole core, discovered by the group of Vassilev from Hoffmann-La Roche [124].

1.3 Aims of the study

The versatile functions of the TRAIL-TRAIL-R system and the tumor suppressor protein p53 in the development and progression of cancer are not understood in detail by now. TRAIL-R2 is transcriptionally regulated by p53. Accordingly, p53-directed anti-tumor therapies also aim to potentiate cell death in wild type p53-expressing malignant cells by enhancing TRAIL-R2 expression at the plasma membrane [75,125–128]. Controversially, TRAIL-R2 is commonly overexpressed in tumors, but it is mainly located intracellular in the cytosol and nucleus.

Preliminary results indicated an interaction between TRAIL-R2 and p53 in the nucleus of colon carcinoma HCT116 and pancreatic ductal adenocarcinoma AsPC-1 cells. Moreover, p53 proteins levels were elevated in HCT116 cells after siRNA-mediated knockdown of TRAIL-R2 expression (unpublished data).

While regulation of TRAIL-R2 expression by p53 has been well characterized, the recent discovery of pro-tumoral functions of endogenous-level expression of plasma membrane TRAIL-R2 [38–40,43] and nuclear TRAIL-R2 [48] in conjunction with above mentioned preliminary results, gave rise to the hypothesis that there might be a negative feedback regulation of p53 by TRAIL-R2. In order to answer this assumption, the present study aimed to address the following aspects:

- i) Examination of TRAIL-R2 and p53 interaction in A549 lung carcinoma cells, in order to assess whether the TRAIL-R2-p53 interaction observed in HCT116 and AsPC-1 cells represents rather a general phenomenon or tumor entity specific one.
- ii) Determination of the TRAIL-R2 status-associated transcriptional output of p53, in order to assess the functional outcome of the TRAIL-R2-p53 interaction.
- iii) Analyses of the impact of TRAIL-R2 on p53 transcriptional and protein level, in order to gain an insight into the molecular mechanisms underlying the TRAIL-R2-mediated modulation of p53.
- iv) Screening of proteins that potentially participate in the TRAIL-R2-p53 regulatory axis, in order to identify novel TRAIL-R2 co-factors.

2. Material

2.1 Chemicals and Reagents

Chemical/ Reagent	Manufacturer
5-Fluoruracil	UKSH pharmacy
Arsenic trioxide (ATO)	UKSH pharmacy
Bio-Rad Protein Assay Dye	Bio-Rad Laboratories, Hercules, USA
Bovine Serum Albumin (BSA)	Biomol GmbH, Hamburg; Germany
Bromphenol blue	Sigma-Aldrich, St. Louis, USA
cOmplete ULTRA Tablets Mini Protease Inhibitor Cocktail	Hoffmann-La Roche, Basel, Switzerland
Cycloheximide	Sigma-Aldrich, St. Louis, USA
Developer G153	Agfa, Mortsel, Belgium
Dimethyl sulfoxide (DMSO)	Sigma-Aldrich, St. Louis, USA
Dithiothreitol (DTT)	Carl Roth, Karlsruhe, Germany
DNA Ladder	Thermo Fisher Scientific, Waltham, USA
Dulbecco's phosphate-buffered saline	Thermo Fisher Scientific, Waltham, USA
Ethanol	Carl Roth, Karlsruhe, Germany
FcR blocking reagent	Miltenyi Biotec GmbH, Bergisch-Gladbach, Germany
Fetal calf serum (FCS)	PAN Biotech, Aidenbach, Germany
Formaldehyde solution 37 %	Sigma-Aldrich, St. Louis, USA
GelRed Nucleic Acid Gel Stain	Biotium, Hayward, USA
GeneRuler 100 bp DNA Ladder	Thermo Fisher Scientific, Waltham, USA
GlutaMAX -I (100X)	Thermo Fisher Scientific, Waltham, USA
Glycerol	Sigma-Aldrich, St. Louis, USA
Glycine	Carl Roth, Karlsruhe, Germany
Hoechst 33342	Sigma Aldrich, St. Louis, USA
Hydrochloric acid, 25%	J.T. Baker, Griesheim, Germany
IS Mounting Medium	diavona, Hamburg, Germany

Isopropanol 70 %	Th. Geyer, Renningen, Germany
Lipofectamine® 2000	Thermo Fisher Scientific, Waltham, USA
Lipofectamine® RNAi/ MAX	Thermo Fisher Scientific, Waltham, USA
Magnesium chloride	Merck Milipore, Darmstadt, Germany
Maxima SYBR Green/ ROX	Thermo Fisher Scientific, Waltham, USA
MG132	Merck Millipore, Burlington, USA
Non-fat dried milk powder, blotting grade	Carl Roth, Karlsruhe, Germany
Nutlin 3a	Sigma-Aldrich, St. Louis, USA
OptiMEM® I (1x): HEPES, 2.4g/L sodium bicarbonate, L-Glutamine	Life Technologies, Carlsbad, USA
PhosSTOP Phosphatase Inhibitor Cocktail Tablets	Hoffmann-La Roche, Basel, Switzerland
Pierce ECL Plus Western Blotting Substrate	Thermo Fisher Scientific, Waltham, USA
Pierce ECL Western Blotting Substrate	Thermo Fisher Scientific, Waltham, USA
Pierce Protein A/G Magnetic Beads	Thermo Fisher Scientific, Waltham, USA
Potassium chloride	Merck Milipore, Darmstadt, Germany
PR-619	Merck Milipore, Darmstadt, Germany
Protein G Sepharose 4 Fast Flow	GE Healthcare, Chicago, USA
Rapid Fixer G354	Agfa, Mortsel, Belgium
Recombinant human sTRAIL/Apo2L	PeproTech, Hamburg, Germany
RNAse	Sigma-Aldrich, St. Louis, USA
Rotiphorese 50x TAE Buffer	Carl Roth, Karlsruhe, Germany
RPMI 1640 Medium	Thermo Fisher Scientific, Waltham, USA
SDS (10%)	Applichem, Darmstadt, Germany
siRNA buffer	Horizon Discovery, Cambridge, UK
Sodium chloride	J.T. Baker, Griesheim, Germany
Sodium pyruvate 100 mM (100x)	Thermo Fisher Scientific, Waltham, USA
Spectra Multicolor Broad Range Protein Ladder	Thermo Fisher Scientific, Waltham, USA
TaqMan Gene Expression Assay	Thermo Fisher Scientific, Waltham, USA
TaqMan Universal PCR Master Mix	Thermo Fisher Scientific, Waltham, USA

TRIS-Base	Merck Millipore, Burlington, USA
Trypsin EDTA 10x	Merck Millipore, Burlington, USA
Tween 20	Merck Millipore, Burlington, USA
Universal-Agarose, peqGOLD	PEQLAB - Life Science, Germany
zVAD-fmk	Bachem, Bubendorf, Switzerland

2.2 Buffers

Buffer	Formulation
RIPA-Lysis buffer	50 mM Tris-HCl pH 7.5 150 mM NaCl 0.2 % (v/v) SDS 1 % (v/v) IGEPAL CA-630 0.5 % w/v Sodium deoxycholate
IP-Lysis buffer (whole cell lysates)	30 mM Tris-HCl pH 7.4 120 mM NaCl 1 % (v/v) Glycerol 1 % (v/v) Triton X 100
Cell fractionation buffers (cytosolic, nuclear preparations)	<u>Hypotonic buffer:</u> 10 mM HEPES pH 7 10 mM KCl 0.2 mM EDTA 1 mM DTT <u>Nuclear-lysis buffer:</u> 30 mM Tris-HCl pH 7.4 120 mM NaCl 1 % Glycerol 0.5 % NP-40
Cell fractionation buffers (cytosolic, nuclear, chromatin preparations)	<u>Buffer A:</u> 10 mM HEPES pH 7.9

	10 mM KCl 1.5 mM MgCl ₂ 0.34 M Saccharose 10 % Glycerol
	<u>Buffer B:</u> 3 mM EDTA 0.2 mM EGTA
Laemmli running buffer	25 mM Tris-HCl 1% (w/v) SDS 192 mM Glycin
Laemmli loading buffer	250 mM Tris-HCL pH 6.8 8 % (w/v) SDS 0.04 % Bromphenol blue 40 % Glycerol 200 mM DTT
Transfer buffer	25 mM Tris HCl 20 % (v/v) Methanol 192 mM Glycin
TBS-T buffer	10 mM Tris-HCl pH 7.6 150 mM NaCl 0,1% (v/v) Tween 20
TBS buffer	10x TBS: 1 M NaCl 1 M Tris HCl pH 7.6
Blocking buffer	5 % (w/v) milk/ TBS-T 5 % (w/v) BSA/ TBS-T
MACS buffer	2 % FCS 1 mM EDTA

	in PBS pH 7.4
--	---------------

2.3 Cell culture material

2.3.1 Cell lines

Cell line	Origin	Reference
HCT116	Human colorectal adenocarcinoma cell line isolated from the primary tumor of a Caucasian male. This cell line has a mutation in codon 13 of the ras proto-oncogene. HCT116 cells were kindly provided by Bert Vogelstein.	[129,130]
A549	Human lung carcinoma cells line isolated from a 58-year-old Caucasian male. A549 wild type and TRAIL-R2 knockout cells were kindly provided by Henning Walczak.	[131]

2.3.2 Culture media

Usage	Formulation
A549	RPMI 1640 medium 10% (v/v) FCS
HCT116	1% (v/v) Sodium pyruvate 1% (v/v) Glutamax

2.3.3 Plasmids

Plasmid	Characterization	Promoter	Selection Agent (Eukaryotes)	Reference
pCR3.1	<i>TNFSF10B</i> (TRAIL-R2 long isoform point mutation R359A)	Cytomegalovirus enhancer-promoter	Geneticin® (G-418)	[132]
pCR3.1	<i>TNFSF10B</i> (TRAIL-R2 short isoform point mutation R330A)	Cytomegalovirus enhancer-promoter	Geneticin® (G-418)	[132]

2.3.4 Short interfering RNAs

siRNA	Manufacturer	Cat. number
siCtrl: control siRNA On-Targetplus® non-targeting pool	Horizon Discovery, Cambridge, UK	D-001810-10
siUSP10: On-Targetplus® human USP10 SMARTpool	Horizon Discovery, Cambridge, UK	J-006062-10-002
siHMGA2: On-Targetplus® human HMGA2 SMARTpool	Horizon Discovery, Cambridge, UK	J-013495-05-0002
siPML: On-Targetplus® human PML siRNA SMARTpool	Horizon Discovery, Cambridge, UK	L-006547-00-0005

2.4 Molecular biological material

2.4.1 Oligonucleotides

Target gene	Manufacturer	Assay ID
TP53	Thermo Fisher Scientific, Waltham, USA	Hs01034249_m1
TATA-box binding protein	Thermo Fisher Scientific, Waltham, USA	Hs00427620_m1
TNFSF10A	Thermo Fisher Scientific, Waltham, USA	Hs00269492_m1
TNFSF10B	Thermo Fisher Scientific, Waltham, USA	Hs00366278_m1
TNFSF10D	Thermo Fisher Scientific, Waltham, USA	Hs00174664_m1
CDKN1A promoter	Cell Signaling Technology, Danvers, USA	6449
MDM2	Thermo Fisher Scientific, Waltham, USA	Hs01066930_m1
BAX	Thermo Fisher Scientific, Waltham, USA	Hs00180269_m1
CDKN1A	Thermo Fisher Scientific, Waltham, USA	Hs00355782_m1

2.4.2 Antibodies

Isotype controls (Clone)	Host (Isotype)	Manufacturer	Cat. number
Isotype (E5Y6Q)	Mouse (IgG _{2a})	Cell Signaling Technology, Danvers, USA	61656
Isotype-APC (11711)	Mouse (IgG ₁)	R&D Systems GmbH, Wiesbaden, Germany	IC002A
Isotype-APC (13303)	Mouse (IgG _{2B})	R&D Systems GmbH, Wiesbaden, Germany	IC0041A
Primary antibodies (Clone)	Host	Manufacturer	Cat. number
BAX	Mouse	BD Transduction Laboratories, Heidelberg, Germany	610982
HMGA2	Rabbit	Cell Signaling Technology, Danvers, USA	5269S
Lamin A/C	Rabbit	Cell Signaling Technology, Danvers, USA	2032
MDM2 (D1V2Z)	Rabbit	Cell Signaling Technology, Danvers, USA	86934S
MDM2 (SMP14)	Mouse	Santa Cruz Biotechnology, Dallas, USA	sc-965
p21 (Waf1/Cip1)	Rabbit	Cell Signaling Technology, Danvers, USA	2947S
p53 (DO-1)	Mouse	Santa Cruz Biotechnology, Dallas, USA	sc-126
p53 (FL393)	Rabbit	Santa Cruz Biotechnology, Dallas, USA	sc-6243
β-Actin	Mouse	Sigma-Aldrich, St. Louis, USA	A5441
TRAIL	Mouse	R&D Systems, Minneapolis, USA	MAB375-500
TRAIL-R1 Mapatumumab	Human	Human Genome Sciences, Rockville, USA	
TRAIL-R1	Rabbit	Merck Millipore, Burlington, USA	AB16955
TRAIL-R1 (HS101)	Mouse	AdipoGen Life Sciences, San Diego, USA	AG-20B-0022

TRAIL-R2	Rabbit	Cell Signaling Technology, Danvers, USA	3696S
TRAIL-R2	Rabbit	ProScience Incorporated, USA	2019
TRAIL-R2 (HS201)	Mouse	AdipoGen Life Sciences, San Diego, USA	AG-20B-0023
TRAIL-R2 Lexatumumab	Human	Human Genome Sciences, Rockville, USA	
TRAIL-R4 (D13H4)	Rabbit	Cell Signaling Technology, Danvers, USA	8049S
USP10	Rabbit	Cell Signaling Technology, Danvers, USA	5553S
α -Tubulin	Rabbit	Epitomics, California, USA	1878-1
PML	Rabbit	Cell Signaling Technology, Danvers, USA	33156
PML (PG-M3)	Mouse	Santa Cruz Biotechnology, Dallas, USA	sc-966
TRAIL-R1-APC (69036)	Mouse	R&D Systems GmbH, Wiesbaden, Germany	FAB347A
TRAIL-R2-APC (71908)	Mouse	R&D Systems GmbH, Wiesbaden, Germany	FAB6311A
TRAIL-R3-APC (90906)	Mouse	R&D Systems GmbH, Wiesbaden, Germany	FAB6302A
TRAIL-R4-APC (104918)	Mouse	R&D Systems GmbH, Wiesbaden, Germany	FAB633A
Secondary antibodies	Host	Manufacturer	Cat. number
Mouse IgG-AF546	Goat	Life Technologies, California, USA	A11003
Rabbit IgG-AF488	Goat	Life Technologies, California, USA	A11008
Mouse IgG-AF488	Goat	Life Technologies, California, USA	A11001
Human IgG-AF546	Goat	Life Technologies, California, USA	A21089

Rabbit IgG-HRP	Goat	Cell Signaling Technology, Danvers, USA	7074S
Mouse IgG-HRP	Horse	Cell Signaling Technology, Danvers, USA	7076S

2.4.3 Consumables

Consumables	Manufacturer
Cell counting chamber SD100	Nexcelom Bioscience, Lawrence, USA
Cell culture multi-well plates, 6-, 12-, 24-, 96-Well	Sarstedt, Nümbrecht, Germany
Cell scraper	Sarstedt, Nümbrecht, Germany
Combitips advanced, 2.5/ 5/ 10 ml	Eppendorf, Hamburg, Germany
Coverslips	Th. Geyer, Renningen, Germany
Falcon Tube 15/ 50 ml	Sarstedt, Nümbrecht, Germany
Filter tips Biosphere tips 10/ 20/ 100/ 1000 µl	Sarstedt, Nümbrecht, Germany
MicroAmp® Optical Adhesive Film	Thermo Fisher Scientific, Waltham, USA
MicroAmp™ Optical 96-Well Reaction Plate	Thermo Fisher Scientific, Waltham, USA
MicroAmp™ Optical Adhesive Film	Thermo Fisher Scientific, Waltham, USA
Microloader pipette tip	Eppendorf, Hamburg, Germany
Microscope slides, adhesive	Th. Geyer, Renningen, Germany
Microtest plate 96-Well	Sarstedt, Nümbrecht, Germany
Nitril-gloves, Nitratex micro-touch	Ansell, Munich, Germany
Novex WedgeWell 4-20% Tris-Glycine Gels 1 mm x 15 Well	Thermo Fisher Scientific, Waltham, USA
Nunc tube 1.8 ml white	Sarstedt, Nümbrecht, Germany
Parafilm M	Bemis, Neenah, USA
Pasteur pipette	Hecht-Assistant, Sondheim, Germany
Pipette tips 20/200/1000 µl	Sarstedt, Nümbrecht, Germany
PVDF-Membrane, Immobilon-P 0.45 µm	Merck Millipore, Darmstadt, Germany

QIAshredder	QIAGEN, Hilden, Germany
Reaction tube, 0.5/ 1.5/ 2 ml	Sarstedt, Nümbrecht, Germany
RNeasy mini plus kit	QIAGEN, Hilden, Germany
Serological pipette 5/ 10/ 25 ml	Sarstedt, Nümbrecht, Germany
Sterile filter Filtropur 0.2 µm	Sarstedt, Nümbrecht, Germany
Syringe 5/20/50 ml	Becton Dickinson, Franklin Lakes, USA
Tissue culture dish, 150 x 20 mm	Sarstedt, Nümbrecht, Germany
Tissue culture flask 25/75/175 cm ²	Sarstedt, Nümbrecht, Germany
Whatman paper 3 mm	GE Healthcare, Chalfont St Giles, UK
X-ray film CL-X Posure Film 8x10 in.	Thermo Fisher Scientific, Waltham, USA

2.4.4 Kit systems

Kit	Manufacturer	Cat. number
Maxima First Strand cDNA Synthesis Kit for RT-qPCR (ECL)	Thermo Fisher Scientific, Waltham, USA	K1642
Pierce BCA Protein Assay Kit	Thermo Fisher Scientific, Waltham, USA	23225
RNeasy Plus Mini Kit	QIAGEN, Hilden	74134
DC Protein Assay Kit II	Bio-Rad Laboratories, Hercules, USA	5000112
SimpleCHIP® Enzymatic Chromatin IP Kit (Agarose beads)	Cell Signaling Technology, Danvers, USA	9002
Venor GeM Classic Mycoplasma Detection Kit	Minerva Biolabs GmbH, Berlin, Germany	11-1025

2.4.5 Software

Software	Manufacturer
ImageJ	National Institute of Health, US
Mendeley Desktop	Mendeley Ltd, New York, US
Microsoft Office 2016	Microsoft Corporation, Redmond, US
Magellan V6.6	Tecan, Männedorf, Switzerland

AIM	Carl Zeiss, Jena, Germany
LSM Image Browser	Carl Zeiss, Jena, Germany
GraphPad Prism 7.01	GraphPad Software, San Diego, USA
StepOne Software V2.1	Applied Biosystems, Foster City, US
FlowJo v10	FlowJo, LCC, Oregon, US

2.4.6 Laboratory Devices

Centrifuge/ Rotors	Manufacturer
Benchtop centrifuge mini Spin plus, Rotor: F-45-12-11	Eppendorf, Hamburg, Germany
Centrifuge 5415 R	Eppendorf, Hamburg, Germany
Rotina 48R	Hettich, Tuttlingen, Germany
Incubators/ Shaker	Manufacturer
CO ₂ -Inkubator HERAcell 150i	Thermo Fisher Scientific, Waltham, USA
Incubator Typ B 6	Heraeus Instruments, Hanau, Germany
Roller mixer RM5	Glaswarenfabrik Karl Hecht, Sondheim v. d. Rhön, Germany
Shaker DUOMAX 1030	Heidolph Instruments, Schwabach, Germany
Thermomixer compact	Eppendorf, Hamburg, Germany
Shaker DUOMAX 1000	Heidolph Instruments, Schwabach, Germany
Shaker Duomax 1000	Heidolph Instruments, Schwabach, Germany
Measuring devices	Manufacturer
Cell counter Cellometer Auto T4	Nexcelom Bioscience, Lawrence, USA
Microplatereader Sunrise	Tecan Group, Männedorf, Switzerland
Spectrophotometer NanoDrop 2000c	Thermo Scientific, Wilmington, USA
StepOne Plus real time PCR system 7900HT Fast	Applied Biosystems, Foster City, US
X-ray film processor Curix 60	AGFA, Mortsel, Belgium

pH-electrode InoLab pH Level 1	WTW, Weilheim, Germany
Thermo cycler T-Gradient	Biometra GmbH, Göttingen, Germany
Thermo Personal Cycler	Biometra GmbH, Göttingen, Germany
FACS Verse cytometer	Becton Dickinson, Franklin Lakes, US
FACS Calibur	Becton Dickinson, Heidelberg, Germany
Microscopes	Manufacturer
Mikroskope ID 03	Carl Zeiss, Jena, Germany
Zeiss LSM 510	Carl Zeiss, Jena, Germany
Other devices	Manufacturer
Analytical balance BP310S	Satorius, Göttingen, Germany
Autoclave CS-Labor 91782	Webeco, Selmsdorf, Germany
Blotting chamber Mini-PROTEAN 3 Cell	Bio-Rad Laboratories, Hercules, USA
Electrophoresis chamber Novex Mini-Cell + XCell SureLock	Thermo Fisher Scientific, Waltham, USA
Magnetic stirrer MR 3001	Heidolph Instruments, Schwabach, Germany
MILLI-Q Reagent water system	Merck Millipore, Darmstadt, Germany
Sonicator PG1029	MSE Scientific Instruments, London, UK
Autoradiography Cassettes	Amersham plc, Little Chalfont, UK
NALGENE Cryo Freezing Container	NALGENE, New York, US
Forma Scientific -80 °C freezer	Thermo Fisher Scientific, Waltham, USA
Lyophilizer Lyovac GT2	Leybold Heraeus, Köln, Germany
Power supply P25 Standard Power Pack	Biometra, Göttingen, Germany
Horizontal agarose gel electrophoresis chamber	Febikon, Köln, Germany
Liquid nitrogen container Chronos	Messer Griesheim, Bad Soden, Germany
Pipettes	Manufacturer
8-channel-pipette 300µl	Eppendorf, Hamburg, Germany
Pipetus	Hirschmann, Eberstadt, Germany
Eppendorf Research Plus 0.1 - 2.5 µl	Eppendorf, Hamburg, Germany

Eppendorf Research Plus 0.5 - 10 µl	Eppendorf, Hamburg, Germany
Eppendorf Research Plus 2 - 20 µl	Eppendorf, Hamburg, Germany
Eppendorf Research Plus 10 - 100 µl	Eppendorf, Hamburg, Germany
Eppendorf Research Plus 20 - 200 µl	Eppendorf, Hamburg, Germany
Eppendorf Research Plus 100 - 1000 µl	Eppendorf, Hamburg, Germany
Sterile benches	Manufacturer
Laminair HB 2472 K	Heraeus Instruments, Hanau, Germany
HERAsafe HS	Thermo Fisher Scientific, Waltham, USA

3. Methods

3.1 Cell biology methods

3.1.1 Cell culture

A549 and HCT116 cells were cultured in RPMI 1640 medium supplemented with FCS (10 %), Glutamine (2 mM) and sodium pyruvate (1 mM). All cells were mycoplasma-free as determined by Venor GeM Classic Mycoplasma Detection Kit.

Cells were passaged as soon as they reached a confluency of around 80-90 %. For this purpose, old cell culture medium was removed, and cells were washed with warm PBS. To detach cells, preheated Trypsin solution was added following incubation for 5-10 min in the incubator at 37 °C, 5 % CO₂. Cell detachment was verified under the microscope. Trypsin reaction was stopped by adding cell culture medium. Cell suspension was transferred to a 50 ml falcon tube and centrifuged at 400 rcf for 5 min at RT. Finally, supernatant was removed, and the cell pellet was resuspended in pre-warmed cell culture medium. For following experiments cells were counted and the desired number of cells was seeded (section 3.1.2). For further cultivation cells were split in a division rate of 1:3 to 1:5 and seeded in a new cell culture flask. Following this protocol cells were regularly passaged, at least two times a week. In addition, HCT116 cells, which were stable transfected with a short hairpin (sh) RNA vector, were positively selected by adding Puromycin (0.5 µg/ ml) to the cell culture medium. There through solely the cells, that kept the vector and express the Puromycin resistance gene, survived.

3.1.2 Determination of the cell number

The number of living cells, that was utilized for respective experiments, was determined by using the cellometer Auto T4. Therefore, 20 µl cell suspension was added to a hemocytometer and cell number was measured. To receive an accurately cell number, cell counting was repeated at least two times. Technical replicates were excluded from further calculations when cell counts differed by more than 10 % from each other.

3.1.3 Cell stimulation

Before stimulation, cells were seeded in 6 well plates and incubated for 24 h at 37 °C and 5 % CO₂. For treatment of the cells the following reagents and final concentrations were utilized: Cycloheximide (10 µg/ ml), inhibitor of *de novo* protein biosynthesis; MG132 (2 µM), inhibitor of the 26S proteasome; 5-FU (10 µM), chemotherapeutic reagent; Nutlin 3a (5 µM), MDM2 inhibitor; Arsenic trioxide (ATO, 5 µM), PML inhibitor; recombinant human TRAIL (20 ng/ ml);

Mapatumumab (10 µg/ ml), anti-TRAIL-R1 agonistic antibody; Lexatumumab (10 µg/ ml), anti-TRAIL-R2 agonistic antibody. Anti-TRAIL neutralizing antibody (1 µg/ ml) as well as zVAD-fmk (20 µM) were directly added to the cell culture medium during cell seeding.

3.1.4 Long-term storage of cells in liquid nitrogen

Cells were stored for long-terms in 10 % DMSO/ FCS in liquid nitrogen. For this purpose, cells were trypsinized, resuspended in fresh medium and centrifuged at 400 rcf for 5 min. Afterwards cell pellet was resuspended in FCS supplemented with 10 % DMSO. Cell suspension was transferred to cryo vials and stored for at least 24 h in a cryo freezing container at -80 °C. Finally, cryo tubes were transferred to liquid nitrogen.

To take cells in culture, frozen cell aliquots were thawed in 37 °C water bath. Thereafter, cells were resuspended in 10 ml cell culture medium and centrifuged at 400 rcf for 5 min at RT. Supernatant was discarded and cell pellet was resuspended in 15 ml cell culture medium. Cells were transferred to a T75 culture flask and incubated at 37 °C and 5 % CO₂. After 24 h cell culture medium was changed.

3.1.5 Small RNA interference

For transient knockdown of USP10, HMGA2 or PML expression, cells were transfected with On-Targetplus® human USP10, human HMGA2 or human PML specific siRNA using Lipofectamine RNAi/ MAX according to manufacturer's instructions. As a control, On-Targetplus® non-targeting pool was utilized. Knockdown was elevated by western blot 48 h to 72 h after transfection.

3.1.6 Overexpression of TRAIL-R2 isoforms

For transient overexpression of TRAIL-R2, cells were transfected with vectors coding for the long or short TRAIL-R2 isoform using Lipofectamine 2000. Since overexpression of TRAIL-R2 promotes cell death by favoring TRAIL-Rs clustering and DISC formation, both constructs carried a point mutation in the death domain (section 2.3.3). In parallel, cells were transfected with an empty vector (pCR3.1). Overexpression was elevated by western blot and immunofluorescence 24 h to 48 h after transfection.

3.2 Biochemical methods

3.2.1 Preparation of whole cell lysates

To prepare whole cell lysates for western blot analysis, cells were seeded in a 6 well plates for at least 24 h. Before harvesting, cells were washed with cold PBS on ice. Depending on the cell confluence, 100-200 μ l RIPA buffer was added to lyse the cells. Cell lysates were frozen for at least 20 min at -80 °C. Afterwards, samples were thawed on ice, lysates were removed using a cell scraper and transferred to a 1.5 ml reaction tube. Samples were sonicated three times for 10 sec. with 10 sec. cooling on ice in between. Finally, Lysates were centrifuged at 16.100 rcf for 15 min at 4 °C and supernatants were transferred to a fresh tube. Protein concentration was estimated using Pierce™ BCA Protein Assay Kit.

3.2.2 Preparation of whole cell lysates for immunoprecipitation

To prepare whole cell lysates for immunoprecipitations at least one T175 flask with a cell confluency of around 80 % was utilized. Cells were washed with cold PBS on ice and lysed in 4 ml IP-lysis buffer per T175 flask. Using a cell scraper, cells were detached and transferred to a 2 ml reaction tube. After incubation on ice for 20 min, samples were centrifuged at 16.100 rcf for 30 min at 4 °C. Supernatants were transferred to a fresh tube and protein concentrations were determined by DC Protein Assay Kit II.

3.2.3 Preparation of nuclear fractions for immunoprecipitation

To prepare nuclear fractions for immunoprecipitation at least one 15 cm cell culture dish with a cell confluency of around 80 % was utilized. Cells were washed with ice cold PBS, lysed with 4 ml hypotonic buffer and transferred to 1.5 ml Eppendorf tubes. Samples were centrifuged at 15.700 rcf for 6 min at 4 °C. Supernatant representing the cytosolic fraction was transferred to a fresh tube and centrifuged again at 15.700 rcf for 30 min at 4 °C. Nuclei pellet was washed three times with hypotonic buffer and nuclei were lysed in 1 ml nuclear lysis buffer afterwards. To break the nuclei a syringe was utilized. Finally, samples were centrifuged at maximum speed for 30 min at 4 °C. Supernatant represents the nuclear fraction. Protein concentration was determined by DC Protein Assay Kit II.

3.2.4 Preparation of cytosolic, nuclear and chromatin fractions

Cells were seeded 24 h before preparation. At least one 15 cm cell cultures dish was utilized per fractionation. For cell fractionation, cells were washed with ice cold PBS, lysed and in 800 μ l buffer A. Cells were removed from the plate with a cell scraper, transferred to a 1.5 ml reaction tube and incubated for 10 min on ice. Afterwards, samples were centrifuged at 1.300 rcf for 4 min at 4 °C. Supernatants, representing the cytosolic fraction, were transferred

to fresh tubes, and were centrifuged again at maximum speed for 15 min at 4 °C to remove cell debris. Nuclei were washed three times with 500 µl buffer A. Thereafter, nuclei were lysed in 200 µl buffer B and incubated on ice for 30 min while occasional vortexing. Afterwards, samples were centrifuged at 1.700 rcf for 5 min at 4 °C. Supernatants, representing the soluble nuclear fraction were transferred to fresh tubes, and centrifuged again at maximum speed for 5 min at 4°C to remove cells debris. Cell pellets were washed three times with 200 µl buffer B. Finally, chromatin pellets were resuspended in 200 µl buffer B, sonicated three times for 20 sec and were centrifuged at maximum speed for 5 min at 4 °C afterwards. Protein concentrations were determined by Bio-Rad Protein Assay Dye (cytosolic fraction) or DC Protein Assay Kit II (nuclear fraction, chromatin fraction).

3.2.5 Protein quantification using Bicinchoninic acid assay

To determine the protein concentration of RIPA-lysates the Pierce™ BCA Protein Assay Kit was utilized. The method is based on two reactions. 1. Peptides containing three or more amino acid residues form a colored complex with Cu^{2+} ions, which are thereby reduced to Cu^+ . 2. Two BCA molecules form a purple-colored complex with the Cu^+ ion produced in the first step. This complex absorbs light at a wavelength of 562 nm. The color intensity is proportional to peptide bonds participating in the reaction [133]. To perform protein determination, RIPA-lysates were diluted 1:10 and a protein standard curve with a range of 1 mg to 15.63 µg with BSA was prepared. Samples were transferred to a 96-Well plate and BCA buffers were added corresponding to manufacturer's protocol. The 96-Well plate was incubated for 40 min at 37 °C. Thereafter, the absorbance of light at a wavelength of 562 nm was measured using the microplate reader Sunrise.

3.2.6 Protein quantification using Lowry assay

To determine the protein concentration of whole cell lysates for IP, cytosolic, nuclear and chromatin fractions the DC (detergent compatible) Protein Assay Kit II was utilized. This colorimetric assay is based on a reduction of Cu^{2+} ions to Cu^+ ions in the presence of peptide bonds and an alkaline pH value. Thereafter, the Cu^+ ions participate in a colorimetric reaction by reducing yellow Folin–Ciocalteu reagent to Molybdenum blue [134]. To perform protein determination, lysates were diluted 1:3 and a protein standard curve with a range of 2 mg to 0.125 µg with BSA was prepared. Samples were transferred to a 96-Well plate and DC buffers were added corresponding to manufacturer's protocol. The 96-Well plate was incubated for 15 min at RT and the absorbance of light at a wavelength of 700 nm was measured using the microplate reader Sunrise.

3.2.7 Protein quantification using Bradford assay

To determine the concentration of cytosolic fractions the Bio-Rad Protein Assay Dye was utilized. The assay is based on the method of Bradford using the properties of Coomassie Brilliant Blue G-250 dye that absorbance maximum shifts from 465 nm to 595 nm when binding to protein occurs. The Coomassie blue dye binds to primarily basic and aromatic amino acid residues, especially arginine [135]. To perform protein determination, cytosolic fractions were diluted 1:3 and a protein standard curve with a range of 1 mg to 15.63 µg with BSA was prepared. Samples were transferred to a 96-Well plate, Bio-Rad protein assay dye was added corresponding to manufacturer's instructions and the 96-Well plate was incubated for 5 min at RT. Thereafter, the absorbance of light at a wavelength of 595 nm was measured using the microplate reader Sunrise.

3.2.8 SDS-Polyacrylamide-gel electrophoresis (SDS-PAGE)

Protein samples were separated and analyzed using the discontinuous electrophoretic system with Tris-Glycine buffers [136]. Gradient gels with a polyacrylamide concentration of 4-20 % were utilized. The protein samples were mixed with Laemmli loading buffer and boiled for 5 min at 95 °C. The electrophoresis was carried out in a vertical chamber system with Laemmli running buffer at 125 V.

3.2.9 Western blotting

During western blot, electrophoretically separated proteins are transferred to a polyvinylidene difluoride (PVDF) membrane [137]. In this work a wet tank blotting system was applied to transfer proteins from SDS gels to PVDF membranes. For this purpose, the holder cassette facing the negative pole was equipped with one foam pad and one filter paper pre-soaked in transfer buffer. The SDS gel was placed thereon, following the PVDF membrane, which was pre-equilibrated in Methanol. Finally, one more wet filter paper and foam pad was placed. Proteins were transferred at 400 mA for 70-90 min on ice. Thereafter, the membrane was washed with ddH₂O, incubated in Methanol for 30 sec. and dried for 20 min at RT. After drying, the membrane was reactivated in Methanol and was incubated for 1 h in 5 % BSA/ TBS-T (w/ v) or 5 % milk/ TBS-T (w/ v) while shaking to block non-specific binding sites. Afterwards, the membrane was incubated with the primary antibody overnight at 4 °C. After washing three times for 10 minutes in TBS-T buffer, the membrane was incubated with a horseradish peroxidase (HRP)-coupled secondary antibody for 1 h at room temperature. Following washing, three times 10 min in TBS-T buffer, the HRP conjugate was detected on the membrane using ECL detection solution (enhanced chemiluminescence system) and Developer G153. Densitometric analysis of band intensities were evaluated using ImageJ [138].

3.2.10 Cell cycle analysis by propidium iodide (PI) staining

Cells were seeded in 6 well plates (1.5×10^5 / well) and grown for 48 h. Cell cycle analysis was performed using propidium iodide staining followed by flow cytometry analysis. Briefly, cells were collected (10 min, 300 rcf, 4°C), washed twice in cold PBS containing 5 mM EDTA (PBSE) and resuspended in 500 µl PBSE. For fixation 500 µl cold Ethanol was added dropwise and incubated for 30 min at RT. Fixed cells were collected by centrifugation and resuspended in 500 µl PBSE. Cells were treated with 20 µg RNase A for 30 min at RT and stained with propidium iodide (PI) by adding 500 µl of a 200 mg/ ml PI-stock solution. Samples were stored at 4°C in the dark until counting using a FACS Verse cytometer.

3.2.11 DNA-fragmentation assay

HCT116 and A549 cells were seeded in 6 well plates (2×10^5 / well) grown for 24 h and stimulated with TRAIL or agonistic anti-TRAIL-R1- (Mapatumumab) or anti-TRAIL-R2 (Lexatumumab) antibodies for 24 h. DNA fragmentation was measured using propidium iodide staining followed by flow cytometry analysis. Briefly, cells and supernatants were collected (10 min, 300 rcf, 4°C), washed with PBS and fixed in 50% Ethanol/ PBS for 30 min at 4°C. Cells were treated with 14 µg/ ml RNase for 30 min at RT and stained with 250 µg/ ml PI/ PBS afterwards. Samples were measured within 1 h using a FACS Calibur. A population size of 30.000 cells was regarded as representative for data evaluation using FlowJo v10.

3.3 Immunological methods

3.3.1 Immunofluorescence

For immunofluorescence stainings cells were seeded, at least for 24 h on cover slips. Cells were washed twice with ice cold TBS on ice and fixed with ice cold 2.5 % PFA/ TBS (w/ v) for 10 min. After washing with TBS, cells were incubated in 100 % methanol for 10 min at -20°C for cell permeabilization. Afterwards, cells were washed again with TBS and unspecific binding sites were blocked with 0.5 % BSA/ TBS (w/ v) for 15 min at RT. Thereafter, cells were incubated with primary antibodies diluted in 0.5 % BSA/ TBS (w/ v) overnight at 4 °C. Subsequently, cells were washed three times with TBS for 5 min on the shaker, following incubation with secondary fluorochrome-labelled antibodies and Hoechst 33342 for 1 h at RT in the dark. Finally, cells were washed three times with TBS and one time with ddH₂O and cover slips were mounted on glass slides using IS Mounting Medium. Confocal LSM was performed using a Zeiss LSM 510.

3.3.2 Flow cytometric analyses of cell surface expression of TRAIL receptors

Cell surface expression levels of TRAIL-Rs were analyzed by flow cytometry. Briefly, cells were detached from culture dishes by treatment with Accutase. Afterwards, cells were washed with cold MACS buffer and FcR-blocking was performed with human FcR blocking reagent according to the manufacturer's instructions. For single stainings of TRAIL-Rs, 2×10^5 cells were incubated for 30 min at 4 °C with APC-conjugated TRAIL-R1, TRAIL-R2, TRAIL-R3 or TRAIL-R4 antibodies. Respective isotype control stainings were performed with APC-conjugated mouse IgG₁ and mouse IgG_{2B} antibodies. Finally, cells were washed twice in cold MACS buffer, resuspended in cold MACS buffer supplemented with 1% PFA and measured within 24 h using a FACSCalibur. A population size of 30,000 cells was regarded as representative for data evaluation using FlowJo v10.

3.3.3 Immunoprecipitation analysis of whole cell lysates

For immunoprecipitation analysis of whole cell lysates 1 mg protein was utilized. To reduce unspecific binding to Protein G Sepharose beads, samples were pre-cleared by incubation with 40 µl beads for 1 h at 4 °C. Afterwards samples were centrifuged for 30 sec. at 3000 rcf, supernatants were transferred to fresh tubes and were used for immunoprecipitation. Lysates were incubated with 10 µg antibody at 4 °C overnight. As a control, samples containing buffer and antibodies were prepared in parallel. On the following day, samples were incubated for 3 h with 40 µl Protein G Sepharose beads. Afterwards, samples were centrifuged for 30 sec. at 3000 rcf and supernatants, representing post-IP samples, were transferred to fresh tubes and stored at -20 °C till further analysis. Bead-antibody-protein complexes were washed five times with IP-Lysis buffer. Finally, antibody-protein complexes were eluted from the beads by Laemmli buffer and boiled for 10 min at 80 °C. IP samples were analyzed by western blotting.

3.3.4 Immunoprecipitation analysis of nuclear fractions

For immunoprecipitation analysis of nuclear fractions 1 mg protein was utilized. Lysates were incubated with 5 µg antibody overnight at 4 °C. As controls, samples containing buffer and antibody or lysate without antibody, were prepared in parallel. On the following day, 25 µl Pierce Protein A/ G Magnetic beads were added to the samples and incubated for 1 h at 4 °C. Afterwards, the bead-antibody-protein complexes were separated from solution by a magnetic rack. Supernatants, containing post-IP samples, were transferred to a fresh tube and stored at -20 °C till further analysis. Beads were washed five times with nuclear-lysis buffer. 40 µl 4x Laemmli buffer and 60 µl nuclear-lysis buffer was added and samples were incubated for 10 min at RT to elute antibody-protein complexes. Finally, the supernatants, containing antibody-protein complexes, was separated from the beads and boiled for 10 min at 95 °C. IP samples were analyzed by western blotting.

3.3.5 Chromatin immunoprecipitation

The chromatin immunoprecipitation (ChIP) assay is a powerful and versatile technique applied to investigate protein-DNA interactions within the natural chromatin context of the cell [139,140]. This assay was used to determine the recruitment of p53 protein to the *CDKN1A* gene promoter. Therefore, 8×10^6 cells were seeded in a 15 cm cell culture dish and were incubated for 24 h at 37 °C and 5 % CO₂. To crosslink proteins to DNA 540 µl of 37 % Formaldehyde solution was added to each cell culture dish containing 20 ml medium. For the following steps, the SimpleChIP® Enzymatic Chromatin IP Kit was used according to manufacturer's instructions. The amount of extracted DNA was quantified via qPCR using Maxima SYBR Green/ ROX master mix and a 7900HT Fast RT-PCR according to manufacturer's instructions. qPCR was performed with a specified amount of ChIP sample per reaction and primers that detect the *CDKN1A* promoter (Table 1). The thermal cycling conditions are listed in Table 2. Enrichment was determined as the fold increase in specific signal relative to the background signal.

Table 1: Master Mix composition per sample for qPCR from ChIP DNA templates.

Component	Volume (µl) per reaction
Nuclease-free H ₂ O	6
Maxima SYBR-Green Reaction Mix (2X)	10
Primers	2
DNA template	2
Total volume	20

Table 2: Thermal cycling conditions for qPCR reaction using SYBR Green.

	Temperature, °C	Time	Number of cycles
Initial denaturation	95	10 min	1
Denaturation	95	15 sec	35
Annealing/Extension	65	60 sec	

3.4 Molecular biology methods

3.4.1 Preparation and quantification of RNA

Cells were harvested, homogenized by QIAshredder and total RNA was isolated using RNeasy Plus Mini Kit according to manufacturer's instructions. RNA concentration was determined using NanoDrop™ 2000/ 2000c spectrophotometer. RNA samples were stored at -80 °C.

3.4.2 Complementary DNA synthesis

Complementary DNA (cDNA) was synthesized from isolated total RNA using the Maxima First Strand cDNA Synthesis Kit according to manufacturer's instructions. cDNA samples were stored at -80 °C.

3.4.3 Quantitative real-time polymerase chain reaction

Quantitative real-time polymerase chain reaction (qPCR) is a powerful and sensitive gene analysis techniques that is utilized for a broad range of applications including quantitative gene expression analysis, genotyping, pathogen detection and measuring RNA interference. In contrast to traditional PCR, qPCR allows to determine the starting concentration of nucleic acid. Every qPCR reaction contains a fluorescent reporter molecule to monitor the accumulation of the PCR product. In relation to the quantity of target amplicon, the amount of fluorescence emitted from the fluorophore increases.

For relative quantification of TRAIL-R1, TRAIL-R2, TRAIL-R4, p53, p21, BAX and MDM2 expression qPCR was performed using TaqMan assays. For this purpose, 9 µl containing 50 ng synthesized cDNA (section 3.4.2) was pipetted into a 96 well PCR plate. Afterwards 11 µl of the respective TaqMan master mix was added (Table 3). Each sample was analyzed in technical triplicates to detect pipetting inaccuracies. The plate was covered with a MicroAmp Optical Adhesive Film and centrifuged at 300 rcf for 5 min to spin down the contents and eliminate air bubbles from the solution. Template amplification and fluorescence measurement was carried out with the 7900HT Fast RT-PCR system and the thermal cycling conditions listed in Table 4. The expression levels were calculated relative to the expression of the housekeeping gene TATA-binding protein (TBP) by $\Delta\Delta\text{CT}$ method. Therefore, the cycle threshold (Ct) was determined and mean Ct-values of technical triplicates were calculated. To exclude variances, Ct-values that differed not more than ± 0.5 from each other were considered only. Finally, gene of interest Ct-values were normalized to respective Ct-values of the housekeeping gene.

Table 3: Master Mix composition per sample for qPCR from cDNA templates.

Component	Volume (μ l) per reaction	Final conc.
TaqMan® Universal PCR Master Mix (2X)	10	1x
TaqMan® Gene Expression Assay (20X)	1	1x
cDNA template + H ₂ O	9	50 ng
Total volume	20	-

Table 4: Thermal cycling conditions for qPCR using TaqMan assays.

Step	Temperature, °C	Time	Number of cycles
Initial denaturation	95	10 min	1
Denaturation	95	15 sec	40
Annealing/Extension	60	60 sec	

3.5 Statistical analysis

Statistical analyses were performed using GraphPad Prism 7.01. Data were tested for normality and equal variance by Shapiro-Wilk and Equal Variance test, respectively. For comparison of two-groups comprising parametric distributed datasets, t-test was applied. Two groups of non-parametric datasets were analyzed with Mann-Whitney Rank Sum test. Statistically significant differences between the groups were assumed at p-values < 0.05 and marked with an asterisk (*).

4. Results

4.1 Determination of TRAIL-receptor levels in A549 and HCT116 wild type and TRAIL-R2 silenced cells

For analyses of the interdependence between TRAIL-R2 and tumor suppressor protein p53 human HCT116 colorectal carcinoma cells and human A549 lung adenocarcinoma cells were utilized. Both cell lines were characterized in detail at the beginning of this study [141]. It could be shown that they express all TRAIL receptors, harbor wild type (WT) p53 and are sensitive to TRAIL-R-mediated cell death induced by TRAIL or TRAIL R1/ R2 agonistic antibodies (see Suppl. Fig. 1 and [141]).

In order to investigate the impact of TRAIL-R2 on p53, HCT116 cells were stable transduced with either a GIPZ lentiviral short hairpin (sh) RNA vector targeting TRAIL-R2 (sh TR2) or a vector encoding a non-silencing RNA sequence (sh ns) as respective control. In addition, A549 TRAIL-R2 knockout cells were generated via clustered regularly interspaced short palindromic repeats (CRISPR)-Cas-9 technology (Thorsten Hartwig). In order to validate the stable knockout/ knockdown of TRAIL-R2 expression in A549 and HCT116 cells and examine effects on TRAIL-R1 and TRAIL-R4 levels, whole cell lysates were analyzed by western blotting and mRNA levels were evaluated by qPCR (Fig. 7). Western blot results validated a total knockout (KO) of TRAIL-R2 in A549 cells. Coincidentally, the protein level of TRAIL-R1 was slightly decreased, while the protein level of TRAIL-R4 was elevated in TRAIL-R2 KO cells compared to WT cells (Fig. 7A). On mRNA level TRAIL-R2 was significantly downregulated by around 47 %. In line with western blotting results, TRAIL-R1 mRNA level was decreased by around 13 % while TRAIL-R4 mRNA level was increased by 60 % in comparison to WT cells (Fig. 7B). HCT116 cells showed a marked downregulation of TRAIL-R2 in knockdown cells compared to control cells. In contrast to A549 cells, the levels of TRAIL-R1 and TRAIL-R4 were not altered on protein level in HCT116 TRAIL-R2 knockdown cells (Fig. 7C). On mRNA level, TRAIL-R2 expression was significantly decreased by 70 % in HCT116 sh TRAIL-R2 cells in comparison to control cells. Notably, similar mRNA levels of TRAIL-R1 were detected in both clones, while the level of TRAIL-R4 was slightly decreased in HCT116 sh TRAIL-R2 cells compared to control cells (Fig. 7D).

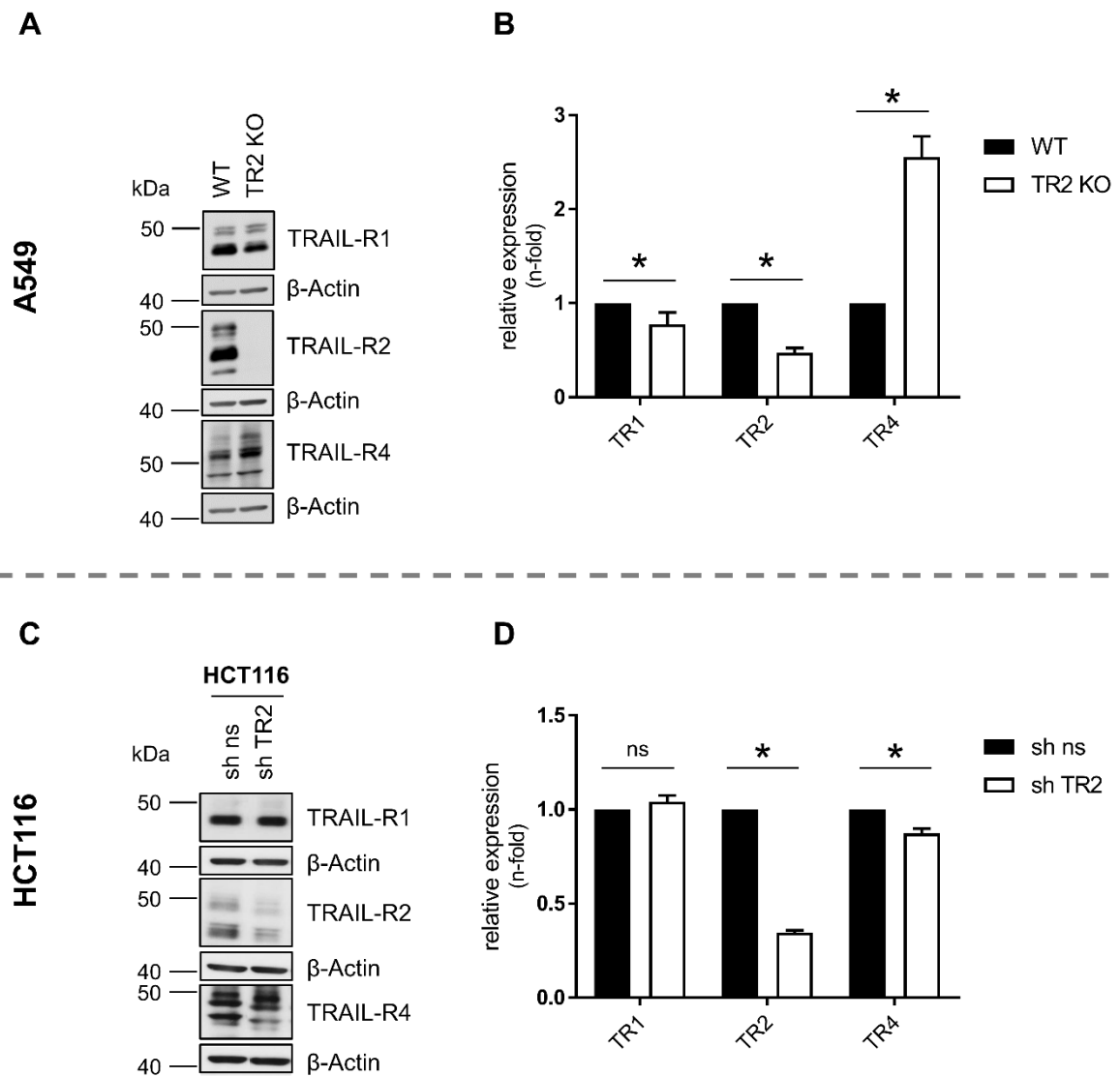


Figure 7: Determination of TRAIL-R levels in A549 and HCT116 wild type and TRAIL-R2 silenced cells.

Whole cell lysates from **(A)** A549 WT and TRAIL-R2 KO and **(C)** HCT116 sh ns and sh TRAIL-R2 were analyzed by western blotting for the protein levels of TRAIL-R1, TRAIL-R2 and TRAIL-R4. β -Actin was analyzed as loading control. **(B, D)** Relative expression of TRAIL-R1, TRAIL-R2 and TRAIL-R4 (normalized to TBP) was analyzed by qPCR in **(B)** A549 WT and TRAIL-R2 KO and **(D)** HCT116 sh ns and sh TRAIL-R2 cells. Bar charts show mean values \pm SD of three independent experiments. TR2 KO, TRAIL-R2 knockout; WT, wild type; sh ns, short hairpin RNA non-silencing; sh TR2, short hairpin RNA TRAIL-R2; TR1, TRAIL-R1; TR2, TRAIL-R2; TR4, TRAIL-R4. * $p < 0.05$

4.2 Activation of p53 upregulates TRAIL-R2 in A549 cells

TRAIL-R2 is a known transcriptional target of p53 [75,128]. In order to confirm this relationship between TRAIL-R2 expression and p53 activation, A549 WT cells were treated with the chemotherapeutic agent 5-Fluorouracil (5-FU). Afterwards, whole cell lysates and nuclear fractions were analyzed by western blotting for the levels of p53 and TRAIL-R2. As shown in Fig. 8, 5-FU led to a strong upregulation of p53 levels. Simultaneously, TRAIL-R2 was upregulated in whole cell lysates, as well as in the nuclear fraction (Fig. 8A, B).

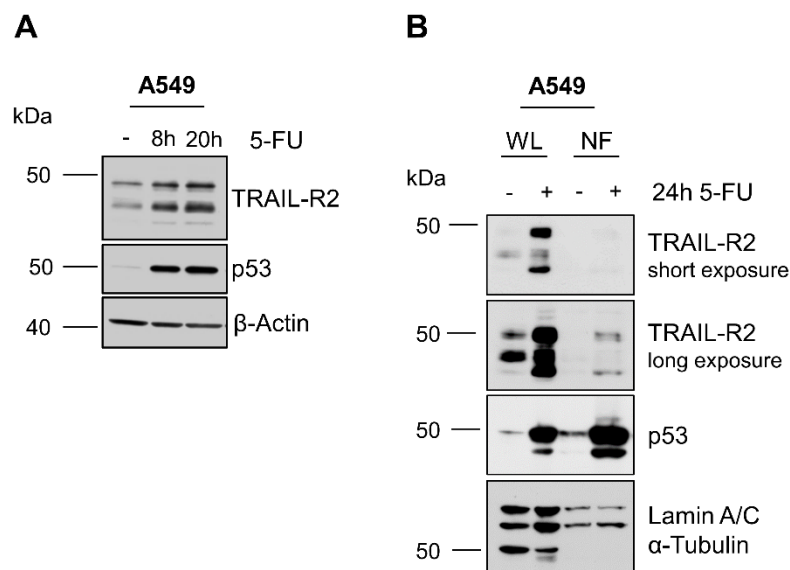


Figure 8: 5-FU treatment leads to increased p53 and TRAIL-R2 protein levels.

A549 cells were treated with 5-FU (10 μ M) for the indicated time periods. Whole cell lysates (**A, B**) and nuclear fractions (**B**) were analyzed by western blotting for the expression of TRAIL-R2 and p53. The levels of β -Actin, α -Tubulin and Lamin A/C were determined as loading and fractionation control. Exposure = decreased/ increased time of light exposure for signal detection. WL, whole cell lysate; NF, nuclear fraction; 5-FU, 5-Fluorouracil.

4.3 TRAIL-R2 interacts with p53

Since both, TRAIL-R2 and p53 are present in the nucleus and each of them has been demonstrated to interact with chromatin and with the microprocessor complex, next it was investigated whether both proteins may interact with each other within the nuclear compartment. For this reason, first the intracellular distribution of TRAIL-R2 and p53 in wild type p53 expressing A549 cells was studied by indirect immunofluorescence staining followed by confocal laser scanning microscopy (LSM) (Fig. 9A). Two different sets of TRAIL-R2 (HS201, Lexa – Lexatumumab) and p53 (FL393, Do-1) specific antibodies were utilized. Immunofluorescence stainings demonstrated a high abundance of both proteins in the cell nucleus as well as TRAIL-R2 and p53 co-localization (Fig. 9A).

In order to further investigate the potential protein-protein interaction of TRAIL-R2 and p53,

both proteins were immunoprecipitated from nuclear extracts of A549 WT and TRAIL-R2 KO cells and protein complexes were analyzed by western blotting (Fig. 9B). As shown in Figure 7, TRAIL-R2 was not detectable in nuclear fractions of A549 TRAIL-R2 KO cells but in A549 WT cells (lane 1 vs. lane 2). Consistently, TRAIL-R2 was only precipitated from nuclear fractions of A549 WT cells (lane 3). A co-precipitation of p53 with TRAIL-R2 was not detected. Interestingly, the protein level of p53 was slightly increased in nuclear fractions of TRAIL-R2 KO cells in comparison to WT cells (lane 1 vs. lane 2). In line with that a higher amount of p53 protein could be precipitated with p53 specific antibody in A549 TRAIL-R2 KO cells compared to control cells (lane 6 vs. lane 7). Of note, the small TRAIL-R2 isoform (around 40 kDa) co-precipitated with p53 from nuclear preparations of A549 WT cells, whereas no band appeared in related samples from TRAIL-R2 KO cells (lane 6 vs. lane 7).

Taken together these results suggest that TRAIL-R2 co-localizes and interacts with p53 in the nucleus in A549 cells.

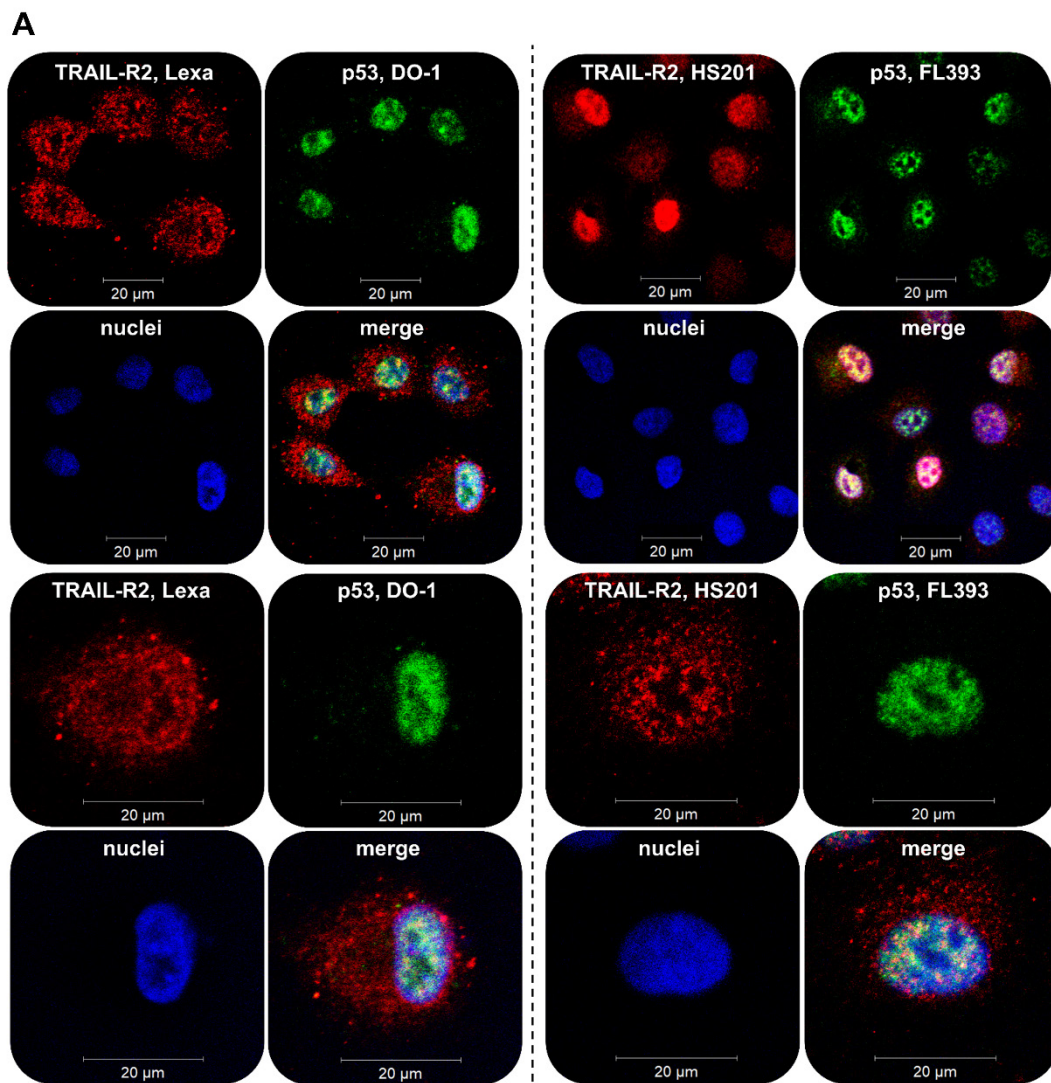


(Figure 9 continued next page)

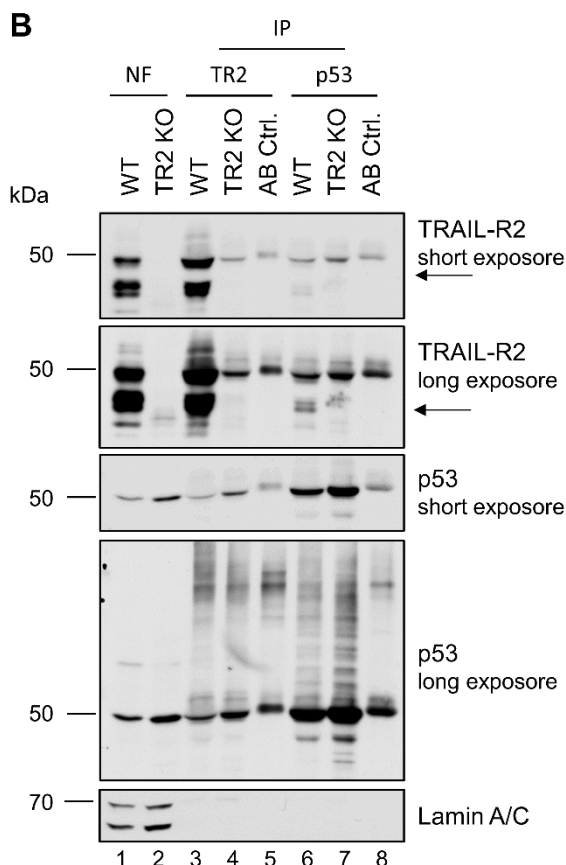


Figure 9: TRAIL-R2 co-localizes and interacts with p53 in the nucleus of A549 cells.

(A) Intracellular distribution of TRAIL-R2 and p53 in A549 cells was analyzed by indirect immunofluorescence following confocal laser scanning microscopy using different TRAIL-R2 (Lexa – Lexatumumab, HS201) or p53 (DO-1, FL393) specific antibodies. Nuclei were stained by Hoechst. (B) TRAIL-R2 and p53 were precipitated from nuclear fractions of A549 WT and TRAIL-R2 KO cells by specific antibodies (TRAIL-R2, HS201; p53, DO-1). Protein complexes were examined by western blotting. As a control antibodies and beads without lysate were analyzed in parallel. The level of Lamin A/C was determined as loading and fractionation control. Exposure = decreased/increased time of light exposure for signal detection. IP, immunoprecipitation; NF, nuclear fraction; AB ctrl., antibody control; TR2 KO, TRAIL-R2 knockout; WT, wild type.

4.4 Impact of TRAIL-R2 status on p53 and its targets

4.4.1 Silencing TRAIL-R2 increases the cellular level of p53 and the expression of its transcriptional targets

Activation of wild type p53 by chemotherapeutic agents enhances both the amount of TRAIL-R2 on the plasma membrane as well as its presence in the nucleus [75,126] (Fig. 8). The results shown in Fig. 9B suggested that knockout of TRAIL-R2 could affect the cellular levels of p53. In order to proof this observation protein levels of p53 and its targets p21, MDM2 and BAX were analyzed in A549 and HCT116 control and TRAIL-R2 knockout/ knockdown cells by western blotting (Fig. 10A, B). Analysis of p53 protein level and p53 targets showed indeed an increased level of p53 itself, and also of p21, BAX and MDM2 in TRAIL-R2 silenced

cells in comparison to respective control cells (Fig. 10A, B). Importantly, consistent with the role of p53 as a transcriptional regulator of p21, BAX and MDM2 expression, the enhanced p53 levels observed in TRAIL-R2 knockout cells correlated with significantly increased mRNA levels of p21, BAX and MDM2 analyzed in A549 cells by qPCR (Fig. 10C). Since p21 is the most prominent target gene of p53, the recruitment of p53 to the p21 promotor was analyzed by chromatin immunoprecipitation (ChIP) of p53 followed by detection of the p21 promotor (*CDKN1A*) via qPCR in A549 cells (Fig. 10D). ChIP results showed a markedly increased enrichment of co-precipitated p21 promotor in A549 TRAIL-R2 KO cells (24.3 \pm 3.3) in comparison to WT cells (13.1 \pm 7.1) (Fig. 10D). As a control, chromatin fractions were analyzed in parallel by western blotting (Fig. 10D). In agreement with data shown in Fig. 9B and 10A the protein level of p53 was enhanced in TRAIL-R2 KO cells in comparison to WT cells. In accordance with the known function of p21 as an inhibitor of the cell cycle progression, knockout of TRAIL-R2 in A549 cells led to G1-phase arrest (Fig. 10E).

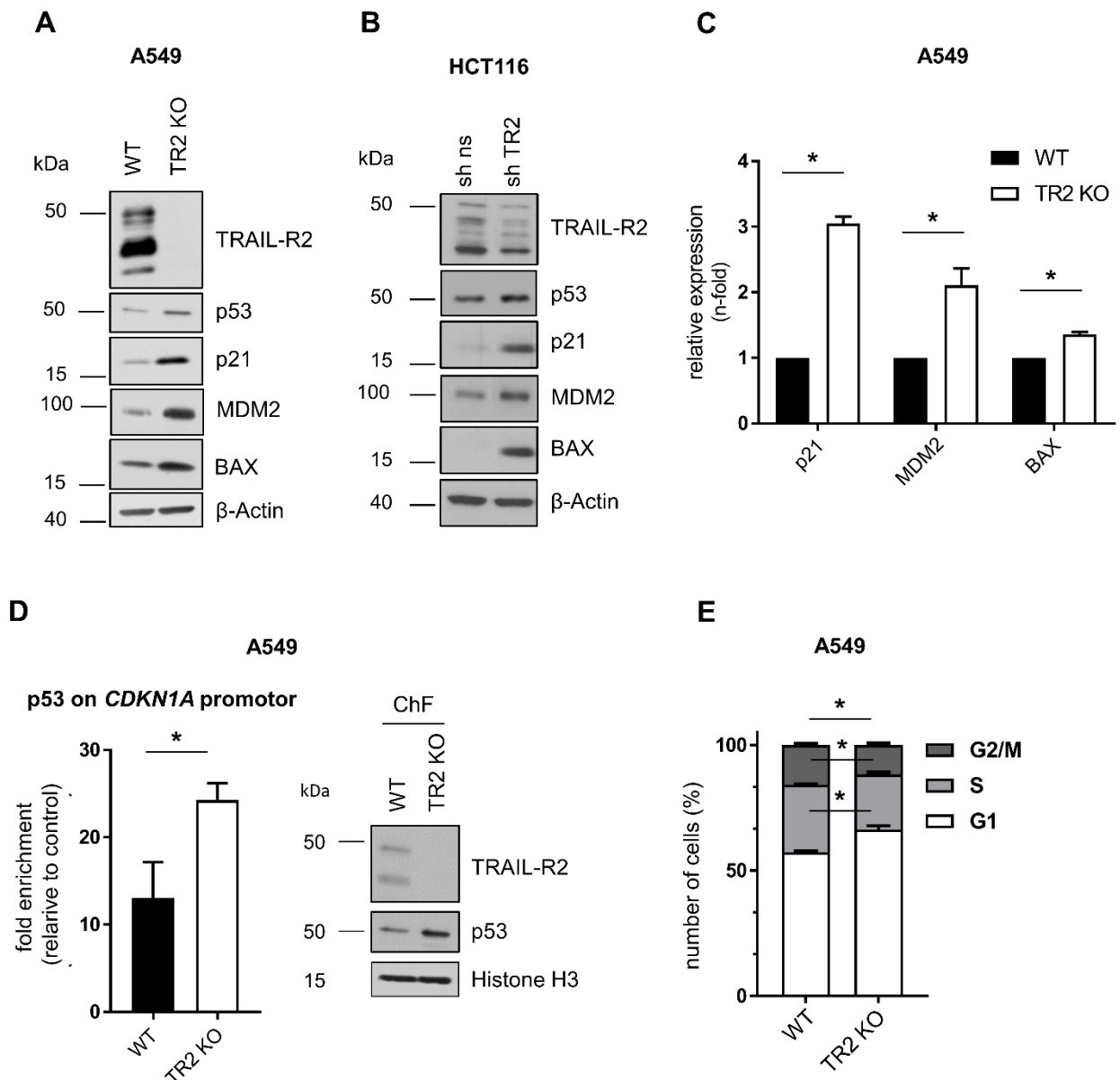


Figure 10: TRAIL-R2 affects the expression of p53 and its targets.

Whole cell lysates of **(A)** A549 WT and TRAIL-R2 KO cells or **(B)** HCT116 sh ns and sh TRAIL-R2 cells were analyzed by western blotting for the protein levels of TRAIL-R2, p53, MDM2, BAX and p21. β -Actin was detected as loading control. **(C)** Relative expression of MDM2, BAX and p21 levels (normalized to TBP) were analyzed in A549 cells by qPCR. Bar chart shows mean values \pm SD of three biological replicates (n=3). **(D)** ChIP was performed with anti-p53 (DO-1) and isotype control antibodies on chromatin preparations harvested from A549 WT and TRAIL-R2 KO cells. The DNA was extracted and qPCR was performed for detection of the *CDKN1A* promotor. Enrichment was determined as the fold increase in specific signal relative to the background signal. Bar chart shows mean values \pm SEM of four biological replicates (n=4). As a control chromatin fractions (ChF) were analyzed for the protein levels of TRAIL-R2 and p53 by western blotting. Histone H3 was determined in parallel as loading control. **(E)** Cell cycle analysis through PI staining followed by flow cytometry of A549 WT and TRAIL-R2 KO cells. Bar chart shows mean values \pm SD of three biological replicates (n=3). ChIP, chromatin immunoprecipitation; TR2 KO, TRAIL-R2 knockout; sh ns, short hairpin RNA non-silencing; sh TR2, short hairpin RNA TRAIL-R2; WT, wild type; qPCR, quantitative real time PCR; PI, propidium iodide. * p<0.05

4.4.2 Overexpression of TRAIL-R2 decreases the cellular p53 level

Since previous results revealed that TRAIL-R2 knockout/ knockdown leads to an upregulation of p53 protein which was accompanied by elevated levels of the p53 targets p21, MDM2 and BAX, next it was investigated whether this effect indeed depends on TRAIL-R2. In order to test this issue A549 cells were transiently transfected with expression vectors coding for the long (TRAIL-R2-long) or short (TRAIL-R2-short) isoform of TRAIL-R2. Since overexpression of TRAIL-Rs promote cell death by favoring TRAIL-Rs clustering leading to DISC formation, both constructs carried a point mutation in the death domain [29]. In parallel, cells were transfected with an empty vector (pCR3.1) as a control. First, the expression and translocation of overexpressed TRAIL-R2-long and short isoforms to the nucleus was verified by immunofluorescence analysis. As shown in Fig. 11A, both TRAIL-R2 isoforms were strongly expressed at the plasma membrane, in the cytosol and nucleus of A549 WT as well as TRAIL-R2 KO cells. In addition, overexpression levels of both TRAIL-R2 isoforms were confirmed by western blotting (Fig. 11B). Both TRAIL-R2 isoforms were strongly expressed and showed specific bands at around 40 kDa and 50 kDa. Moreover, multiple high molecular weight bands between 100 kDa to 260 kDa appeared in TRAIL-R2 overexpression samples, suggesting that both TRAIL-R2 isoforms are present in numerous protein complexes. Furthermore, western blot results validated the previously identified increased p53 protein level in A549 TRAIL-R2 KO cells in comparison to WT cells after transfection with the vector control. Interestingly, overexpression of both TRAIL-R2 isoforms in A549 WT cells and, even more important in TRAIL-R2 KO cells, reduced the protein level of p53 in comparison to respective controls (Fig. 11B). Additionally, markedly decreased protein levels of p53 targets MDM2 and p21 were detected in TRAIL-R2 KO cells overexpressing either TRAIL-R2 isoform (Fig. 11B).

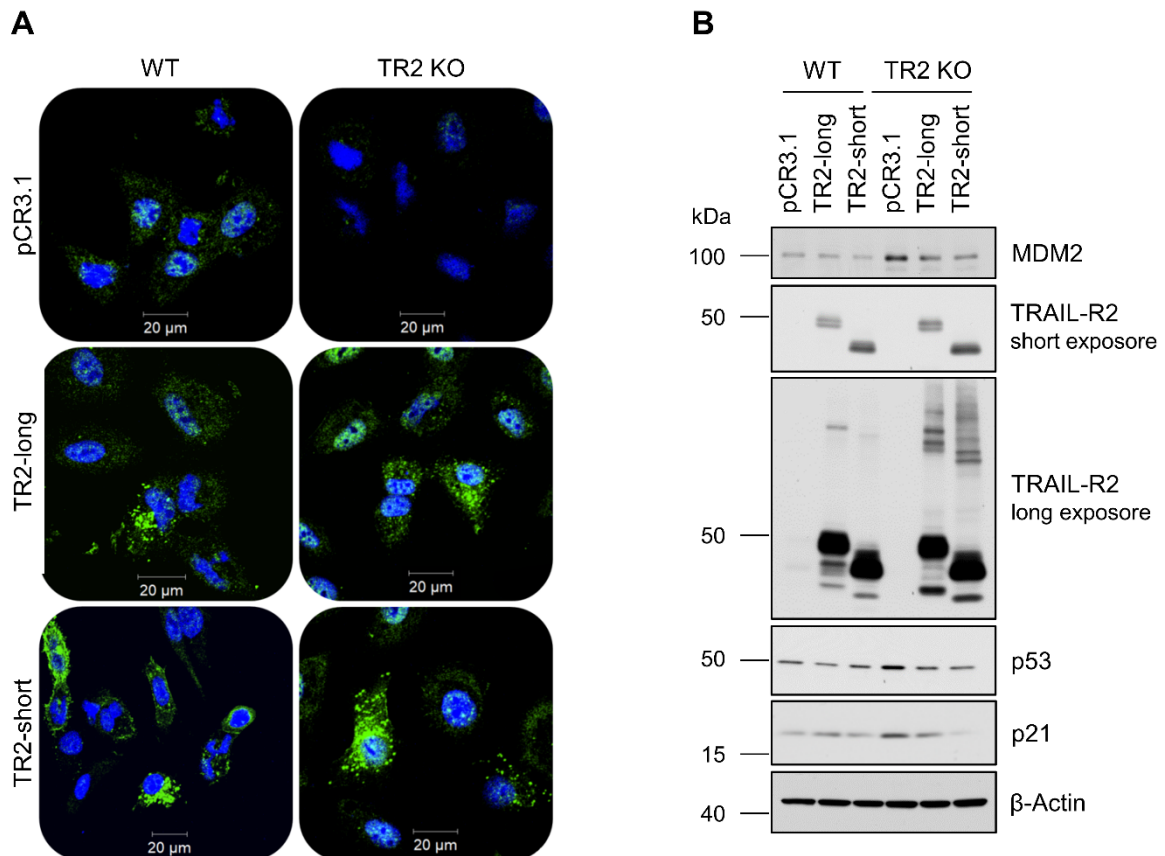


Figure 11: TRAIL-R2 decreases the protein level of p53.

A549 WT and TRAIL-R2 KO cells were transiently transfected with expression vectors coding for the long (TR2-long) or short (TR2-short) isoform of TRAIL-R2, both carrying a point mutation in the death domain. In parallel cells were transfected with an empty vector (pCR3.1) as a control. **(A)** Intracellular distribution of TRAIL-R2 long and short isoform was studied by indirect immunofluorescence followed by confocal laser scanning microscopy 24 h after transfection. Nuclei were stained by Hoechst. **(B)** Protein levels of TRAIL-R2, p53, p21 and MDM2 were analyzed by western blotting 48 h after transfection. The level of β -Actin was determined in parallel and served as loading control. TR2 KO, TRAIL-R2 knockout; sh ns, short hairpin RNA non-silencing; sh TR2, short hairpin RNA TRAIL-R2; WT, wild type.

4.4.3 TRAIL-R2's impact on p53 levels and its transcriptional output does not depend on the activity of caspases

Due to the mutation in the DD the overexpressed TRAIL-R2 isoforms are not able to bind FADD and therefore induce caspase-8 activation. Consequently, the observed TRAIL-R2-mediated effects on p53-levels are supposed to be independent of caspases. In order to validate this conclusion, A549 cells were treated with the broad-spectrum caspase-inhibitor zVAD-fmk and whole cell lysates were analyzed by western blotting (Fig. 12A). As previously identified western blot results showed an increased protein level of p53, MDM2, p21 and BAX in TRAIL-R2 KO cells in comparison to control cells. Importantly, inhibition of caspases by zVAD-fmk did not affect the level of p53, MDM2, p21 and BAX neither in WT and nor in TRAIL-R2 KO A549 cells (Fig. 12A). Furthermore, ChIP of p53 was performed on chromatin

preparations from A549 WT and TRAIL-R2 KO cells followed by detection of the p21 promotor (*CDKN1A*) via qPCR (Fig. 12B). In accordance with western blot results, treatment of A549 cells with zVAD-fmk also did not affect the presence of p53 at the p21 promotor neither in WT nor in TRAIL-R2 KO cells (WT control 7 vs. zVAD-fmk 8.7, TRAIL-R2 KO control 21.4 vs. zVAD-fmk 25.8; Fig. 12B).

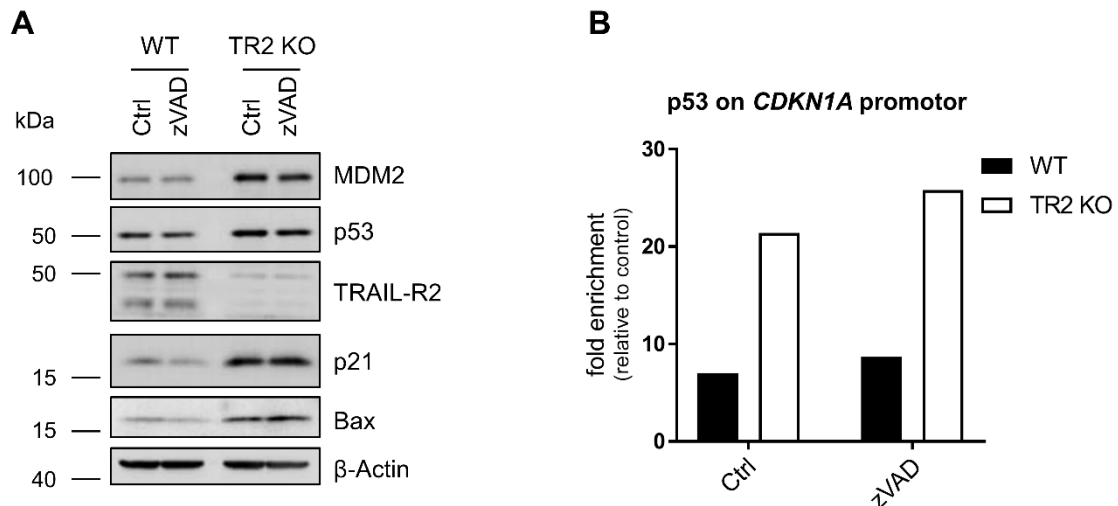


Figure 12: TRAIL-R2 impacts p53 levels independent of caspases.

(A) A549 cells were treated with zVAD-fmk (20 μ M) for 48 h. Whole cell lysates were analyzed by western blotting for the expression of TRAIL-R2, p53, MDM2, BAX and p21. β -Actin was detected as loading control. **(B)** A549 cells were treated with zVAD-fmk (20 μ M) for 24 h. ChIP was performed with anti-p53 and isotype control antibodies on chromatin preparations harvested from A549 WT and TRAIL-R2 KO cells. The DNA was extracted and qPCR was performed for detection of the *CDKN1A* promotor. Enrichment was determined as the fold increase in signal relative to the background signal. Bar chart shows results from one representative experiment ($n=1$). ChIP, chromatin immunoprecipitation; WT, wild type; TR2 KO, TRAIL-R2 knockout; zVAD, broad-spectrum caspase inhibitor.

4.4.4 TRAIL-R2 affects p53 independent of TRAIL

Since TRAIL stimulation induces various TRAIL-R-mediated pathways such as NF- κ B and ERK [38,39,43], the influence of TRAIL on the TRAIL-R2-mediated modulation of p53 protein levels was examined. Therefore, A549 WT and TRAIL-R2 KO cells were treated either with TRAIL (20 ng/ml; 6 h and 24 h) or anti-TRAIL antibody (1 μ g/ml; 48 h) neutralizing endogenous TRAIL (Fig. 13A). As carried out with data shown before, western blot analysis of whole cell lysates showed increased p53, MDM2 and p21 levels in TRAIL-R2 KO cells in comparison to control cells. Neither TRAIL stimulation nor anti-TRAIL treatment affected protein levels of p53, MDM2 and p21 in WT and TRAIL-R2 KO A549 cells (Fig. 13A).

In order to validate western blot results ChIP of p53 was performed using chromatin preparations from A549 WT and TRAIL-R2 KO cells untreated or treated with anti-TRAIL antibody for 24 h (Fig. 13B). As previously shown in Fig. 10 and 12, comparison of untreated control samples revealed an enrichment of precipitated p21 promotor in A549 TRAIL-R2 KO

cells (WT 7 vs. TRAIL-R2 KO 21.4). In agreement with western blot data (Fig. 13A), neutralizing endogenous TRAIL did not affect the presence of p53 at the p21 promoter in both clones (WT control 7 vs. anti-TRAIL 8.7; TRAIL-R2 KO control 21.4 vs. anti-TRAIL 20.1; Fig. 13B). In conclusion, these results suggest that TRAIL-R2 affects p53 independent of TRAIL.

Taken together, silencing of TRAIL-R2 increases the level of p53 and the expression of its transcriptional targets p21, MDM2 and BAX. *Vice versa* overexpression of TRAIL-R2-long or short isoform in TRAIL-R2 knockout cells decreased the level of p53 and its transcriptional targets. This impact of TRAIL-R2 on p53 level is independent of caspase activation as well as TRAIL. With regard to the previous finding that p53 and TRAIL-R2 interact with each other in the nucleus, these results highly indicate a mechanistic link between TRAIL-R2 and p53 expression/ activity, a question that is addressed in the following in more detail.

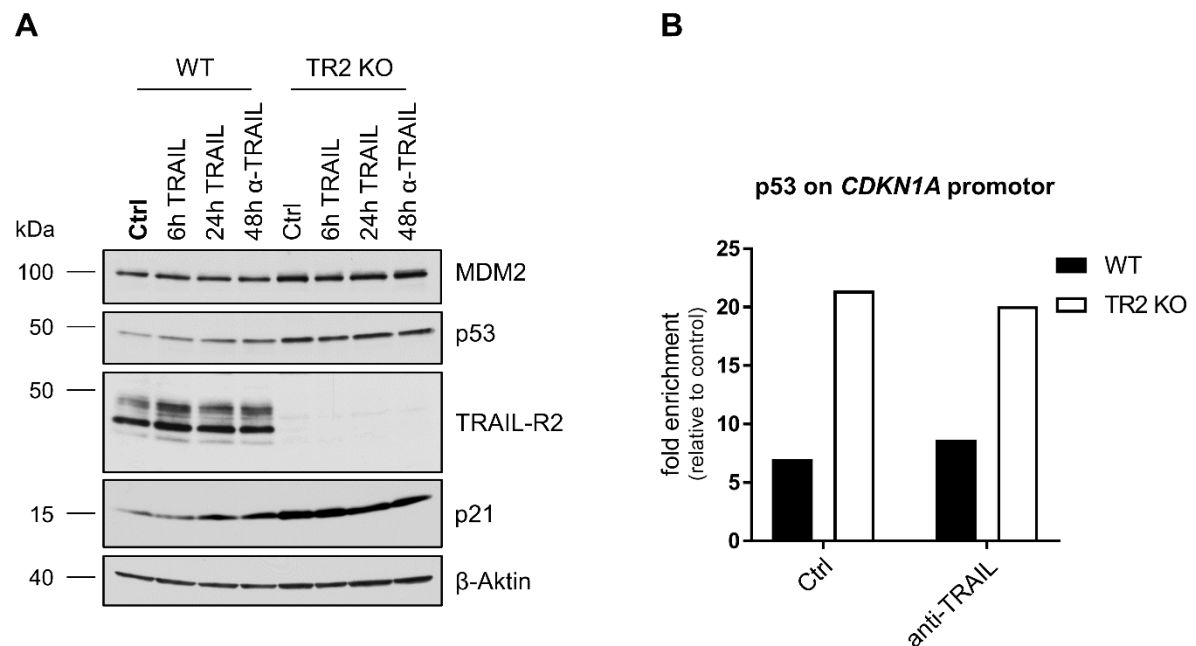


Figure 13: TRAIL-R2 affects p53 TRAIL-independent.

(A) A549 cells were treated with TRAIL (20 ng/ ml) or anti-TRAIL (1 µg/ ml) neutralizing antibody for the indicated time periods. Whole cell lysates were analyzed by western blotting for the expression of TRAIL-R2, p53, MDM2 and p21. The level of β-Actin was determined in parallel and served as loading control. **(B)** A549 cells were treated with anti-TRAIL (1 µg/ ml) neutralizing antibody for 24 h. ChIP was performed with anti-p53 and isotype control antibodies on chromatin preparations harvested from A549 WT and TRAIL-R2 KO cells. The DNA was extracted and qPCR was performed for detection of the *CDKN1A* promotor. Enrichment was determined as the fold increase in signal relative to the background signal. Bar chart shows results from one representative experiment (n=1). ChIP, chromatin immunoprecipitation; WT, wild type; TR2 KO, TRAIL-R2 knockout.

4.5 Analysis of the regulatory mechanism by which TRAIL-R2 affects the protein level of p53

4.5.1 TRAIL-R2 affects p53 protein stability

To gain an insight into the molecular mechanisms underlying the TRAIL-R2-mediated modulation of p53 protein levels, next it was examined whether TRAIL-R2 influences the transcription of the p53 gene. Therefore, the amount of p53 mRNA was quantified in A549 and HCT116 control and TRAIL-R2 knockout/ knockdown cells by qPCR (Fig. 14A, B). Results showed that p53 mRNA level was hardly altered by TRAIL-R2 status in both cell lines. This raises the hypothesis that TRAIL-R2 impacts p53 protein.

In order to investigate whether TRAIL-R2 may affect the stability of p53, its half-life was compared in A549 and HCT116 control and TRAIL-R2 knockout/ knockdown cells. Therefore, cells were treated for different time periods with Cycloheximide (CHX), an inhibitor of *de novo* protein synthesis, and the level of p53 protein was analyzed by western blotting (Fig. 14C, D). Western blot analyses showed that p53 was almost completely degraded 1 h after treatment with CHX in control cells, whereas p53 levels were still detectable up to 4 h after protein biosynthesis blockade in TRAIL-R2 knockout/ knockdown cells (Fig. 14C, D). Quantification of p53 protein levels by densitometry allowed the determination of the protein half-life. As shown in Fig. 14E, F knockout or knockdown of TRAIL-R2 strongly increased the half-life of p53. In agreement with the elevated p53 level in TRAIL-R2 silenced cells, the p53 targets MDM2 and p21 were also enhanced in TRAIL-R2 knockdown/ knockout cells in comparison to respective controls. In order to examine whether the impact of TRAIL-R2 on p53 protein stability represents a p53-specific phenomenon, protein levels of c-Myc and Nrf2, which are also characterized by a short half-life, were analyzed in parallel in A549 cells (Fig. 14C). Interestingly, western blot analysis revealed that the stability of c-Myc and Nrf2 was not influenced by TRAIL-R2.

In conclusion, these findings indicate that knockdown/ knockout of TRAIL-R2 extends the half-life of p53 protein in A549 and HCT116 cells in comparison to control cells. Therefore, TRAIL-R2 might affect p53 protein level by decreasing its protein stability, a hypothesis that is addressed in more detail in following experiments.

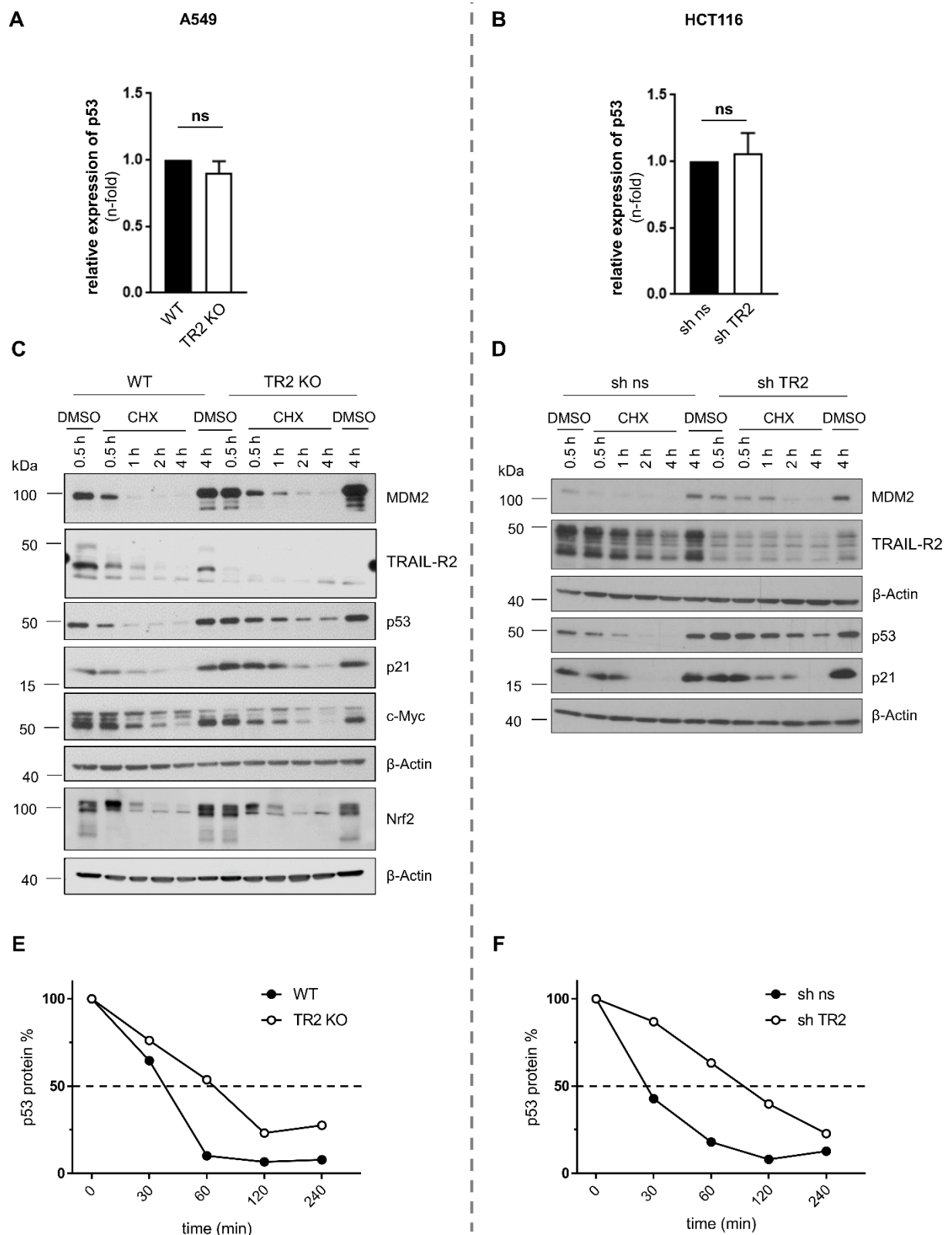


Figure 14: TRAIL-R2 affects p53 protein stability.

(A, B) Relative expression of p53 (normalized to TBP) was analyzed by qPCR in (A) A549 WT and TRAIL-R2 KO cells as well as (B) HCT116 sh ns and sh TRAIL-R2 cells. Bar charts show mean values \pm SEM of three independent experiments. (C) A549 WT and TRAIL-R2 KO as well as (D) HCT116 sh ns and sh TRAIL-R2 cells were treated with Cycloheximide (10 μ g/ml) for the indicated time periods or DMSO as a control. Whole cell lysates were analyzed by western blotting. The level of β -Actin was determined as loading control. (E, F) p53 protein levels were quantified by densitometry, normalized to β -Actin and plotted against time. CHX, Cycloheximide; ns, not significant; WT, wild type; TR2 KO, TRAIL-R2 knockout; sh ns, short hairpin RNA non-silencing; sh TR2, short hairpin RNA TRAIL-R2.

4.5.2 TRAIL-R2-mediated p53 degradation depends on the ubiquitin-proteasome-system

P53, such as multiple other proteins, is degraded by the ubiquitin-proteasome-system (UPS) [92,93]. In order to investigate whether TRAIL-R2 impacts p53 protein stability by affecting p53 degradation via the UPS, A549 and HCT116 control and TRAIL-R2 knockout/ knockdown cells were treated with MG132, a 26S proteasome inhibitor, for 4 h. Afterwards, p53 levels were analyzed by western blotting (Fig. 15A, B). MG132 led to the accumulation of p53 in both cell lines. As already shown, inhibition of TRAIL-R2 expression, either in HCT116 or in A549 cells, also resulted in elevated p53 levels. Importantly, concomitant inhibition of the proteasome in these cells did not further increase the p53 protein level in TRAIL-R2 knockout/ knockdown cells compared to respective MG132-treated control cells (Fig. 15A, B). Notably, the protein level of p53 was equivalent in control and TRAIL-R2 knockout/ knockdown cells after MG132 treatment. These data support the view that TRAIL-R2 negatively regulates the stability of p53 protein by promoting its proteasomal degradation.

A key regulator of p53 ubiquitination is MDM2 [92,93]. Upon binding, MDM2 ubiquitylates p53 leading to its proteasomal degradation. In order to examine, whether TRAIL-R2-mediated p53 destabilization depends on MDM2, A549 cells were treated with Nutlin 3a, which inhibits MDM2-p53 interaction and thereby protects p53 from ubiquitination followed by proteasomal degradation (Fig. 16A). As previously shown, the p53 level was elevated in whole cell lysate from untreated A549 TRAIL-R2 KO cells in comparison to respective WT cells. After treatment with Nutlin 3a, p53 protein was accumulated and importantly, Nutlin 3a-treated WT cells showed a p53 level similar to respective TRAIL-R2 KO cells. Thus, blocking the interaction

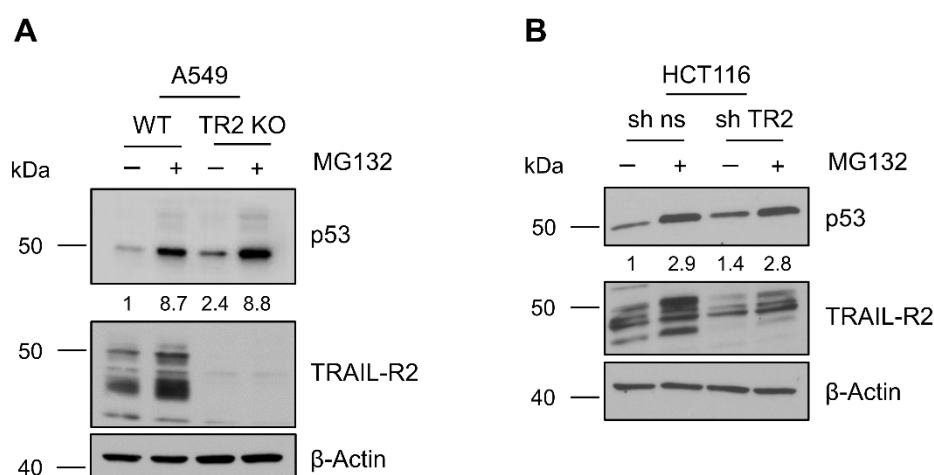


Figure 15: TRAIL-R2 decreases p53 levels via ubiquitin-proteasome-dependent degradation.

(A) A549 WT and TRAIL-R2 KO as well as (B) HCT116 sh ns and sh TRAIL-R2 cells were treated with MG132 (2 μ M) for 4 h or DMSO as a control. Whole cell lysates were analyzed by western blotting for the expression of TRAIL-R2 and p53. The level of β -Actin was detected as loading control. P53 protein levels were quantified by densitometry and normalized to respective β -Actin levels. Data are presented as fold-changes relative to WT control. WT, wild type; TR2 KO, TRAIL-R2 knockout; MG132, proteasome inhibitor.

between MDM2 and p53 attenuates the difference in p53 protein level between WT and TRAIL-R2 KO cells. Moreover, TRAIL-R2 levels were also enhanced after Nutlin 3a treatment in WT cells, a finding that might be explained by the accumulation of activated p53, which mediates the upregulation of TRAIL-R2 expression on transcriptional level (Fig. 16A).

In order to analyze the effect of Nutlin 3a on p53 in more detail, ChIP targeting p53 located at the p21 promotor was performed using chromatin preparations from A549 WT and TRAIL-R2 KO cells treated or not with Nutlin 3a for 24 h (Fig. 16B). ChIP analysis revealed that Nutlin 3a strongly enhanced the presence of p53 at the p21 promoter in both WT (untreated 7 vs. Nutlin 3a 66.3) and TRAIL-R2 KO cells (untreated 21.4 vs. Nutlin 3a 118.1). Notably, p53 levels bound to p21 promotor were still higher in TRAIL-R2 KO cells than in WT cells after Nutlin 3a treatment (Fig. 16B).

Summing up, these results revealed that TRAIL-R2 negatively regulates the stability of p53 protein by promoting its proteasomal degradation and an involvement of MDM2.

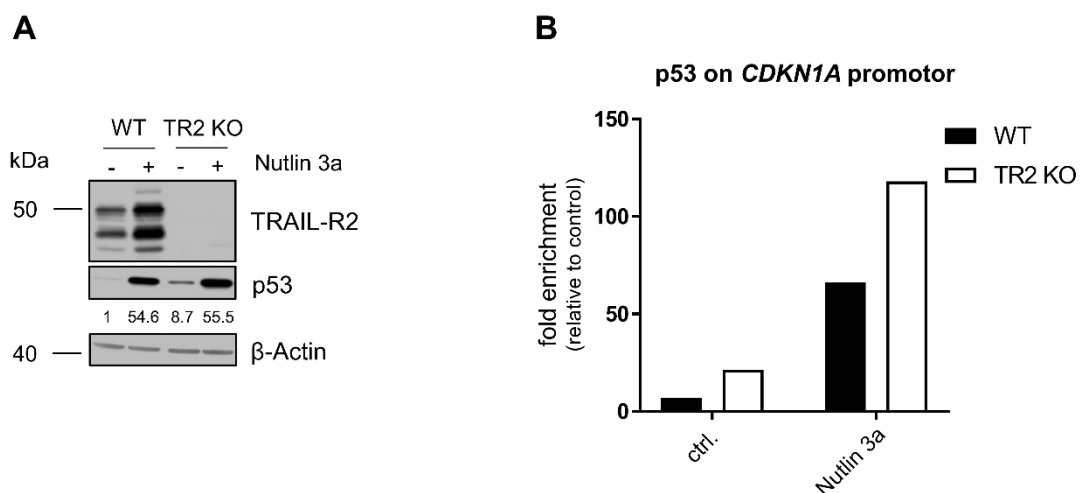


Figure 16: MDM2 impacts the TRAIL-R2-mediated p53 destabilization.

(A) A549 WT and TRAIL-R2 KO cells were treated with Nutlin 3a (5 μ M) for 24 h. Whole cell lysates were analyzed by western blotting for the expression of TRAIL-R2 and p53. The level of β -Actin was determined in parallel as loading control. P53 protein level was quantified by densitometry and normalized to respective β -Actin levels. Data are presented as fold-changes relative to WT control. **(B)** A549 WT and TRAIL-R2 KO cells were treated with Nutlin 3a (5 μ M) for 4 h. ChIP was performed with anti-p53 and isotype control antibodies on chromatin preparations harvested from A549 WT and TRAIL-R2 KO cells. The DNA was extracted, and qPCR was performed using primers that detected the *CDKN1A* promotor. Enrichment was determined as the fold increase in signal relative to the background signal. Bar chart shows results from one representative experiment (n=1). ChIP, chromatin immunoprecipitation; WT, wild type; TR2 KO, TRAIL-R2 knockout; Nutlin 3a, MDM2 inhibitor.

4.5.3 TRAIL-R2 co-localizes with MDM2 in the nucleus

To get more insights into the TRAIL-R2-p53-MDM2 regulatory axis the interaction of p53 and MDM2 in the presence and absence of TRAIL-R2, as well as the interaction between TRAIL-R2 and MDM2 was analyzed by immunofluorescence in A549 cells. Results showed a high abundance of p53 and MDM2 in the nucleus as well as a co-localization of MDM2 and p53 in WT and TRAIL-R2 KO cells (Fig. 17A). Interestingly, TRAIL-R2 also co-localized with MDM2 in the nucleus of A549 WT cells (Fig. 17B). In order to further investigate the potential protein-protein interaction of TRAIL-R2 and MDM2, immunoprecipitation experiments of nuclear fractions from A549 WT and TRAIL-R2 KO cells were carried out and protein complexes were analyzed by western blotting (Fig. 17C). Lysate control samples showed elevated p53 and MDM2 protein levels in TRAIL-R2 KO cells in comparison to control cells (lane 1 vs. lane 2). In line with that immunoprecipitates showed a higher amount of p53 pulled down with specific antibody as well as a higher amount of co-precipitated MDM2 in A549 TRAIL-R2 KO cells compared to control cells (lane 6 vs. lane 7). As shown previously (Fig. 9B), analysis of protein complexes revealed a co-precipitation of TRAIL-R2 with p53 solely in WT cells (lane 6 vs. lane 7). Since a small amount of MDM2 was detected in TRAIL-R2 precipitates from TRAIL-R2 KO cells, but not in respective precipitates from WT cells (lane 4 vs. lane 3), this might be due to unspecific binding. Thus, TRAIL-R2 and MDM2 did not co-precipitate.

Taken together, immunofluorescence analysis and immunoprecipitation experiments revealed an interaction of p53 and MDM2 independent of the TRAIL-R2 status in A549 cells. Immunoprecipitations suggest that TRAIL-R2 does not directly interact with MDM2. However, results from immunofluorescence analyses indicated that TRAIL-R2 is present in protein complexes with p53 and MDM2. These results raise the hypothesis that besides MDM2 another, by now unidentified factor, might participate in the TRAIL-R2-p53 regulatory axis to modulate p53 protein levels. In order to address this assumption, the role of potential co-players was examined in following experiments.

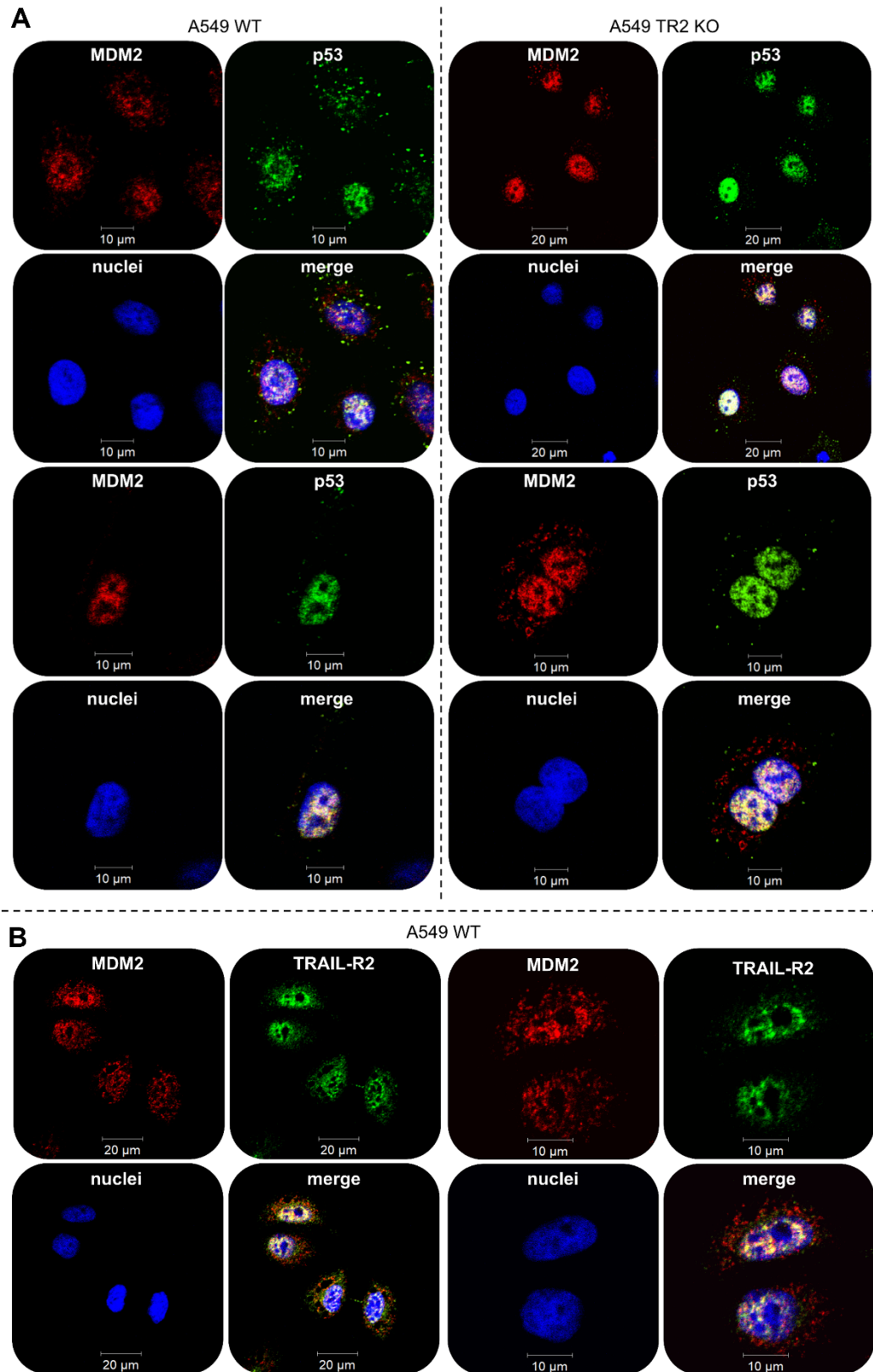


(Figure 17 continued next page)

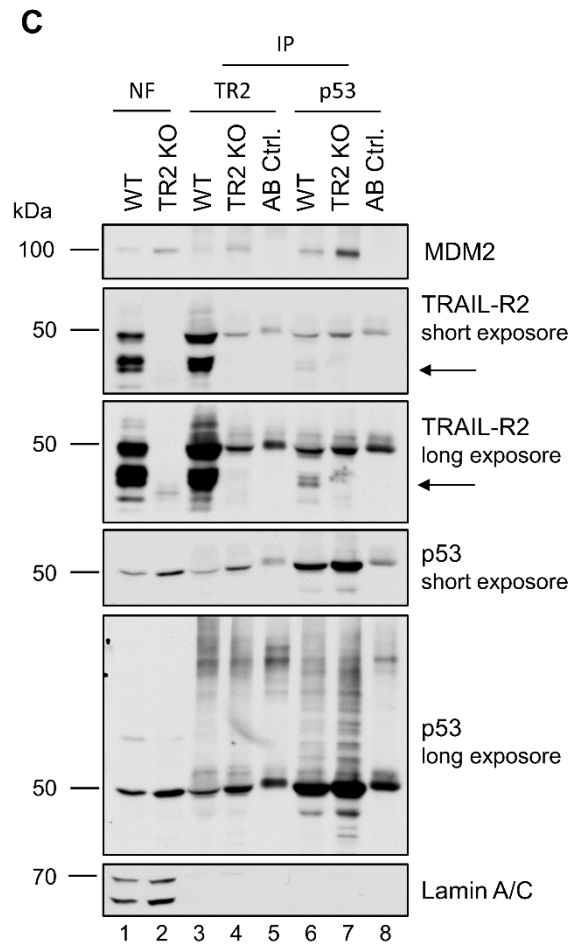


Figure 17: MDM2, p53 and TRAIL-R2 co-localize in the nucleus of A549 cells, but MDM2 does not co-precipitate with TRAIL-R2.

(A, B) Intracellular distribution of **(A)** MDM2 (SMP14) and p53 (FL393) as well as **(B)** MDM2 (SMP14) and TRAIL-R2 (Lexatumumab) in A549 cells was analyzed by indirect immunofluorescence following confocal laser scanning microscopy. Nuclei were stained by Hoechst. **(C)** TRAIL-R2 (HS201) and p53 (DO-1) were precipitated from nuclear fractions of A549 WT and TRAIL-R2 KO cells by specific antibodies and protein complexes were analyzed by western blotting. As a control antibodies and beads without lysate were analyzed in parallel. Lamin A/C was detected as loading control. Exposure = decreased/ increased time of light exposure for signal detection. IP, immunoprecipitation; AB ctrl., antibody control; WT, wild type; TR2 KO, TRAIL-R2 knockout; TR2, TRAIL-R2.

4.5.4 TRAIL-R2 does not affect the deubiquitination activity of USP10 towards p53

In addition to ubiquitin ligases the protein level of p53 is maintained by multiple other factors such as phosphorylation, acetylation or deubiquitination. Previous mass-spectrometric analysis of the working group regarding pancreatic ductal adenocarcinoma (PDAC) Panc89 cells revealed that TRAIL-R2 might interact with the deubiquitination enzyme USP10. USP10 is able to directly interact with p53 and remove its ubiquitin moieties, thereby counteracting its proteasomal degradation [104]. Thus, the possible interaction between TRAIL-R2 and USP10 was further investigated by immunofluorescence and immunoprecipitation analysis in A549 cells.

Immunofluorescence analysis showed that USP10 was present in the cytosol and in the nucleus of A549 WT and TRAIL-R2 KO cells. Moreover, results showed a co-localization of USP10 with p53 in the nuclei of A549 WT and TRAIL-R2 KO cells (Fig. 18A). Interestingly, analyses also displayed that USP10 co-localizes with TRAIL-R2 in both the nucleus and cytoplasm of A549 WT cells (Fig. 18B).

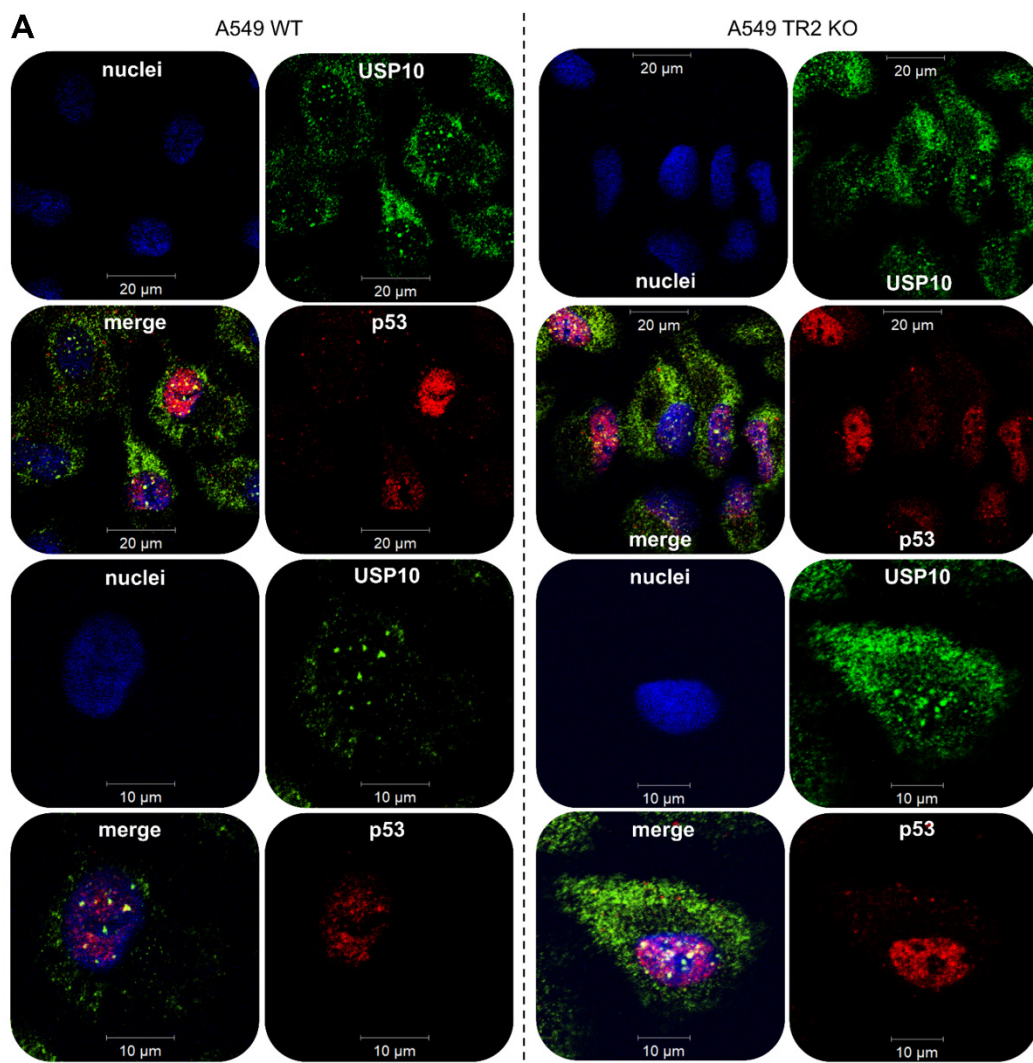


(Figure 18 continued next page)

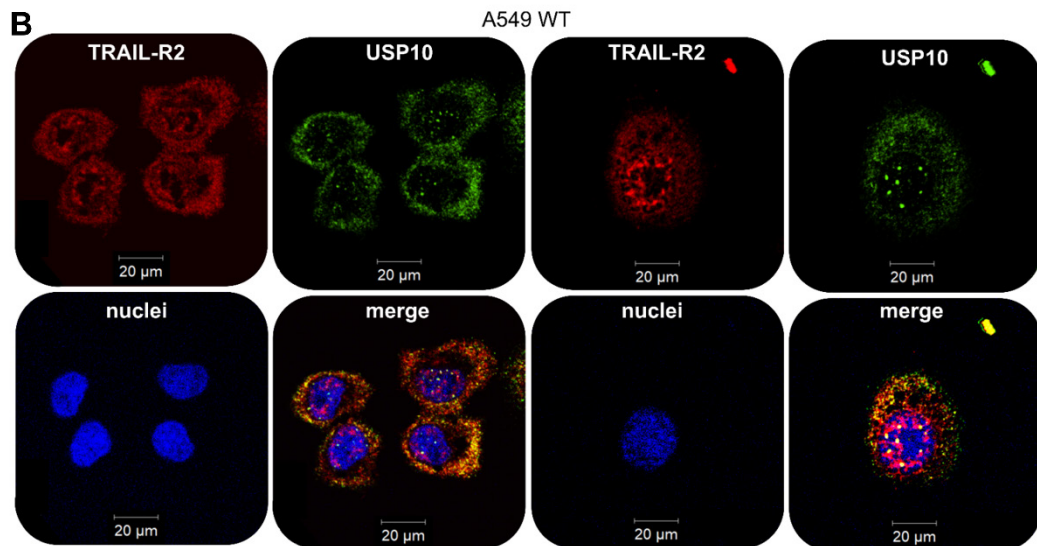


Figure 18: USP10 co-localizes with TRAIL-R2 and p53 in the cytosol and nucleus.

The intracellular distribution of **(A)** USP10 and p53 (DO-1) and **(B)** USP10 and TRAIL-R2 (HS201) was analyzed by indirect immunofluorescence following confocal laser scanning microscopy in A549 cells. Nuclei were stained by Hoechst. WT, wild type; TR2 KO, TRAIL-R2 knockout.

In order to further characterize a potential protein-protein interaction between TRAIL-R2 and USP10, immunoprecipitation experiments of whole cell lysates from A549 cells were performed (Fig. 19A). Indeed, western blot analyses of TRAIL-R2 immunoprecipitates showed a co-precipitation of USP10 with TRAIL-R2 in A549 WT cells. Moreover, immunoprecipitations of p53 revealed a co-precipitation of USP10 in TRAIL-R2 KO cells, but precipitating USP10, p53 co-precipitated in both, WT and TRAIL-R2 KO cells (Fig. 19A).

Upon DNA damage, USP10 translocates from the cytosol to the nucleus where it deubiquitylates and, thereby, stabilizes p53 [142]. Therefore, the intracellular distribution of USP10 in A549 WT and TRAIL-R2 KO cells was examined by cell fractionation and immunofluorescence analysis (Fig. 19B, C). Cell fractionation quality was assessed by detection of α -Tubulin, CRM1 and Histone H3, which are exclusively present or absent in distinct cellular compartments. Evaluation of TRAIL-R2 levels showed that most of the intracellularly located receptor was present in the soluble nuclear and chromatin fraction. As already shown, p53 protein level was increased in whole cell lysates of A549 TRAIL-R2 KO cells in comparison to control cells. According to its known intracellular distribution, p53 was found in all three fractions, but no marked difference in the amount of p53 between WT and TRAIL-R2 KO cells was detected (Fig. 19B). In contrast, the amount of USP10 was similar in whole cell lysates from A549 WT and TRAIL-R2 KO cells, but its intracellular distribution markedly varied between WT and TRAIL-R2 KO cells. Hence, western blot analysis of cellular fractions revealed less USP10 in the cytosolic and chromatin fraction of TRAIL-R2 KO cells compared to control cells, but notably higher USP10 levels in the soluble nuclear fraction of

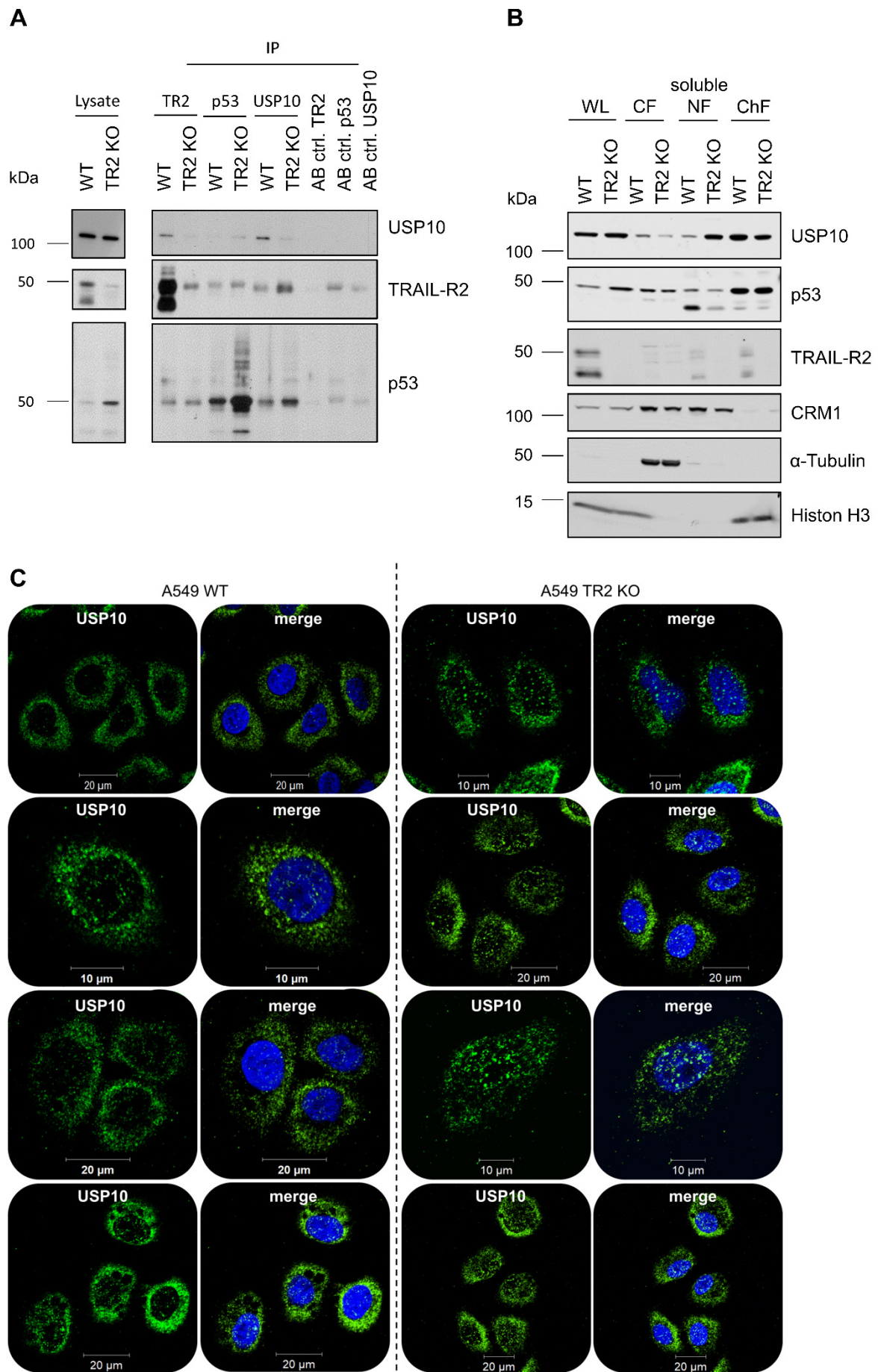


Figure 19: USP10 interacts with p53 and TRAIL-R2 in A549 cells and is located to a higher extent in the nucleus of TRAIL-R2 KO cells than WT cells.

(A) TRAIL-R2, p53 and USP10 were precipitated from whole cell lysates of A549 WT and TRAIL-R2 KO cells by specific antibodies. Protein complexes were examined by western blotting. **(B)** Whole cell lysates (WL), cytosolic (CF), soluble nuclear (NF) and chromatin fractions (ChF) from A549 WT and TRAILR2 KO cells were prepared and analyzed by western blotting. CRM1, Histone H3 and α -Tubulin were analyzed in parallel and served as loading and fractionation quality control. **(C)** Cellular distribution of USP10 was analyzed by indirect immunofluorescence following laser scanning microscopy in A549 WT and TRAIL-R2 KO cells. WT, wild type; TR2 KO, TRAIL-R2 knockout; IP, immunoprecipitation.

A549 TRAIL-R2 KO cells than in WT cells (Fig. 19B). Noteworthy, results from western blotting analyses of cell fractionations were fostered by immunofluorescence stainings of USP10 in A549 WT and TRAIL-R2 KO cells (Fig. 19C). In detail, USP10 was detectable in the cytosol and in the nucleus where it aggregated in small clusters. Comparison of USP10 distribution in A549 WT and TRAIL-R2 KO cells indicated that USP10 is located to a markedly higher extent in the nucleus of TRAIL-R2 KO cells (Fig. 19C).

4.5.6 USP10 is not involved in TRAIL-R2-mediated destabilization of p53

In order to further investigate the regulatory relationship between TRAIL-R2 and USP10, USP10 was transiently knocked down via short interfering RNA (siRNA). For this purpose, A549 WT and TRAIL-R2 KO cells were transfected with USP10 specific or control siRNA and whole cell lysates were analyzed by western blotting 48 h after transfection (Fig. 20A). In addition, whole cell lysates from non-transfected cells were analyzed in parallel. Western blot analyses showed an equal protein amount of USP10 in WT and TRAIL-R2 KO cells and an efficient USP10 knockdown was confirmed. The level of TRAIL-R2 was similar in lysates from WT control and WT siCtrl cells, while the TRAIL-R2 level in WT siUSP10 cells was slightly decreased. TRAIL-R2 was not detectable in lysates from TRAIL-R2 KO cells. The protein level of p53 was increased in TRAIL-R2 KO cells compared to control cells. This difference in p53 levels was diminished after transfection with control as well as USP10 siRNA (Fig. 20A). However, densitometric analysis of p53 protein level highlighted that USP10 knockdown was not associated with a significant reduction of the increased p53 levels in A549 TRAIL-R2 KO cells (siCtrl 2.1 vs. siUSP10 1.8; Fig. 20B). In line with this finding, the protein levels of the p53 targets MDM2 and p21 were markedly higher in untransfected, siCtrl and siUSP10 A549 TRAIL-R2 KO cells than in respective WT cells.

In order to examine the effect of USP10 knockdown on p53 protein stability in A549 WT and TRAIL-R2 KO cells in more detail, CHX chase assays were performed (Fig. 20C, D). Western blot analyses of whole cell lysates from A549 WT and TRAIL-R2 KO cells transfected with control siRNA (Fig. 20C) or USP10 siRNA (Fig. 20D) followed by CHX treatment revealed that

the protein stability of p53 was increased in both, control siRNA and siUSP10 transfected TRAIL-R2 KO cells compared to control cells. In line with that also the p21 protein level was markedly higher in A549 TRAIL-R2 KO cells than WT cells over the whole time course of 4 h independent of USP10 knockdown.

Taken together, it could be shown that USP10 co-localizes and interacts with p53 and TRAIL-R2. Nevertheless, results suggest that USP10 is not involved in TRAIL-R2-mediated p53 destabilization.

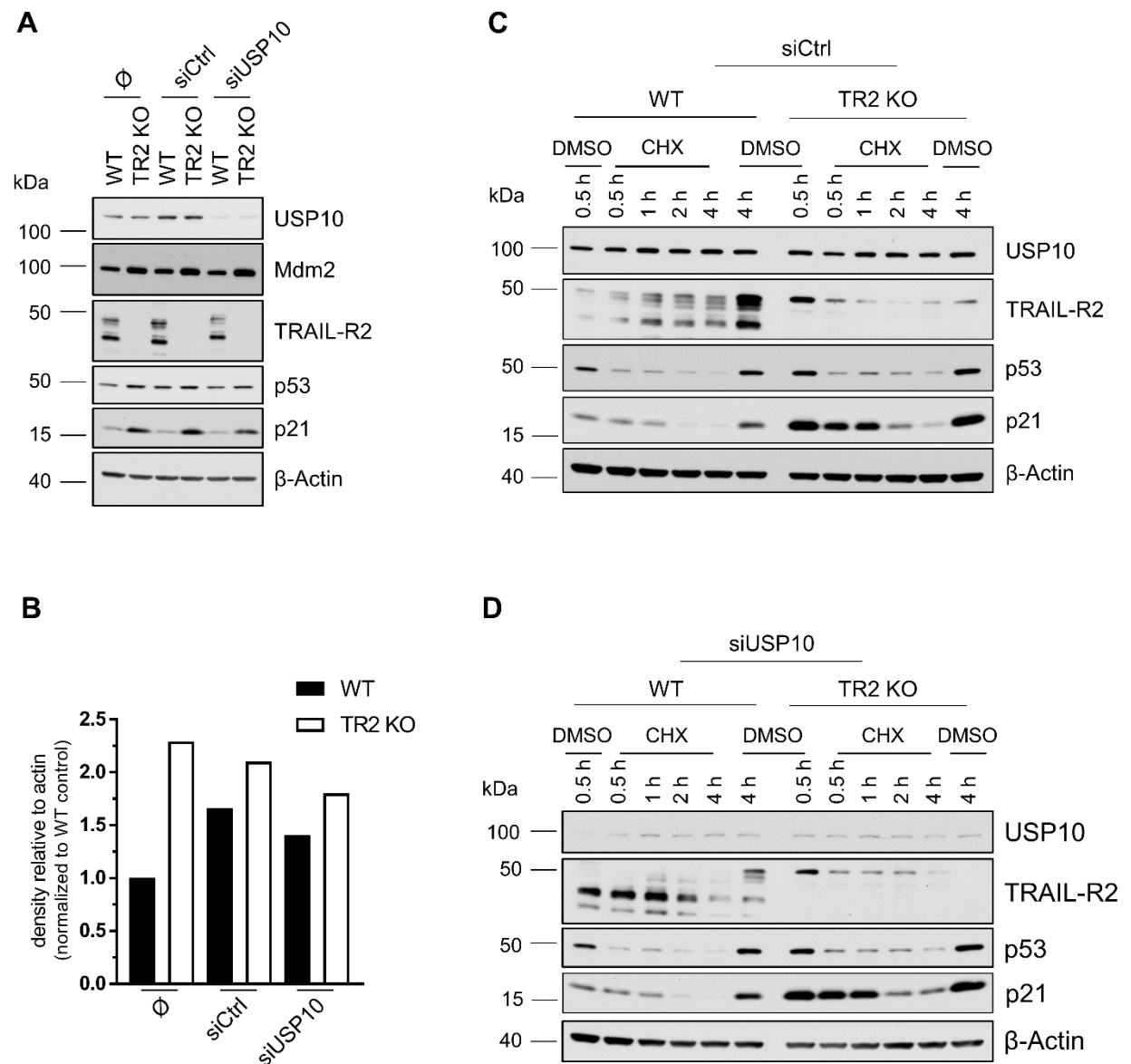


Figure 20: SiRNA-mediated knockdown of USP10 does not affect the increased p53 stability in A549 TRAIL-R2 KO cells.

(A) A549 WT and TRAIL-R2 KO cells were transiently transfected with control (siCtrl) or USP10 siRNA (siUSP10). After 48 h whole cell lysates were analyzed by western blotting. (B) P53 band intensities were analyzed by densitometry and the intensity of each band was normalized to the respective β -Actin. Data are presented as fold-changes relative to WT control. (C, D) A549 WT and TRAIL-R2 KO cells were transiently transfected as described in (A). In addition, cells were treated with Cycloheximide (10 μ g/ml) or with DMSO as a control for the indicated time periods and whole cell lysates were analyzed by western blotting. β -Actin was detected in parallel and served as loading control. WT, wild type; TR2 KO, TRAIL-R2 knockout; CHX, Cycloheximide.

4.5.5 Deubiquitinases are not involved in TRAIL-R2-mediated destabilization of p53

The previously shown results from RNA interference experiments indicated that TRAIL-R2 regulates p53 protein stability independent of USP10. However, a broad range of other deubiquitinases exist, which might be involved in TRAIL-R2-mediated p53 destabilization. In order to address this issue, A549 WT and TRAIL-R2 KO cells were treated for different time periods with the broad spectrum deubiquitinase inhibitor PR-619 and/ or CHX. Afterwards, whole cell lysates were analyzed by western blotting (Fig. 21A, B). PR-619 led to a slight increase of p53 after 1 h, 2 h and 4 h in A549 WT and TRAIL-R2 KO cells. In line with this finding, MDM2, p21 and TRAIL-R2 levels were likewise elevated, indicating that PR-619 treatment caused p53 activation. Interestingly, p53 was almost completely degraded in WT cells after 0.5 h treatment with CHX alone or in combination with PR-619 (Fig. 21A). In contrast,

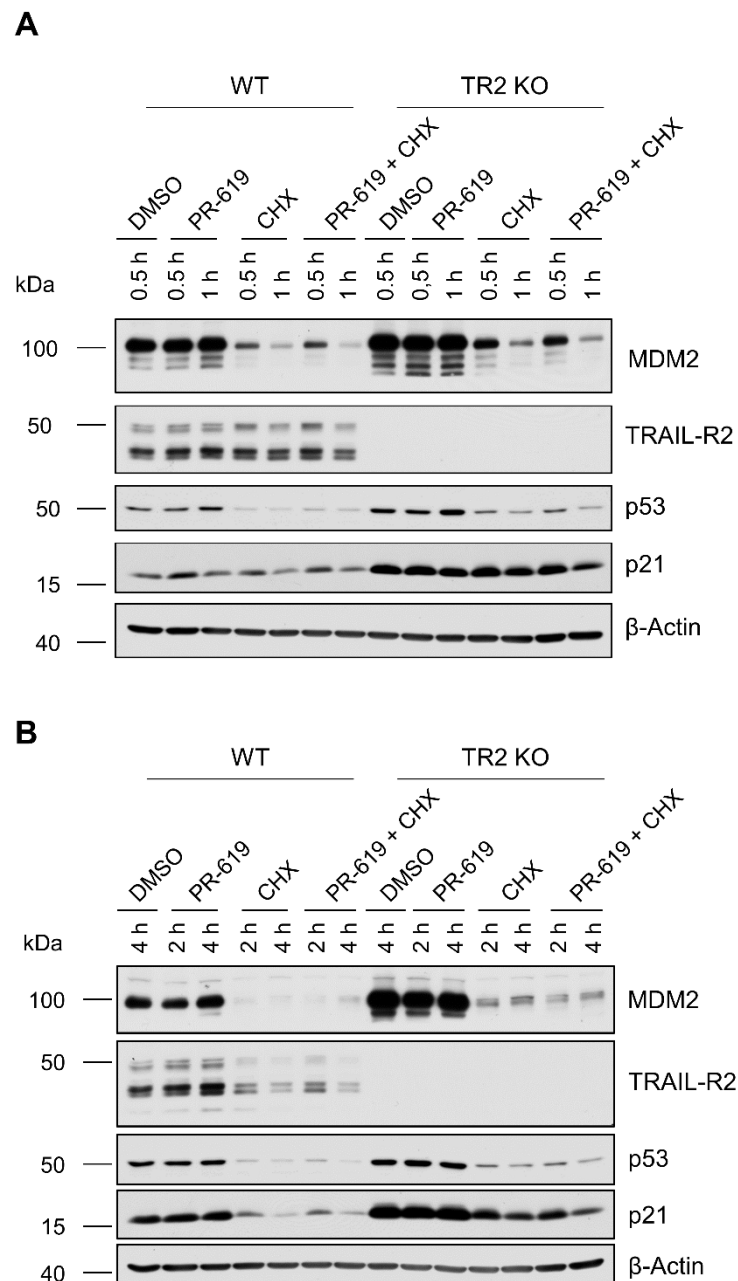


Figure 21: TRAIL-R2 affects p53 protein stability independent of deubiquitinating enzymes in A549 cells.

A549 WT and TRAIL-R2 KO cells were treated with CHX (10 µg/ml) and/ or PR-619 (8 µM) for (A) 0.5 h and 1 h as well as (B) 2 h and 4 h. β -Actin was analyzed as loading control. CHX, Cycloheximide; PR-619, broad spectrum deubiquitinase inhibitor; WT, wild type; TR2 KO, TRAIL-R2 knockout.

p53 was still detectable in TRAIL-R2 KO cells after 4 h treatment with CHX alone or in combination with PR-619 (Fig. 21B).

These results suggest that TRAIL-R2 impacts p53 protein stability independent of deubiquitinases.

4.5.6 TRAIL-R2 affects p53 protein level independent of HMGA2

On the trace of finding a co-factor that participates with TRAIL-R2 and MDM2 in destabilizing p53, next HMGA2 was examined. HMGA2 interacts with p53 and MDM2, promotes p53 ubiquitination and degradation and supports thereby colorectal cancer progression [143]. Interestingly, a regulatory link between TRAIL-R2 and HMGA2 was described. TRAIL-R2 interacts with the core components of the microprocessor complex thereby inhibiting the maturation of miRNA let-7. This leads to enhanced expression of let-7 target HMGA2 [48]. Based on these findings a possible interrelationship between TRAIL-R2, p53 and HMGA2 was investigated. Therefore, first the regulatory role of TRAIL-R2 on HMGA2 expression was examined in A549 cells. A549 WT and TRAIL-R2 KO cells were transiently transfected with vectors coding for the long and short isoform of TRAIL-R2 or with an empty vector, respectively. Then, whole cell lysates were analyzed for the expression level of TRAIL-R2 and HMGA2 (Fig. 22). Western blot results showed that the HMGA2 level was strongly decreased in TRAIL-R2 KO cells in comparison to control cells. Of note, after re-expression of TRAIL-R2 long or short isoform HMGA2 levels were elevated in both A549 WT and TRAIL-R2 KO cells. These results clearly show that TRAIL-R2 regulates the expression of HMGA2.

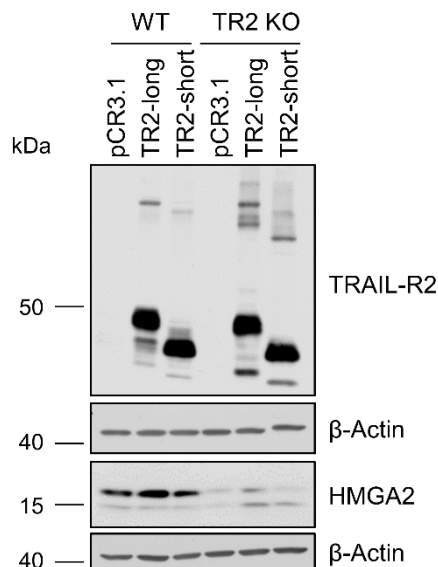


Figure 22: TRAIL-R2 overexpression upregulates HMGA2 levels.

A549 WT and TRAIL-R2 KO cells were transiently transfected with expression vectors coding for the long (TRAIL-R2-long) or short (TRAIL-R2-short) isoforms of TRAIL-R2, both carrying a point mutation in the death domain, or with an empty vector (pCR3.1). Protein levels of TRAIL-R2 and HMGA2 were detected in whole cell lysates by western blotting 48 h after transfection. β -Actin was analyzed as loading control. WT, wild type; TR2 KO, TRAIL-R2 knockout.

Based on these findings, it was next investigated whether TRAIL-R2 impacts p53 protein level via HMGA2. For this purpose, A549 WT and TRAIL-R2 KO cells were transiently transfected with control (siCtrl) or HMGA2 specific siRNA (siHMGA2). Whole cell lysates were analyzed by western blotting 24 h, 48 h and 72 h after transfection, respectively (Fig. 23). As already repeatedly shown, p53 level was elevated in TRAIL-R2 KO cells compared to WT cells. Knockdown of HMGA2 was confirmed by western blotting and silencing was most efficient 48 h and 72 h after transfection. Interestingly, knockdown of HMGA2 led to a decreased p53 protein level in A549 WT cells, while no difference was detected in TRAIL-R2 KO cells in comparison to respective control transfected cells. In line with the alterations observed in p53 protein level, levels of p21 and MDM2 were decreased after HMGA2 knockdown in A549 WT cells, but not altered in TRAIL-R2 KO cells (Fig. 23).

In summary, these data show that TRAIL-R2 promotes HMGA2 expression in A549 cells. HMGA2 has an impact on p53 protein levels in A549 WT cells, but plays a minor role in TRAIL-R2 KO cells. However, the previously described regulatory role of HMGA2 on p53 degradation [143] could not be identified in A549 cells.

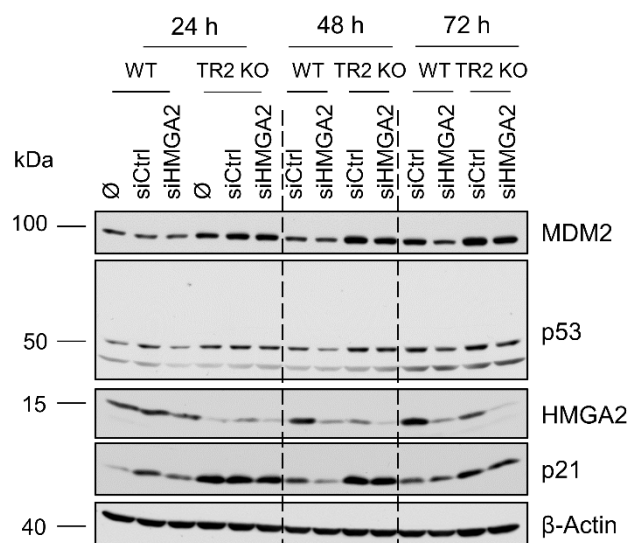
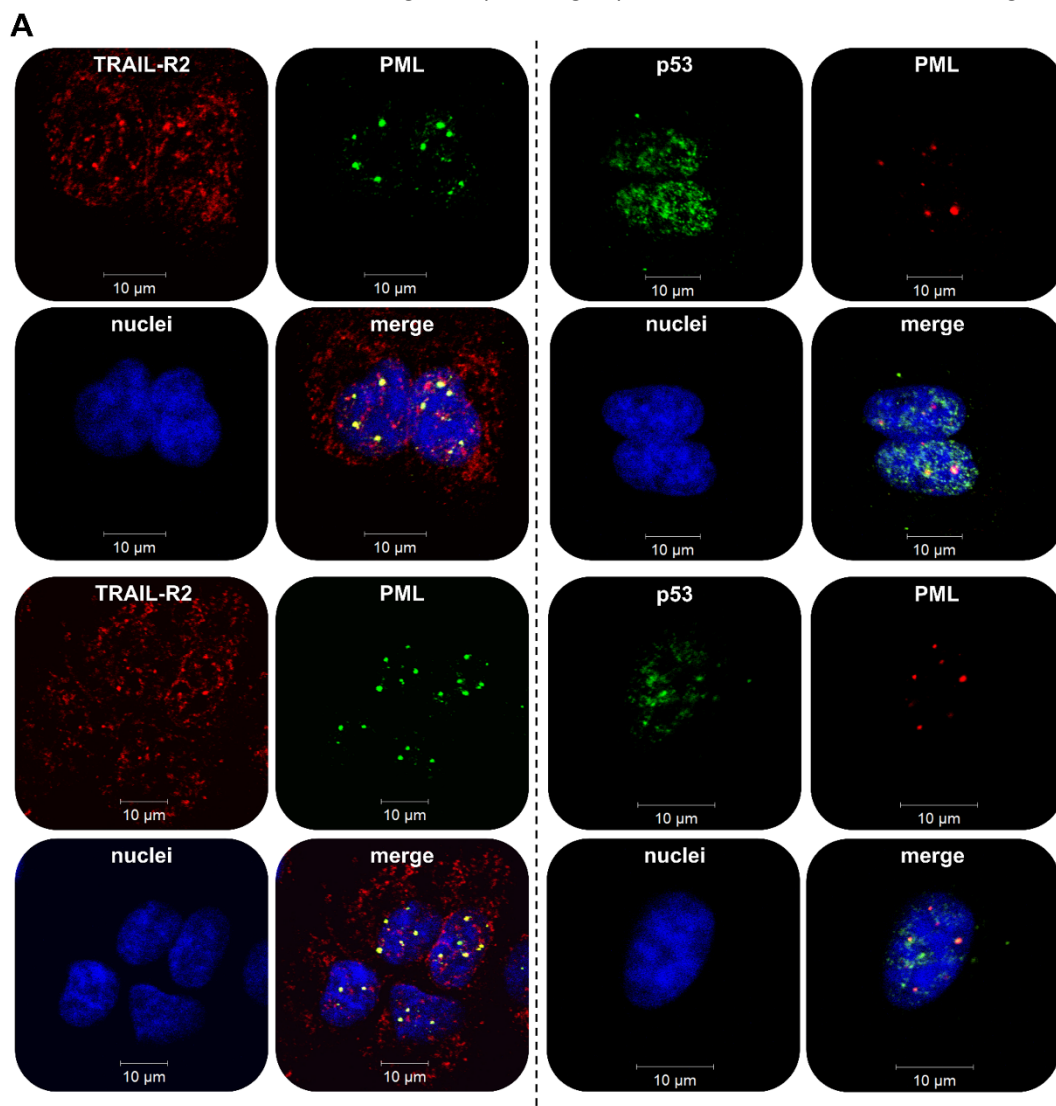


Figure 23: siRNA-mediated knockdown of HMGA2 does not affect increased p53 stability in A549 TRAIL-R2 KO cells

A549 WT and TRAIL-R2 KO cells were transiently transfected with control siRNA (siCtrl) or HMGA2 siRNA (siHMGA2). After 24 h, 48 h and 72 h whole cell lysates were analyzed by western blotting for the protein levels of MDM2, p53, HMGA2 and p21. The level of β -Actin was determined in parallel and served as loading control. WT, wild type; TR2 KO, TRAIL-R2 knockout.

4.5.7 TRAIL-R2 co-localizes with PML protein in distinct nuclear domains

The staining pattern of nuclear p53 and TRAIL-R2 showed a co-localization of both in distinct sub-nuclear regions that resemble PML NBs. PML NBs are membraneless super-assembled subnuclear organelles that play a key role in governing the recruitment, stability and function of nuclear proteins such as p53 [110,111,144]. Among other mechanisms, PML NBs can activate p53 by inhibiting MDM2 [107]. Given the pivotal role of PML in controlling p53 and MDM2 activity and based on the staining pattern of p53 and nTRAIL-R2 revealing their co-localization in distinct sub-nuclear regions (see Fig. 9), immunofluorescence stainings of A549



(Figure 24 continued next page)

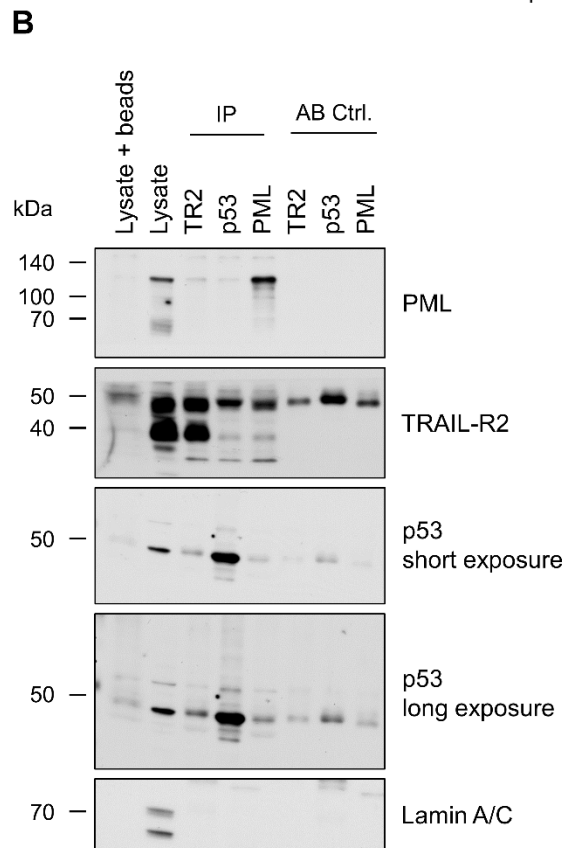


Figure 24: TRAIL-R2 co-localizes and interacts with PML in the nucleus of A549 cells.

(A) Intracellular distribution of TRAIL-R2 (Lexatumumab) and PML (PG-M3) as well as p53 (FL393) and PML (PG-M3) in A549 cells was analyzed by indirect immunofluorescence following confocal laser scanning microscopy.

(B) TRAIL-R2, p53 and PML were precipitated from nuclear fractions of A549 WT cells by specific antibodies (TRAIL-R2, HS201; p53, DO-1; PML, PG-M3). As controls nuclear fraction and beads as well as antibodies and beads were analyzed in parallel. Protein complexes were examined by western blotting. Exposure = decreased/increased time of light exposure for signal detection. AB Ctrl, antibody control.

cells for PML, TRAIL-R2 and p53 were performed. Immunofluorescence stainings displayed PML in distinct nuclear dots and in numerous of these co-localizing with TRAIL-R2 as well as p53 (Fig. 24A). In order to support a potential TRAIL-R2-PML interaction, immunoprecipitation of TRAIL-R2, p53 and PML from nuclear extracts of A549 WT cells were performed and protein complexes were analyzed by western blotting (Fig. 24B). In accordance with immunofluorescence stainings, PML protein was detected in a complex with both p53 and TRAIL-R2 (Fig. 24B).

In summary, TRAIL-R2 co-localizes and interacts with PML in the nucleus of A549 WT cells implying a potential involvement of PML NBs in the TRAIL-R2-p53 regulatory pathway.

To gain an insight into a potential involvement of PML in the TRAIL-R2-p53 regulatory axis, next it was investigated, whether the disruption of PML-NBs could affect the impact of TRAIL-R2 on p53 protein level. Therefore A549 cells were treated with arsenic trioxide (ATO), an agent that leads to the oxidation of PML followed by its oligomerization, polyubiquitination

and subsequent degradation [145,146]. Within 4 h of ATO treatment, oligomers and polyubiquitination products of PML at molecular weights higher than 170 kDa were formed and degraded between 8 h and 24 h of ATO treatment (Fig. 25A). Interestingly, the levels of PML protein in all its variants between 70 and 110 kDa [147] were lower in A549 WT cells when compared to TRAIL-R2 KO cells. After 4 h treatment with ATO a slightly different band pattern was seen and a portion of the 110 kDa PML protein [147] was more resistant to ATO treatment until 24 h. Importantly, in control cells the amount of p53 protein as well as the expression of TRAIL-R2 increased along with the loss of PML during ATO treatment. Such effect of ATO on p53 was not visible in TRAIL-R2 KO A549 cells. Thus, under conditions of PML NB destruction, the expression level of TRAIL-R2 and p53 were not reciprocal as seen under regular conditions, indicating that p53 degradation is not forced by TRAIL-R2 anymore. In order to confirm the role of PML in the TRAIL-R2-mediated p53 destabilization, its expression in A549 cells was knocked down by siRNA (Fig. 25B). Along with the considerable loss of PML after siRNA treatment for 48 h and 72 h, the protein level of p53 in A549 WT cells was clearly elevated. By contrast, in TRAIL-R2 KO cells, the higher level of p53 observed in untreated cells was not affected by the knockdown of PML. This again indicates that the effect of TRAIL-R2 on the stability of p53 depends on PML. Therefore, TRAIL-R2 likely modulates the PML-p53 axis to facilitate inhibition of p53 in cancer cells.

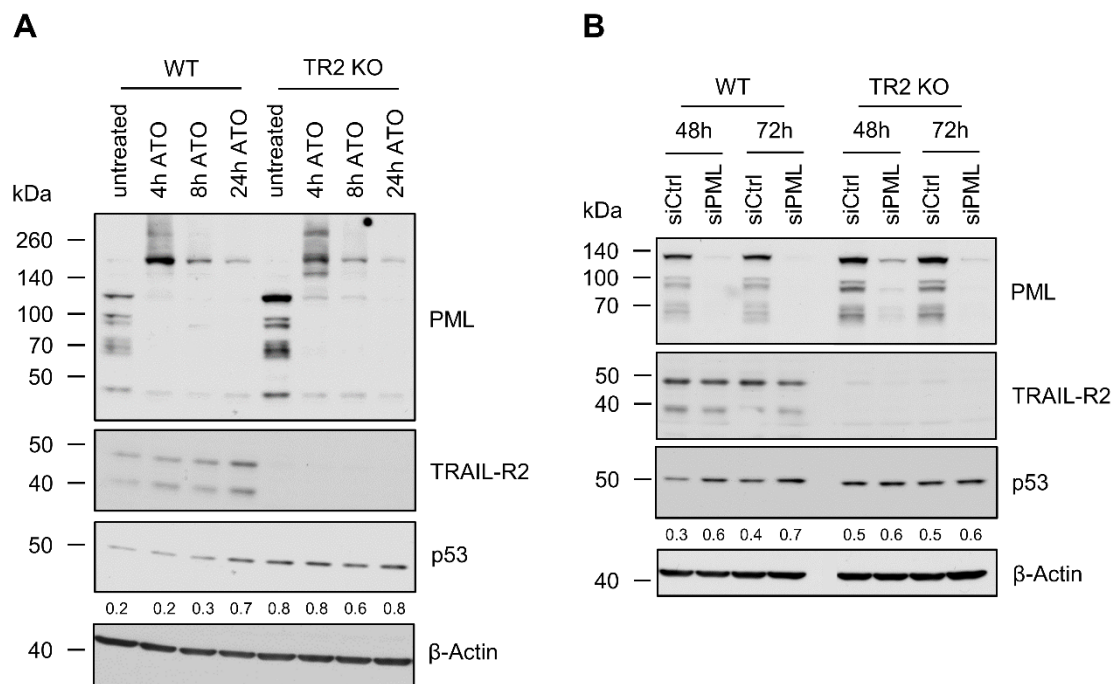


Figure 25: TRAIL-R2-mediated decrease of p53 stability depends on PML.

(A) A549 WT and TRAIL-R2 KO cells were treated with Arsenic trioxide (ATO; 5 μ M) for indicated time periods. The expression of PML, TRAIL-R2 and p53 was analyzed in whole cell lysates by western blotting. **(B)** A549 WT and TRAIL-R2 KO cells were transiently transfected with PML siRNA (siPML) or control siRNA (siCtrl). Protein levels of PML, TRAIL-R2 and p53 were analyzed by western blotting 48 h and 72 h after transfection. The level of β -Actin was determined in parallel and served as loading control. P53 protein level was quantified by densitometry and normalized to β -Actin. ATO, Arsenic trioxide; WT, wild type; TR2 KO, TRAIL-R2 knockout.

5. Discussion

It has been shown that binding of TRAIL to its plasma membrane receptors TRAIL-R1 and TRAIL-R2 induces apoptosis in neoplastic cells but not in normal, healthy cells [54,55]. Accordingly, this biological principle has been exploited for the development of cancer-selective therapeutic strategies. However, many tumor cells are either primarily resistant to TRAIL or rapidly acquire resistance. In addition to their ability to trigger the apoptotic pathway, TRAIL-Rs also activate various pro-inflammatory signal transduction pathways such as NF- κ B, MAP-Kinases, Src and AKT which promote invasion, migration and metastasis in apoptosis resistant cancers [33–40,43]. These TRAIL induced functions of TRAIL-Rs are linked to their presence at the plasma membrane. In addition to a plasma membrane localization TRAIL-Rs are also present intracellularly in the cytosol and nucleus. In the nucleus TRAIL-R2 was shown to execute tumor promoting functions by regulating the maturation of miRNA let-7, which in turn is a known negative regulator of the expression of various proliferation-driving proteins [48]. Consistently, a high intracellular abundance of TRAIL-R2 was correlated with worse patient prognosis [46]. Nevertheless, the functions of nTRAIL-R2 are still not understood in detail by now. Recently, TRAIL death receptors were reported to associate with the chromatin fraction indicating that this is just the beginning of the story about the functions of these proteins in their nuclear localization. In fact, in the present study a novel mechanism was uncovered how nTRAIL-R2 executes its tumor promoting function. TRAIL-R2 interacts with the tumor suppressor protein p53 in the nucleus, destabilizes p53 protein and thereby inhibits its transcriptional output. Thus, nTRAIL-R2 is a novel negative regulator of tumor suppressor protein p53.

5.1 Interrelationship between TRAIL-R2 and p53

The essential role of tumor suppressor protein p53 in human tumorigenesis is widely accepted. Commonly, p53 functions are compromised in tumor cells as a result of mutations or protein inactivation. As a consequence of p53 dysregulation hallmarks of cancer are affected, including apoptosis resistance, uncontrolled cell proliferation as well as activation of migration and invasion [69]. The recovery of p53's tumor suppressor activity is an effective strategy for cancer treatment. Consequently, multiple chemotherapeutic agents intent to activate wild type p53. Activated p53 induces the expression of several transcriptional targets, including TRAIL-R2, in order to sensitize the cells to TRAIL-mediated apoptosis [75]. The combination of TRAIL with chemotherapeutic agents was shown to be particularly effective in killing malignant cells that express wild type p53, presumably through induction of TRAIL-R2 cell surface expression [148]. Interestingly, the present study indicates that p53 activation by chemotherapeutic agent 5-FU also enhances the presence of TRAIL-R2 in the nucleus of A549

cells. Furthermore, a co-localization as well as an interaction of TRAIL-R2 and p53 in the nucleus of A549 cells was uncovered by immunofluorescence and immunoprecipitation analysis. Similar results were obtained for HCT116 and AsPC-1 cells (unpublished data), suggesting that the interaction of TRAIL-R2 and p53 occurs in tumor cells from different cancer entities. nTRAIL-R2 and p53 were both shown to interact with the components of the microprocessor complex Drosha and p68 thereby interfering with the miRNA biogenesis machinery [48,149]. Therefore, the presence of TRAIL-R2 and p53 in protein complexes containing interaction partners of both of them, might explain the observed interaction. To clarify whether the TRAIL-R2-p53 interaction is based on direct or indirect protein-protein association as well as whether this is restricted to wild type p53 needs further examinations. Nevertheless, also a functional interrelation between TRAIL-R2 and p53 has been identified in A549 and HCT116 cells. Knockout/ knockdown of TRAIL-R2 was associated with elevated p53 protein levels as well as an increased expression of its targets p21, MDM2 and BAX in A549 and HCT116 cells. *Vice versa*, overexpression of TRAIL-R2, either short or long isoforms, decreased the protein levels of p53 as well as p21 and MDM2 in A549 cells. Consistent with the role of p53 as a transcriptional regulator of p21, MDM2 and BAX expression, the enhanced p53 levels observed in TRAIL-R2 knockout cells correlated with significantly increased mRNA levels of p21, MDM2 and BAX. In accordance, ChIP analysis revealed a higher abundance of p53 at the p21 promoter in A549 TRAIL-R2 KO cells compared to WT cells. These observations are confirmed by dual luciferase reporter gene assays performed in HCT116 cells (unpublished data). Constructs containing a luciferase gene under the control of the p21 promoter were analyzed in HCT116 p53 wildtype and HCT116 p53 knockout cells with or without transient TRAIL-R2 knockdown. Knockdown of TRAIL-R2 led to the activation of the p21 promoter in HCT116 p53 wild type cells, but no difference in luciferase activity could be detected between control and TRAIL-R2 knockdown in HCT116 p53 knockout cells. Taken together, these results strongly indicate that TRAIL-R2 modulates p53 protein levels and thereby its transcriptional output. Even more important, this might result in a functional readout, since knockout of TRAIL-R2 in A549 cells led to cell cycle arrest in G1-phase. Similar results could be obtained with HCT116 cells (unpublished data). The cell cycle arrest might be explained by the elevated p21 levels in these cells, since the function of p21 as an inhibitor of cell cycle progression is well established [150]. Consequently, nTRAIL-R2 might benefit WT p53-expressing cancer cells by regulating p53 levels and its transcriptional outcome thereby promoting proliferation.

Recently, caspase-8, which is well known for its cytosolic function as a mediator of death receptor signaling, was identified as a novel negative regulator of p53 in human cancers [151–153]. In the nucleus, caspase-8 cleaves the ubiquitin-specific peptidase 28 (USP28) thereby inactivating its de-ubiquitinating activity leading to p53 destabilization. Depletion of caspase-8 was correlated with G2/ M arrest, stabilization of p53 and induction of p53-dependent intrinsic

apoptosis in malignant cells. Hence, this novel non-canonical role of nuclear caspase-8 results in degradation of p53 protein shifting cell fate from apoptosis towards mitosis. In line with this mechanism, in multiple tumors an upregulated expression and nuclear localization of caspase-8 was observed, which was correlated with treatment resistance and poor clinical outcome [153]. On the basis of the described role of nuclear caspase-8 on p53 stability, it was analyzed whether caspase-8 activation functions as a mediator of TRAIL-R2 induced p53 destabilization. Interestingly, data presented in figure 12 and 13 suggest that the TRAIL-R2-mediated reduction of p53 stability does not depend on this non-canonical function of nuclear caspase-8. Firstly, a mutation, which abolishes caspase-8 activation in the DD of the overexpressed TRAIL-R2 constructs, and secondly, treatment with the broad-spectrum caspase inhibitor zVAD-fmk, could not impede the impact of TRAIL-R2 on p53. Hence, caspase-8 has no mediatory function between TRAIL-R2 and p53.

Since TRAIL ligation to its receptors can induce multiple signaling pathways [33–38,40], but also the translocation of TRAIL-Rs from the plasma membrane to the nucleus [47], the role the ligand has to be taken into consideration when investigating the functions of TRAIL-Rs. Receptor translocation is TRAIL dose dependent and can be inhibited by antibody that is able to neutralize TRAIL. Moreover, recombinant TRAIL as well as endogenous TRAIL co-localize with TRAIL-R1 and TRAIL-R2 in the nucleus, suggesting that the ligand is shuttled bound to its receptors from the plasma membrane to the nucleus [47]. Like TRAIL-R2, TRAIL also belongs to the target genes of p53 [154]. Thus, p53 activation not only enhances the expression levels of TRAIL-R2, but also the levels of its ligand TRAIL. In turn, TRAIL stimulates nuclear translocation of TRAIL-Rs, whereas nTRAIL-R2 inhibits p53, suggesting a negative feedback loop. Therefore, the impact of TRAIL on the interdependence between TRAIL-R2 and p53 was examined by treating A549 cells with recombinant TRAIL or TRAIL neutralizing antibody. Strikingly, neither stimulation of cells with recombinant TRAIL nor treatment with neutralizing TRAIL antibody had an impact on the protein levels of p53 and its targets in A549 WT and TRAIL-R2 KO cells. In accordance, treatment of A549 WT and TRAIL-R2 KO cells with neutralizing anti-TRAIL antibody had no influence on the amount of p53 recruited to the p21 promoter. Experiments with luciferase gene reporter assays under control of the p21 promoter in HCT116 cells supported these observations, since treatment with neutralizing anti-TRAIL antibody had no impact on the p53-mediated activation of the p21 promoter in these cells (unpublished data). In line with that, previously uncovered intracellular functions of TRAIL-Rs were also described to be TRAIL-independent. This includes, TRAIL-R1 and TRAIL-R2 cytoplasmic actions during unfolded protein response (UPR) contributing to unresolved ER stress-induced cell death [51,52]. Here, it has been shown that misfolded proteins can act as ligands to activate cytoplasmic TRAIL-R2 leading to assemble of pro-apoptotic caspase-8-activating complexes [53]. Moreover, the interference of nTRAIL-R2 with the microprocessor complex and the thereof resulting inhibition of let-7 miRNA maturation

was also shown to be independent of TRAIL. Blocking endogenous TRAIL by neutralizing antibody had no impact on the intracellular distribution of TRAIL-R2, the expression level of let-7 target HMGA2 and cell proliferation [48].

Taken together, TRAIL-R2 and p53 interact with each other in the nucleus of cells from different tumor entities, where TRAIL-R2 impacts p53 protein levels as well as its transcriptional output independent of caspases and TRAIL.

5.2 TRAIL-R2 destabilizes p53 protein

p53 expression is tightly regulated on protein level, e.g. by various post-translational modifications such as ubiquitination, phosphorylation and acetylation [83]. In unstressed cells, p53 is kept at low levels through its continuous degradation via the UPS, whereas upon cellular stress p53 degradation is attenuated. In line with these well-established observations, p53 was almost fully degraded in A549 and HCT116 control cells 1 h after treatment with CHX, an inhibitor of *de novo* protein biosynthesis. Importantly, the half-life of p53 was prolonged to at least 4 h in TRAIL-R2 knockout/ knockdown A549 and HCT116 cells. Notably, knockout/ knockdown of TRAIL-R2 had no impact on the mRNA level of p53 suggesting that TRAIL-R2 does not interfere with p53 transcription, but rather destabilizes p53 protein. This hypothesis is confirmed by experiments using the 26S proteasome inhibitor MG132. Blocking of the proteasomal degradation pathway resulted in p53 protein accumulation, as described previously [155], and even more important, MG132 treatment abolished the difference in p53 protein level between control and TRAIL-R2 knockout/ knockdown A549/ HCT116 cells. Thus, blocking the conventional p53 degradation pathway via the UPS prevents TRAIL-R2-mediated p53 destabilization.

Prior to degradation, proteins need to be modified with ubiquitin for the recognition by the proteasome. The regulation of protein degradation by ubiquitination is a mechanism known for a broad range of proteins. A key regulator of p53 ubiquitination is MDM2 [92,93]. Upon binding, MDM2 ubiquitylates p53 leading to its proteasomal degradation. Therefore, the role of MDM2 in TRAIL-R2-mediated p53 destabilization was addressed by usage of the small molecule inhibitor Nutlin 3a, an agent which specifically binds to the p53-binding pocket on MDM2 thereby blocking MDM2-p53 interaction. Nutlin 3a treatment, abolished the difference in p53 protein level between A549 control and TRAIL-R2 KO cells. This observation raises the hypothesis that TRAIL-R2 plays a regulatory role in MDM2-mediated p53 ubiquitination.

The modulation of MDM2 activity as a mechanism to escape p53 tumor suppressor functions was described previously in cancer. For instance, Chao *et al.* showed that overexpressed pleckstrin homology domain-containing protein (PHLDB3) reduces p53 protein levels via binding to MDM2, thereby, promoting MDM2-mediated ubiquitination and degradation of p53. Thus, PHLDB3 overexpression increases proliferation and impedes apoptosis induction of wild

type p53 harboring cancer cells. In addition, PHLDB3 was identified as a p53 target, suggesting a regulatory feedback loop [156]. A related mechanism was described for another protein. The ankyrin repeat oncoprotein gankyrin, which is commonly expressed at high levels in hepatocellular carcinomas, binds to MDM2, facilitates p53-MDM2 binding and thereby increases ubiquitination and degradation of p53. Moreover, gankyrin enhances MDM2 auto-ubiquitination in the absence of p53 [157]. Sui *et al.* found that the transcription factor YY1 (Yin Yang 1) forms a ternary complex with p53 and MDM2, thereby promoting MDM2-mediated p53 ubiquitination [158]. Moreover, Wu *et al.* reported that UBE4B (ubiquitination factor E4B) promoted p53 degradation in a similar manner in brain tumors [159].

Although immunofluorescence analysis displayed that TRAIL-R2 and MDM2 co-localize or at least occur in the same protein clusters, an interaction of both proteins could not be confirmed by immunoprecipitation experiments. Thus, the destabilizing effect of TRAIL-R2 on p53 seems to depend on MDM2, but the lack of TRAIL-R2-MDM2 interaction suggests mechanisms different from that utilized by PHLDB3, gankyrin, YY1 and UBE4B. Nevertheless, MDM2-regulated p53 turnover has been shown to be affected by several other proteins, of which some will be discussed in the following sections concerning their potential role in the TRAIL-R2-MDM2-p53 regulatory axis.

5.3 TRAIL-R2 destabilizes p53 independent of deubiquitinases

Besides ubiquitin ligases, p53 stability is also regulated by ubiquitin peptidases like USP10 [104]. USP10 specifically deubiquitinates p53 and this way counteracts MDM2-mediated ubiquitination and degradation of p53 [104]. In the present study USP10 was shown to co-localize and co-precipitate with TRAIL-R2 in A549 cells pointing to a possible role of USP10 in TRAIL-R2-mediated destabilization of p53. Here, TRAIL-R2 might block the interaction between USP10 and p53 thereby inhibiting USP10 deubiquitination activity on p53 and promotes p53 proteasomal degradation. Consequently, TRAIL-R2 deficiency would rescue USP10-p53 association and thereby indirectly stabilize p53 protein. Supporting this hypothesis, USP10-p53 co-precipitation was only detected in lysates from A549 TRAIL-R2 KO cells but not in lysates from control cells. Moreover, p53 levels were slightly decreased in both A549 WT and TRAIL-R2 KO cells due to siRNA-mediated USP10 knockdown, suggesting that USP10 plays a role in the regulation of p53 stability in both cell lines. However, A549 WT and TRAIL-R2 KO cells showed still a difference in p53 protein level after USP10 knockdown. This could be explained by some extant USP10 which might compensate USP10 downregulation. Moreover, besides USP10 other deubiquitinases are also able to regulate p53 ubiquitination, such as HAUSP [102]. In order to examine the role of deubiquitinases in the TRAIL-R2-mediated p53 destabilization, A549 cells were treated with the pan-deubiquitinase inhibitor

PR-619. However, blocking deubiquitinases did not affect the difference of p53 protein stability in A549 control and TRAIL-R2 KO cells.

Under unstressed conditions USP10 is mainly localized in the cytosol, where it deubiquitinates p53 enabling its re-entry into the nucleus. Upon DNA damage, ATM phosphorylates USP10 inducing its translocation to the nucleus, where it deubiquitinates and activates p53 [104]. Interestingly, the present study revealed that the intracellular distribution of USP10 varied in dependence of the TRAIL-R2 status in A549 cells. Concretely, cell fractionation experiments showed an increased abundance of USP10 in the nucleus of A549 TRAIL-R2 KO cells compared to control cells, while the total USP10 protein level was not altered. Therefore, the increased nuclear USP10 levels in TRAIL-R2 KO cells suggest that either the DNA damage response is induced or at least ATM is activated in TRAIL-R2 KO cells in comparison to WT cells. In turn, this assumption implies that TRAIL-R2 somehow inhibits the DNA damage response or at least USP10 phosphorylation and translocation to the nucleus. ATM persists in an inactive state in resting cells but can be activated by a complex composed of meiotic recombination 11 homolog 1 (MRE11), DNA repair protein RAD50, and phosphopeptide-binding Nijmegen breakage syndrome protein 1 (NBS1). The Mre11–Rad50–Nbs1 (MRN) complex plays a key role in the initial and sustained responses to DNA double-strand breaks, stalled replication forks, dysfunctional telomeres and viral DNA infection [160]. P53 is well known for its role as a main regulator in the cellular response to DNA damage. Several mechanisms have been shown to stabilize and activate p53 after DNA damage including its phosphorylation by ATM which inhibits MDM2 binding [161,162].

In summary, deubiquitinases are not involved in the TRAIL-R2-p53 feedback loop, but the intracellular distribution of USP10 seems to be affected by the TRAIL-R2 status. Certainly, this observation needs further investigation and will be part of future studies.

5.4 TRAIL-R2 impacts p53 independent of HMGA2

HMGA2 was described to directly interact via its three AT-hook domains (amino acids 1-83) with p53's tetramerization domain (amino acids 294-393) in colon carcinoma HCT116, LoVo and RKO cells. Moreover, HMGA2 associates with the central acidic and zinc finger domains of MDM2 (amino acids 111-360). Within this protein complex HMGA2 promotes MDM2-mediated p53 ubiquitination and degradation [143]. Consequently, elevated HMGA2 levels have been shown to promote colorectal cancer aggressiveness by modulation of the transcription of p53 target genes as well as cell cycle progression and inhibition of apoptosis [143,163,164]. Another member of the HMGA family, high mobility group A1 (HMGA1) was also described as an oncogene. Interestingly, HMGA1 associates with the tetramerization domain of p53 in thyroid cancer cells. HMGA1-p53 interaction resulted in a reduced p53 DNA-binding activity, subsequently inhibiting target gene expression [165]. TRAIL-R2 interacts with

components of the microprocessor complex thereby inhibiting the maturation of miRNA let-7. This leads in particular to an enhanced expression of let-7 targets Lin28B and HMGA2 [48]. Hence, the already known link between TRAIL-R2, HMGA2 and p53 raised the hypothesis that nTRAIL-R2 indirectly interferes with p53 protein degradation via promoting HMGA2 expression.

Indeed, WT cells showed higher HMGA2 levels than TRAIL-R2 KO cells and TRAIL-R2 overexpression was associated with increased HMGA2 levels. In order to address the role of HMGA2 on p53 stability in the potential MDM2-TRAIL-R2-p53 interaction network of the present cell system, HMGA2 siRNA-mediated knockdown experiments were performed. Interestingly, HMGA2 knockdown did not lead to the expected elevated, but to diminished p53 protein level in control cells. In contrast, p53 protein level was hardly affected by HMGA2 knockdown in TRAIL-R2 KO cells, presumably because of the low HMGA2 basal level in these cells.

In conclusion, these data suggest that TRAIL-R2 mediates p53 destabilization independent of HMGA2 in A549 cells. Moreover, the previously described impact of HMGA2 on p53 stability in colon cancer cells could not be observed in A549 lung carcinoma cells.

5.5 TRAIL-R2 interacts with PML

PML NBs are spheres associated with the nuclear matrix. PML is the key organizer of these domains recruiting a variety of proteins. Functionally, PML bodies can sequester, modify or degrade partner proteins and were proposed to regulate multiple nuclear functions [111]. Consistently, numerous p53 regulators, including ATM, ATR, Chk2, SIRT1, HIPK2, HAUSP and MDM2, are found in PML NBs that are organized in response to cellular stress [110,166,167]. PML can protect p53 from MDM2-mediated ubiquitination and subsequent degradation by recruiting Chk2 and p53 into PML NBs. Thereby, PML promotes p53-Chk2 interaction, which in turn causes a prolonged stress-induced phosphorylation of p53 on serine 20, a site of Chk2. Phosphorylation of p53 on serine 20 inhibits p53-MDM2 interaction protecting p53 from ubiquitination and subsequent proteasomal degradation [108]. HIPK2 enhances p53-dependent transcription by phosphorylating p53 at serine 46 in PML NBs [168]. Moreover, PML can directly inhibit MDM2-mediated ubiquitination of p53 via binding to MDM2 [107]. In addition, PML enhances p53 stability by sequestering MDM2 to the nucleolus in response to DNA damage [169]. In order to adjust p53 activity, MDM2 can be released from PML via activation of big MAP kinase 1 (BMK1) which disrupts PML-MDM2 interaction [170]. Thus, in dependence of the architecture of NBs, PML is able to induce both, p53 stabilization and destabilization. Interestingly, in the present study immunofluorescence and immunoprecipitation experiments, identified TRAIL-R2 as a novel potential interaction partner of PML. Moreover, PML knockdown as well as PML NB disruption by ATO led to an increased

p53 protein level in TRAIL-R2-expressing cells to similar extent as the knockout of TRAIL-R2 itself, whereas no alteration of p53 level was seen by PML knockdown in TRAIL-R2 KO cells. This indicates that the TRAIL-R2-mediated decrease of p53 stability depends on PML. Given the pivotal role of PML in controlling p53 stability, PML might be involved in TRAIL-R2-mediated destabilization of p53. A recent study reported that mitotic arrest deficient 1 (Mad1), which is frequently upregulated in human breast cancer, is able to displace MDM2 from PML, favoring p53 ubiquitination and triggering tumorigenesis [171]. Mad1 interacts with its C-terminal SUMO-interacting motif (SIM) domain with SUMO (small ubiquitin-related modifier) chains on PML N-terminus. These PML SUMO chains are frequently used by other proteins to bind to PML NBs [111]. Whether the interaction of TRAIL-R2 with PML involves sumoylation, as well as whether the structure of TRAIL-R2 contains a putative SIM needs further investigations. Mad1 induces p53 destabilization by displacing MDM2 from nucleoli through direct binding to PML after DNA damage. Consequently, Mad1 indirectly attenuates p53 stability and p21 expression, a mechanism that causes inhibition of the DNA damage induced cell death *in vitro* and promotes orthotopic mammary tumor growth *in vivo* [171].

In order to examine whether TRAIL-R2 might affect p53 similar to Mad1 further investigations are needed, which address whether PML is critical for TRAIL-R2-p53 interaction, whether TRAIL-R2 affects MDM2 distribution and in particular, whether this leads to tumor progression by inhibition of the DNA damage response. Moreover, since PML NBs play a key role in multiple cellular pathways including transcriptional regulation, DNA damage responses, cell proliferation, apoptosis and viral infection defence [110,111,172,173], nTRAIL-R2 might impact far more than p53 stability by modulating PML NBs.

6. Conclusion

TRAIL-R2 is commonly expressed at high levels in malignant cells but is mainly localized to the nucleus. A high intracellular abundance of TRAIL-R2 was correlated with worse patient prognosis. One mechanism by which nTRAIL-R2 executes its tumor promoting functions represents the regulation of the maturation of miRNA let-7, which in turn is a known negative regulator of the expression of various proliferation-driving proteins [48]. A second mechanism, how TRAIL-R2 executes its tumor promoting functions, could be uncovered in the present study. This mechanism is based on a regulatory feedback signaling loop between nTRAIL-R2 and p53 in wild type p53 expressing cancer cells. In this model, activated p53 transcriptionally upregulates TRAIL-R2 expression. Increased TRAIL-R2 expression subsequently leads to elevated levels of nTRAIL-R2, which destabilizes p53 involving the activity of the ubiquitin ligase MDM2. Consequently, p53 becomes degraded by the proteasome and cannot exert its tumor suppressive functions. In addition, TRAIL-R2 was identified as a novel interaction partner of PML, which represents the core component of PML NBs. Given the pivotal role of PML in controlling p53 and MDM2 activity, PML might be involved in TRAIL-R2-mediated destabilization of p53 and/ or might function as a platform that facilitates TRAIL-R2-p53-MDM2 interaction (Fig. 26).

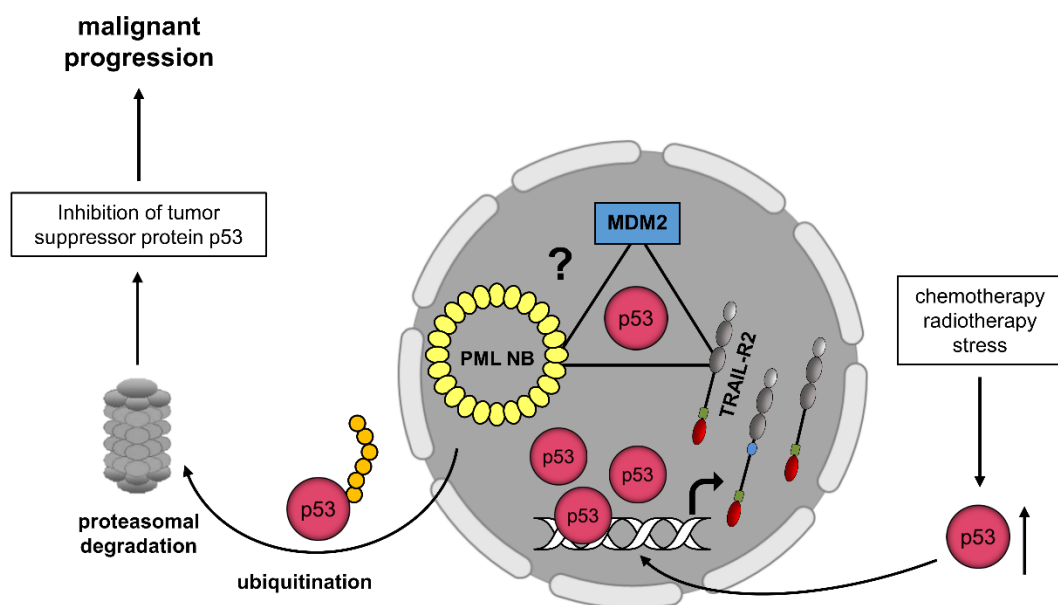


Figure 26: TRAIL-R2 is a negative regulator of p53.

In its nuclear location, TRAIL-R2 interacts with the tumor suppressor protein p53. This interaction causes the destabilization of p53 and its subsequent proteasomal degradation. Thereby, nTRAIL-R2 interferes with the tumor suppressor function of wildtype p53. Ubiquitin ligase MDM2 and PML might assist TRAIL-R2. Since p53 is a positive regulator of TRAIL-R2 expression and chemotherapy leads to the activation of p53, this regulatory p53-nTRAIL-R2 feedback signaling might represent a crucial mechanism how malignant cells expressing wild type p53 escape p53-mediated tumor suppression and acquire an even more aggressive phenotype.

The common abundance of p53 mutations in various tumor entities and the role of p53 in a comprehensive network of cellular signaling pathways clearly highlights the importance of p53 tumor suppressor functions in cancer development. A detailed understanding of p53 signaling pathways as well as the complex regulation of p53 protein stability and activity is essential for the improvement of existing, and the development of future cancer therapy strategies, including powerful drug combinations that increase the selectivity and safety of chemotherapy by ensuring the protection of normal cells and tissues.

In conclusion, the uncovered potential nTRAIL-R2-p53 regulatory feedback signaling loop might represent a crucial mechanism by which malignant cells expressing wild type p53 could escape p53-mediated tumor suppression and acquire an even more aggressive phenotype. Moreover, this mechanism might provide an explanation for the correlation between a high intracellular abundance of TRAIL-R2 and worse patient prognosis. Since chemo- and radiotherapy in cancer treatment are known to activate p53 in wild type p53 tumor cells, this mechanism potentially has a serious impact on tumor evolution under common therapeutic regimens. However, it still has to be examined whether nTRAIL-R2 and p53 interact directly or indirectly and whether other regulators like MDM2 and PML are involved in the interaction. Even more important, understanding the detailed mechanism(s) by which nTRAIL-R2 destabilizes p53, might open opportunities to develop pharmacological inhibitors and a novel targeted therapeutic intervention in the future.

7. References

1. Wiley, S.R.; Schooley, K.; Smolak, P.J.; Din, W.S.; Huang, C.P.; Nicholl, J.K.; Sutherland, G.R.; Smith, T.D.; Rauch, C.; Smith, C.A.; et al. Identification and characterization of a new member of the TNF family that induces apoptosis. *Immunity* **1995**.
2. Kawakubo, T.; Okamoto, K.; Iwata, J.I.; Shin, M.; Okamoto, Y.; Yasukochi, A.; Nakayama, K.I.; Kadowaki, T.; Tsukuba, T.; Yamamoto, K. Cathepsin E prevents tumor growth and metastasis by catalyzing the proteolytic release of soluble TRAIL from tumor cell surface. *Cancer Res.* **2007**.
3. Zou, J.; Zhu, F.; Liu, J.; Wang, W.; Zhang, R.; Garlisi, C.G.; Liu, Y.H.; Wang, S.; Shah, H.; Wan, Y.; et al. Catalytic Activity of Human ADAM33. *J. Biol. Chem.* **2004**.
4. Pan, G.; Ni, J.; Wei, Y.F.; Yu, G.I.; Gentz, R.; Dixit, V.M. An antagonist decoy receptor and a death domain-containing receptor for TRAIL. *Science (80-.).* **1997**.
5. Walczak, H.; Degli-esposti, M.A.; Johnson, R.S.; Smolak, P.J.; Waugh, J.Y.; Boiani, N.; Timour, M.S.; Gerhart, M.J.; Schooley, K.A.; Smith, C.A.; et al. TRAIL-R2: a novel apoptosis-mediating receptor for. **1997**, *16*, 5386–5397.
6. Mongkolsapaya, J.; Grimes, J.M.; Chen, N.; Xu, X.N.; Stuart, D.I.; Jones, E.Y.; Screaton, G.R. Structure of the TRAIL-DR5 complex reveals mechanisms conferring specificity in apoptotic initiation. *Nat. Struct. Biol.* **1999**, *6*, 1048–1053.
7. Emery, J.G.; McDonnell, P.; Burke, M.B.; Deen, K.C.; Lyn, S.; Silverman, C.; Dul, E.; Appelbaum, E.R.; Eichman, C.; DiPrinzio, R.; et al. Osteoprotegerin is a receptor for the cytotoxic ligand TRAIL. *J. Biol. Chem.* **1998**.
8. Ashkenazi, A. Targeting death and decoy receptors of the tumour-necrosis factor superfamily. *Nat. Rev. Cancer* **2002**.
9. LeBlanc, H.N.; Ashkenazi, A. Apo2L/TRAIL and its death and decoy receptors. *Cell Death Differ.* **2003**, *10*, 66–75.
10. Merino, D.; Lalaoui, N.; Morizot, A.; Schneider, P.; Solary, E.; Micheau, O. Differential Inhibition of TRAIL-Mediated DR5-DISC Formation by Decoy Receptors 1 and 2. *Mol. Cell. Biol.* **2006**, *26*, 7046–7055.
11. Sanlioglu, A.D.; Korcum, A.F.; Pestereli, E.; Erdogan, G.; Karaveli, S.; Savas, B.; Griffith, T.S.; Sanlioglu, S. TRAIL death receptor-4 expression positively correlates with

- the tumor grade in breast cancer patients with invasive ductal carcinoma. *Int. J. Radiat. Oncol. Biol. Phys.* **2007**, *69*, 716–23.
12. Lalaoui, N.; Morlé, A.; Mérino, D.; Jacquemin, G.; Iessi, E.; Morizot, A.; Shirley, S.; Robert, B.; Solary, E.; Garrido, C.; et al. TRAIL-R4 Promotes Tumor Growth and Resistance to Apoptosis in Cervical Carcinoma HeLa Cells through AKT. *PLoS One* **2011**, *6*, e19679.
 13. Takahashi, N.; Udagawa, N.; Suda, T. A New Member of Tumor Necrosis Factor Ligand Family, ODF/OPGL/TRANCE/RANKL, Regulates Osteoclast Differentiation and Function. *Biochem. Biophys. Res. Commun.* **1999**, *256*, 449–455.
 14. Simonet, W.S.; Lacey, D.L.; Dunstan, C.R.; Kelley, M.; Chang, M.S.; Lüthy, R.; Nguyen, H.Q.; Wooden, S.; Bennett, L.; Boone, T.; et al. Osteoprotegerin: A novel secreted protein involved in the regulation of bone density. *Cell* **1997**.
 15. Wu, G.S.; Burns, T.F.; Zhan, Y.; Alnemri, E.S.; El-Deiry, W.S. Molecular cloning and functional analysis of the mouse homologue of the KILLER/DR5 tumor necrosis factor-related apoptosis-inducing ligand (TRAIL) death receptor. *Cancer Res.* **1999**.
 16. Wang, T.T.Y.; Jeng, J. Coordinated regulation of two TRAIL-R2/KILLER/DR5 mRNA isoforms by DNA damaging agents, serum and 17 β -estradiol in human breast cancer cells. *Breast Cancer Res. Treat.* **2000**.
 17. Falschlehner, C.; Schaefer, U.; Walczak, H. Following TRAIL's path in the immune system. *Immunology* **2009**.
 18. Takeda, K.; Smyth, M.J.; Cretney, E.; Hayakawa, Y.; Kayagaki, N.; Yagita, H.; Okumura, K. Critical role for tumor necrosis factor-related apoptosis-inducing ligand in immune surveillance against tumor development. *J. Exp. Med.* **2002**.
 19. Macher-Goeppinger, S.; Aulmann, S.; Tagscherer, K.E.; Wagener, N.; Haferkamp, A.; Penzel, R.; Brauckhoff, A.; Hohenfellner, M.; Sykora, J.; Walczak, H.; et al. Prognostic value of tumor necrosis factor-related apoptosis-inducing ligand (TRAIL) and TRAIL receptors in renal cell cancer. *Clin. Cancer Res.* **2009**, *15*, 650–659.
 20. Ozawa, F.; Friess, H.; Kleeff, J.; Xu, Z.W.; Zimmermann, A.; Sheikh, M.S.; Büchler, M.W. Effects and expression of TRAIL and its apoptosis-promoting receptors in human pancreatic cancer. *Cancer Lett.* **2001**.
 21. Kretz, A.L.; Trauzold, A.; Hillenbrand, A.; Knippschild, U.; Henne-Bruns, D.; von Karstedt, S.; Lemke, J. Trailblazing strategies for cancer treatment. *Cancers (Basel)*. **2019**.

22. Kerr, J.F.R.; Wyllie, A.H.; Currie, A.R. Apoptosis: A basic biological phenomenon with wide-ranging implications in tissue kinetics. *Br. J. Cancer* **1972**.
23. Dickens, L.S.; Powley, I.R.; Hughes, M.A.; MacFarlane, M. The 'complexities' of life and death: Death receptor signalling platforms. *Exp. Cell Res.* **2012**, *318*, 1269–1277.
24. Dickens, L.S.; Boyd, R.S.; Jukes-Jones, R.; Hughes, M.A.; Robinson, G.L.; Fairall, L.; Schwabe, J.W.R.; Cain, K.; MacFarlane, M. A Death Effector Domain Chain DISC Model Reveals a Crucial Role for Caspase-8 Chain Assembly in Mediating Apoptotic Cell Death. *Mol. Cell* **2012**.
25. Hughes, M.A.; Powley, I.R.; Jukes-Jones, R.; Horn, S.; Feoktistova, M.; Fairall, L.; Schwabe, J.W.R.; Leverkus, M.; Cain, K.; MacFarlane, M. Co-operative and Hierarchical Binding of c-FLIP and Caspase-8: A Unified Model Defines How c-FLIP Isoforms Differentially Control Cell Fate. *Mol. Cell* **2016**.
26. Falschlehner, C.; Emmerich, C.H.; Gerlach, B.; Walczak, H. TRAIL signalling: Decisions between life and death. *Int. J. Biochem. Cell Biol.* 2007.
27. Schug, Z.T.; Gonzalvez, F.; Houtkooper, R.H.; Vaz, F.M.; Gottlieb, E. BID is cleaved by caspase-8 within a native complex on the mitochondrial membrane. *Cell Death Differ.* **2011**, *18*, 538–48.
28. Wei, M.C.; Lindsten, T.; Mootha, V.K.; Weiler, S.; Gross, A.; Ashiya, M.; Thompson, C.B.; Korsmeyer, S.J. tBID, a membrane-targeted death ligand, oligomerizes BAK to release cytochrome c. *Genes Dev.* **2000**.
29. Pan, G.; O'Rourke, K.; Dixit, V.M. Caspase-9, Bcl-X(L), and Apaf-1 form a ternary complex. *J. Biol. Chem.* **1998**.
30. Deveraux, Q.L.; Takahashi, R.; Salvesen, G.S.; Reed, J.C. X-linked IAP is a direct inhibitor of cell-death proteases. *Nature* **1997**.
31. Grootjans, S.; Vanden Berghe, T.; Vandenabeele, P. Initiation and execution mechanisms of necroptosis: An overview. *Cell Death Differ.* 2017.
32. Kretz, A.L.; Von Karstedt, S.; Hillenbrand, A.; Henne-Bruns, D.; Knippschild, U.; Trauzold, A.; Lemke, J. Should we keep walking along the trail for pancreatic cancer treatment? Revisiting TNF-related apoptosis-inducing ligand for anticancer therapy. *Cancers (Basel)*. 2018.
33. Siegmund, D.; Klose, S.; Zhou, D.; Baumann, B.; Röder, C.; Kalthoff, H.; Wajant, H.; Trauzold, A. Role of caspases in CD95L- and TRAIL-induced non-apoptotic signalling

- in pancreatic tumour cells. *Cell. Signal.* **2007**, *19*, 1172–1184.
34. Trauzold, A.; Wermann, H.; Arlt, A.; Schütze, S.; Schäfer, H.; Oestern, S.; Röder, C.; Ungefroren, H.; Lampe, E.; Heinrich, M.; et al. CD95 and TRAIL receptor-mediated activation of protein kinase C and NF- κ B contributes to apoptosis resistance in ductal pancreatic adenocarcinoma cells. *Oncogene* **2001**, *20*, 4258–4269.
 35. Zauli, G.; Sancilio, S.; Cataldi, A.; Sabatini, N.; Bosco, D.; Di Pietro, R. PI-3K/Akt and NF- κ B/I κ B α pathways are activated in Jurkat T cells in response to TRAIL treatment. *J. Cell. Physiol.* **2005**, *202*, 900–911.
 36. Azijli, K.; Yuvaraj, S.; Peppelenbosch, M.P.; Würdinger, T.; Dekker, H.; Joore, J.; van Dijk, E.; Quax, W.J.; Peters, G.J.; de Jong, S.; et al. Kinome profiling of non-canonical TRAIL signaling reveals RIP1-Src-STAT3-dependent invasion in resistant non-small cell lung cancer cells. *J. Cell Sci.* **2012**, *125*, 4651–61.
 37. Azijli, K.; Weyhenmeyer, B.; Peters, G.J.; De Jong, S.; Kruyt, F.A.E. Non-canonical kinase signaling by the death ligand TRAIL in cancer cells: Discord in the death receptor family. *Cell Death Differ.* **2013**, *20*, 858–868.
 38. Trauzold, A.; Siegmund, D.; Schniewind, B.; Sipos, B.; Egberts, J.; Zorenkov, D.; Emme, D.; Röder, C.; Kalthoff, H.; Wajant, H. TRAIL promotes metastasis of human pancreatic ductal adenocarcinoma. *Oncogene* **2006**, *25*, 7434–7439.
 39. von Karstedt, S.; Conti, A.; Nobis, M.; Montinaro, A.; Hartwig, T.; Lemke, J.; Legler, K.; Annenwarter, F.; Campbell, A.D.; Taraborrelli, L.; et al. Cancer Cell-Autonomous TRAIL-R Signaling Promotes KRAS-Driven Cancer Progression, Invasion, and Metastasis. *Cancer Cell* **2015**, *27*, 561–573.
 40. Hoogwater, F.J.H.; Nijkamp, M.W.; Smakman, N.; Steller, E.J.A.; Emmink, B.L.; Westendorp, B.F.; Raats, D.A.E.; Sprick, M.R.; Schaefer, U.; Van Houdt, W.J.; et al. Oncogenic K-Ras Turns Death Receptors Into Metastasis-Promoting Receptors in Human and Mouse Colorectal Cancer Cells. *Gastroenterology* **2010**.
 41. Lafont, E.; Kantari-Mimoun, C.; Draber, P.; De Miguel, D.; Hartwig, T.; Reichert, M.; Kupka, S.; Shimizu, Y.; Taraborrelli, L.; Spit, M.; et al. The linear ubiquitin chain assembly complex regulates TRAIL-induced gene activation and cell death. *EMBO J.* **2017**.
 42. Bertrand, M.J.M.; Milutinovic, S.; Dickson, K.M.; Ho, W.C.; Boudreault, A.; Durkin, J.; Gillard, J.W.; Jaquith, J.B.; Morris, S.J.; Barker, P.A. cIAP1 and cIAP2 Facilitate Cancer Cell Survival by Functioning as E3 Ligases that Promote RIP1 Ubiquitination. *Mol. Cell*

2008.

43. Hartwig, T.; Montinaro, A.; von Karstedt, S.; Sevko, A.; Surinova, S.; Chakravarthy, A.; Taraborrelli, L.; Draber, P.; Lafont, E.; Arce Vargas, F.; et al. The TRAIL-Induced Cancer Secretome Promotes a Tumor-Supportive Immune Microenvironment via CCR2. *Mol. Cell* **2017**, *65*, 730-742.e5.
44. Kojima, Y.; Nakayama, M.; Nishina, T.; Nakano, H.; Koyanagi, M.; Takeda, K.; Okumura, K.; Yagita, H. Importin β 1 protein-mediated nuclear localization of Death Receptor 5 (DR5) limits DR5/Tumor Necrosis Factor (TNF)-related apoptosis-inducing ligand (TRAIL)-induced cell death of human tumor cells. *J. Biol. Chem.* **2011**, *286*, 43383–43393.
45. Zhang, B.; Chen, J.-J.; Shen, J.H.-C.; Rosado, L.R.; Zhang, Y.; Di, X. Mislocalization of death receptors correlates with cellular resistance to their cognate ligands in human breast cancer cells. *Oncotarget* **2012**, *3*, 833.
46. Bertsch, U.; Röder, C.; Kalthoff, H.; Trauzold, A. Compartmentalization of TNF-related apoptosis-inducing ligand (TRAIL) death receptor functions: Emerging role of nuclear TRAIL-R2. *Cell Death Dis.* **2014**, *5*, 1–10.
47. Mert, U.; Adawy, A.; Scharff, E.; Teichmann, P.; Willms, A.; Haselmann, V.; Colmorgen, C.; Lemke, J.; von Karstedt, S.; Fritsch, J.; et al. TRAIL Induces Nuclear Translocation and Chromatin Localization of TRAIL Death Receptors. *Cancers (Basel)*. **2019**, *11*, 1167.
48. Haselmann, V.; Kurz, A.; Bertsch, U.; Hübner, S.; Olempska-Müller, M.; Fritsch, J.; Häslner, R.; Pickl, A.; Fritsche, H.; Annewanter, F.; et al. Nuclear death receptor trail-r2 inhibits maturation of let-7 and promotes proliferation of pancreatic and other tumor cells. *Gastroenterology* **2014**, *146*, 278–290.
49. Boyerinas, B.; Park, S.M.; Hau, A.; Murmann, A.E.; Peter, M.E. The role of let-7 in cell differentiation and cancer. *Endocr. Relat. Cancer* **2010**, *17*, 19–36.
50. Jun, K.H.; Jung, J.H.; Choi, H.J.; Shin, E.Y.; Chin, H.M. HMGA1/HMGA2 protein expression and prognostic implications in gastric cancer. *Int. J. Surg.* **2015**.
51. Dufour, F.; Rattier, T.; Constantinescu, A.A.; Zischler, L.; Morlé, A.; Mabrouk, H. Ben; Humblin, E.; Jacquemin, G.; Szegezdi, E.; Delacote, F.; et al. TRAIL receptor gene editing unveils TRAIL-R1 as a master player of apoptosis induced by TRAIL and ER stress. *Oncotarget* **2017**, *8*, 9974–9985.
52. Lu, M.; Lawrence, D.A.; Marsters, S.; Acosta-Alvear, D.; Kimmig, P.; Mendez, A.S.;

- Paton, A.W.; Paton, J.C.; Walter, P.; Ashkenazi, A. Opposing unfolded-protein-response signals converge on death receptor 5 to control apoptosis. *Science (80-)*. **2014**, *345*, 98–101.
53. Lam, M.; Marsters, S.; Ashkenazi, A.; Walter, P. Misfolded proteins bind and activate death receptor 5 to trigger apoptosis during unresolved endoplasmic reticulum stress. *Elife* **2020**.
54. Walczak, H.; Miller, R.E.; Ariail, K.; Gliniak, B.; Griffith, T.S.; Kubin, M.; Chin, W.; Jones, J.; Woodward, a; Le, T.; et al. Tumoricidal activity of tumor necrosis factor-related apoptosis-inducing ligand in vivo. *Nat. Med.* **1999**, *5*, 157–163.
55. Ashkenazi, A.; Pai, R.C.; Fong, S.; Leung, S.; Lawrence, D.A.; Marsters, S.A.; Blackie, C.; Chang, L.; McMurtrey, A.E.; Hebert, A.; et al. Safety and Antitumor Activity of Recombinant Soluable Apo2 Ligand. *J. Clin. Investig.* **1999**, *104*, 155–162.
56. Lemke, J.; Von Karstedt, S.; Zinngrebe, J.; Walczak, H. Getting TRAIL back on track for cancer therapy. *Cell Death Differ.* **2014**, *21*, 1350–1364.
57. Ashkenazi, A.; Pai, R.C.; Fong, S.; Leung, S.; Lawrence, D.A.; Marsters, S.A.; Blackie, C.; Chang, L.; McMurtrey, A.E.; Hebert, A.; et al. Safety and antitumor activity of recombinant soluble Apo2 ligand. *J. Clin. Invest.* **1999**.
58. De Loeff, M.; De Jong, S.; Kruyt, F.A.E. Multiple interactions between cancer cells and the tumor microenvironment modulate TRAIL signaling: Implications for TRAIL receptor targeted therapy. *Front. Immunol.* **2019**, *10*, 1–15.
59. Linzer, D.I.H.; Levine, A. Characterization of a 54K Dalton cellular SV40 tumor antigen present in SV40-transformed cells and uninfected embryonal carcinoma cells. *Cell* **1979**.
60. Finlay, C.A.; Hinds, P.W.; Levine, A.J. The p53 proto-oncogene can act as a suppressor of transformation. *Cell* **1989**.
61. Takahashi, T.; Nau, M.M.; Chiba, I.; Birrer, M.J.; Rosenberg, R.K.; Vinocour, M.; Levitt, M.; Pass, H.; Gazdar, A.F.; Minna, J.D. p53: A frequent target for genetic abnormalities in lung cancer. *Science (80-)*. **1989**.
62. Baker, S.J.; Fearon, E.R.; Nigro, J.M.; Hamilton, S.R.; Preisinger, A.C.; Jessup, J.M.; Vantuinen, P.; Ledbetter, D.H.; Barker, D.F.; Nakamura, Y.; et al. Chromosome 17 deletions and p53 gene mutations in colorectal carcinomas. *Science (80-)*. **1989**.
63. Lane, D.P. p53, guardian of the genome. *Nature* 1992.

64. Baptiste, N.; Friedlander, P.; Chen, X.; Prives, C. The proline-rich domain of p53 is required for cooperation with anti-neoplastic agents to promote apoptosis of tumor cells. *Oncogene* **2002**.
65. Toledo, F.; Lee, C.J.; Krummel, K.A.; Rodewald, L.-W.; Liu, C.-W.; Wahl, G.M. Mouse Mutants Reveal that Putative Protein Interaction Sites in the p53 Proline-Rich Domain Are Dispensable for Tumor Suppression. *Mol. Cell. Biol.* **2007**.
66. El-Deiry, W.S.; Kern, S.E.; Pietenpol, J.A.; Kinzler, K.W.; Vogelstein, B. Definition of a consensus binding site for p53. *Nat. Genet.* **1992**.
67. Foord, O.S.; Bhattacharya, P.; Reich, Z.; Rotter, V. A DNA binding domain is contained in the C-terminus of wild type p53 protein. *Nucleic Acids Res.* **1991**.
68. Chillemi, G.; Kehrhoesser, S.; Bernassola, F.; Desideri, A.; Dö, V.; Levine, A.; Melino, G. Structural Evolution and Dynamics of the p53 Proteins.
69. Levine, A. The many faces of p53: something for everyone. 524 | *J. Mol. Cell Biol.* **2019**, 524–530.
70. Biegging, K.T.; Mello, S.S.; Attardi, L.D. Unravelling mechanisms of p53-mediated tumour suppression. *Nat. Rev. Cancer* 2014.
71. Karimian, A.; Ahmadi, Y.; Yousefi, B. Multiple functions of p21 in cell cycle, apoptosis and transcriptional regulation after DNA damage. *DNA Repair (Amst)*. 2016.
72. Delavaine, L.; La Thangue, N.B. Control of E2F activity by p21(Waf1/Cip1). *Oncogene* **1999**.
73. Aubrey, B.J.; Kelly, G.L.; Janic, A.; Herold, M.J.; Strasser, A. How does p53 induce apoptosis and how does this relate to p53-mediated tumour suppression? *Cell Death Differ.* **2018**, 25, 104–113.
74. Liu, X.; Yue, P.; Khuri, F.R.; Sun, S.-Y. p53 upregulates death receptor 4 expression through an intronic p53 binding site. *Cancer Res.* **2004**, 64, 5078–83.
75. Takimoto, R.; El-Deiry, W.S. Wild-type p53 transactivates the KILLER/DR5 gene through an intronic sequence-specific DNA-binding site. *Oncogene* **2000**, 19, 1735–1743.
76. Suzuki, H.I.; Yamagata, K.; Sugimoto, K.; Iwamoto, T.; Kato, S.; Miyazono, K. Modulation of microRNA processing by p53. *Nature* **2009**.
77. Léveillé, N.; Elkon, R.; Davalos, V.; Manoharan, V.; Hollingworth, D.; Vrieling, J.O.; Le

- Sage, C.; Melo, C.A.; Horlings, H.M.; Wesseling, J.; et al. Selective inhibition of microRNA accessibility by RBM38 is required for p53 activity. *Nat. Commun.* **2011**.
78. Krell, J.; Stebbing, J.; Carissimi, C.; Dabrowska, A.F.; Giorgio, A. De; Frampton, A.E.; Harding, V.; Fulci, V.; Macino, G.; Colombo, T.; et al. TP53 regulates miRNA association with AGO2 to remodel the miRNA-mRNA interaction network. *Genome Res.* **2016**.
79. Liu, J.; Zhang, C.; Zhao, Y.; Feng, Z. MicroRNA Control of p53. *J. Cell. Biochem.* **2017**.
80. Chéne, P. Inhibiting the p53-Mdm2 interaction: an important target for cancer therapy. **2003**.
81. Walerych, D.; Kudla, G.; Gutkowska, M.; Wawrzynow, B.; Muller, L.; King, F.W.; Helwak, A.; Boros, J.; Zyllich, A.; Zyllich, M. Hsp90 chaperones wild-type p53 tumor suppressor protein. *J. Biol. Chem.* **2004**.
82. Liang, S.H.; Clarke, M.F. Regulation of p53 localization. *Eur. J. Biochem.* 2001.
83. Liu, Y.; Tavana, O.; Gu, W. p53 modifications: exquisite decorations of the powerful guardian. *J. Mol. Cell Biol.* **2019**, 564–577.
84. Kruse, J.P.; Gu, W. Modes of p53 Regulation. *Cell* **2009**, 137, 609–622.
85. Kruse, J.-P.; Gu, W. SnapShot: p53 Posttranslational Modifications. *Cell* **2008**, 133.
86. Gu, W.; Roeder, R.G. Activation of p53 sequence-specific DNA binding by acetylation of the p53 C-terminal domain. *Cell* **1997**.
87. Luo, J.; Su, F.; Chen, D.; Shiloh, A.; Gu, W. Deacetylation of p53 modulates its effect on cell growth and apoptosis. *Nature* **2000**.
88. Espinosa, J.M.; Emerson, B.M. Transcriptional regulation by p53 through intrinsic DNA/chromatin binding and site-directed cofactor recruitment. *Mol. Cell* **2001**.
89. Ito, A.; Kawaguchi, Y.; Lai, C.H.; Kovacs, J.J.; Higashimoto, Y.; Appella, E.; Yao, T.P. MDM2-HDAC1-mediated deacetylation of p53 is required for its degradation. *EMBO J.* **2002**.
90. Iyer, N.G.; Özdag, H.; Caldas, C. p300/CBP and cancer. *Oncogene* 2004.
91. Brooks, C.L.; Gu, W. Ubiquitination, phosphorylation and acetylation: The molecular basis for p53 regulation. *Curr. Opin. Cell Biol.* 2003, 15, 164–171.
92. Haupt, Y.; Maya, R.; Kazaz, A.; Oren, M. Mdm2 promotes the rapid degradation of p53. *Nature* **1997**, 387, 296–299.

93. Kubbutat, M.H.G.; Jones, S.N.; Vousden, K.H. Regulation of p53 stability by Mdm2. *Nature* **1997**, *387*, 299–303.
94. Brooks, C.L.; Gu, W. p53 ubiquitination: Mdm2 and beyond. *Mol. Cell* **2006**, *21*, 307–315.
95. Li, M.; Brooks, C.L.; Wu-Baer, F.; Chen, D.; Baer, R.; Gu, W. Mono- Versus Polyubiquitination: Differential Control of p53 Fate by Mdm2. *Science (80-.)*. **2003**, *302*, 1972–1975.
96. Wu, X.; Bayle, J.H.; Olson, D.; Levine, A. The p53-mdm-2 autoregulatory feedback loop. *Genes Dev.* **1993**, *7*, 1126–1132.
97. Zhang, Y.; Xiong, Y.; Yarbrough, W.G. ARF promotes MDM2 degradation and stabilizes p53: ARF-INK4a locus deletion impairs both the Rb and p53 tumor suppression pathways. *Cell* **1998**.
98. Zhang, Y.; Lu, H. Signaling to p53: Ribosomal Proteins Find Their Way. *Cancer Cell* **2009**.
99. Brady, C.A.; Attardi, L.D. p53 at a glance. *J. Cell Sci.* **2010**.
100. Wade, M.; Li, Y.C.; Wahl, G.M. MDM2, MDMX and p53 in oncogenesis and cancer therapy. *Nat. Rev. Cancer* **2013**, *13*, 83–96.
101. Cummins, J.M.; Rago, C.; Kohli, M.; Kinzler, K.W.; Lengauer, C.; Vogelstein, B. Tumour suppression: disruption of HAUSP gene stabilizes p53. *Nature* **2004**.
102. Li, M.; Chen, D.; Shiloh, A.; Luo, J.; Nikolaev, A.Y.; Qin, J.; Gu, W. Deubiquitination of p53 by HAUSP is an important pathway for p53 stabilization. *Nature* **2002**.
103. Sheng, Y.; Saridakis, V.; Sarkari, F.; Duan, S.; Wu, T.; Arrowsmith, C.H.; Frappier, L. Molecular recognition of p53 and MDM2 by USP7/HAUSP. *Nat. Struct. Mol. Biol.* **2006**.
104. Yuan, J.; Luo, K.; Zhang, L.; Chevillat, J.C.; Lou, Z. USP10 Regulates p53 Localization and Stability by Deubiquitinating p53. *Cell* **2010**, *140*, 384–396.
105. Chao, C.C.K. Mechanisms of p53 degradation. *Clin. Chim. Acta* **2014**.
106. Guo, A.; Salomoni, P.; Luo, J.; Shih, A.; Zhong, S.; Gu, W.; Pandolfi, P.P. The function of PML in p53-dependent apoptosis. *Nat. Cell Biol.* **2000**.
107. Kurki, S.; Latonen, L.; Laiho, M. Cellular stress and DNA damage invoke temporally distinct Mdm2, p53 and PML complexes and damage-specific nuclear relocalization. *J. Cell Sci.* **2003**.

108. Louriya-Hayon, I.; Grossman, T.; Sionov, R.V.; Alsheich, O.; Pandolfi, P.P.; Haupt, Y. The promyelocytic leukemia protein protects p53 from Mdm2-mediated inhibition and degradation. *J. Biol. Chem.* **2003**, *278*, 33134–33141.
109. Langley, E.; Pearson, M.; Faretta, M.; Bauer, U.M.; Frye, R.A.; Minucci, S.; Pelicci, P.G.; Kouzarides, T. Human SIR2 deacetylates p53 and antagonizes PML/p53-induced cellular senescence. *EMBO J.* **2002**.
110. Li, Y.; Ma, X.; Wu, W.; Chen, Z.; Meng, G. PML Nuclear Body Biogenesis, Carcinogenesis, and Targeted Therapy. *Trends in Cancer* 2020.
111. Lallemand-Breitenbach, V.; de Thé, H. PML nuclear bodies. *Cold Spring Harb. Perspect. Biol.* 2010.
112. Vousden, K.H.; Lane, D.P. p53 in health and disease. *Nat. Rev. Mol. Cell Biol.* 2007.
113. Brosh, R.; Rotter, V. When mutants gain new powers: news from the mutant p53 field. *Nat. Rev. Cancer* **2009**, *9*, 701–13.
114. Muller, P.A.J.; Vousden, K.H. P53 mutations in cancer. *Nat. Cell Biol.* 2013, *15*, 2–8.
115. Kim, E.; Deppert, W. Transcriptional activities of mutant p53: When mutations are more than a loss. *J. Cell. Biochem.* **2004**.
116. Gaiddon, C.; Lokshin, M.; Ahn, J.; Zhang, T.; Prives, C. A Subset of Tumor-Derived Mutant Forms of p53 Down-Regulate p63 and p73 through a Direct Interaction with the p53 Core Domain. *Mol. Cell. Biol.* **2001**.
117. Strano, S.; Fontemaggi, G.; Costanzo, A.; Rizzo, M.G.; Monti, O.; Baccharini, A.; Sal, G. Del; Levrero, M.; Sacchi, A.; Oren, M.; et al. Physical interaction with human tumor-derived p53 mutants inhibits p63 activities. *J. Biol. Chem.* **2002**.
118. Di Como, C.J.; Gaiddon, C.; Prives, C. p73 Function Is Inhibited by Tumor-Derived p53 Mutants in Mammalian Cells. *Mol. Cell. Biol.* **1999**.
119. Li, D.; Marchenko, N.D.; Moll, U.M. SAHA shows preferential cytotoxicity in mutant p53 cancer cells by destabilizing mutant p53 through inhibition of the HDAC6-Hsp90 chaperone axis. *Cell Death Differ.* **2011**.
120. Kravchenko, J.E.; Ilyinskaya, G. V.; Komarov, P.G.; Agapova, L.S.; Kochetkov, D. V.; Strom, E.; Frolova, E.I.; Kovriga, I.; Gudkov, A. V.; Feinstein, E.; et al. Small-molecule RETRA suppresses mutant p53-bearing cancer cells through a p73-dependent salvage pathway. *Proc. Natl. Acad. Sci. U. S. A.* **2008**.

121. Foster, B.A.; Coffey, H.A.; Morin, M.J.; Rastinejad, F. Pharmacological rescue of mutant p53 conformation and function. *Science (80-.)*. **1999**.
122. Selivanova, G.; Ryabchenko, L.; Jansson, E.; Iotsova, V.; Wiman, K.G. Reactivation of Mutant p53 through Interaction of a C-Terminal Peptide with the Core Domain. *Mol. Cell. Biol.* **1999**.
123. Niazi, S.; Purohit, M.; Niazi, J.H. Role of p53 circuitry in tumorigenesis: A brief review. *Eur. J. Med. Chem.* **2018**, *158*, 7–24.
124. Vassilev, L.T.; Vu, B.T.; Craves, B.; Carvajal, D.; Podlaski, F.; Filipovic, Z.; Kong, N.; Kammlott, U.; Lukacs, C.; Klein, C.; et al. In Vivo Activation of the p53 Pathway by Small-Molecule Antagonists of MDM2. *Science (80-.)*. **2004**, *303*, 844–848.
125. Meijer, A.; Kruyt, F.A.E.; van der Zee, A.G.J.; Hollema, H.; Le, P.; ten Hoor, K.A.; Groothuis, G.M.M.; Quax, W.J.; de Vries, E.G.E.; de Jong, S. Nutlin-3 preferentially sensitises wild-type p53-expressing cancer cells to DR5-selective TRAIL over rhTRAIL. *Br. J. Cancer* **2013**, *109*, 2685–2695.
126. Zhao, J.; Lu, Y.; Shen, H.-M. Targeting p53 as a therapeutic strategy in sensitizing TRAIL-induced apoptosis in cancer cells. *Cancer Lett.* **2012**, *314*, 8–23.
127. Wu, G.S.; Kim, K.; El-Deiry, W.S. KILLER/DR5, a novel DNA-damage inducible death receptor gene, links the p53-tumor suppressor to caspase activation and apoptotic death. *Adv. Exp. Med. Biol.* **2000**.
128. Wu, G.S.G.; Kim, K.; El-Deiry, W.S.; Burns, T.F.; McDonald, E.R.; Jiang, W.; Meng, R.; Krantz, I.D.; Kao, G.; Gan, D.-D.; et al. KILLER/DR5 is a DNA damage-inducible p53-regulated death receptor gene. *Adv. Exp. Med. Biol.* **2000**, *17*, 141–143.
129. Bunz, F.; Dutriaux, A.; Lengauer, C.; Waldman, T.; Zhou, S.; Brown, J.P.; Sedivy, J.M.; Kinzler, K.W.; Vogelstein, B. Requirement for p53 and p21 to sustain G2 arrest after DNA damage. *Science* **1998**, *282*, 1497–501.
130. Brattain, M.G.; Fine, W.D.; Khaled, F.M.; Thompson, J.; Brattain, D.E. Heterogeneity of Malignant Cells from a Human Colonic Carcinoma. *Cancer Res.* **1981**.
131. Giard, D.J.; Aaronson, S.A.; Todaro, G.J.; Arnstein, P.; Kersey, J.H.; Dosik, H.; Parks, W.P. In Vitro Cultivation of Human Tumors: Establishment of Cell Lines Derived From a Series of Solid Tumors. *JNCI J. Natl. Cancer Inst.* **1973**, *51*, 1417–1423.
132. Fritsche, H.; Heilmann, T.; Tower, R.J.; Hauser, C.; von Au, A.; El-Sheikh, D.; Campbell, G.M.; Alp, G.; Schewe, D.; Chübner, S.; et al. TRAIL-R2 promotes skeletal metastasis

- in a breast cancer xenograft mouse model. *Oncotarget* **2015**, *6*, 9502–9516.
133. Smith, P.K.; Krohn, R.I.; Hermanson, G.T.; Mallia, A.K.; Gartner, F.H.; Provenzano, M.D.; Fujimoto, E.K.; Goeke, N.M.; Olson, B.J.; Klenk, D.C. Measurement of protein using bicinchoninic acid. *Anal. Biochem.* **1985**.
134. Lowry Lowry Protein Assay. *J. Biol. Chem.* **1951**.
135. Bradford, M.M. A rapid and sensitive method for the quantitation of microgram quantities of protein utilizing the principle of protein-dye binding. *Anal. Biochem.* **1976**.
136. Laemmli, U.K. Cleavage of structural proteins during the assembly of the head of bacteriophage T4. *Nature* **1970**, *227*, 680–685.
137. Towbin, H.; Staehelin, T.; Gordon, J. Electrophoretic transfer of proteins from polyacrylamide gels to nitrocellulose sheets: Procedure and some applications. *Proc. Natl. Acad. Sci. U. S. A.* **1979**, *76*, 4350–4354.
138. Rasband, W.S. ImageJ. Bethesda, MD: US National Institutes of Health. *ht tp://rsb. info. nih. gov/ij* **1997**.
139. Orlando, V. Mapping chromosomal proteins in vivo by formaldehyde-crosslinked-chromatin immunoprecipitation. *Trends Biochem. Sci.* **2000**, *25*, 99–104.
140. Kuo, M.H.; Allis, C.D. In vivo cross-linking and immunoprecipitation for studying dynamic Protein:DNA associations in a chromatin environment. *Methods A Companion to Methods Enzymol.* **1999**.
141. Willms, A.; Schitteck, H.; Rahn, S.; Sosna, J.; Mert, U.; Adam, D.; Trauzold, A. Impact of p53 status on TRAIL-mediated apoptotic and non-apoptotic signaling in cancer cells. *PLoS One* **2019**.
142. Satija, Y.K.; Bhardwaj, A.; Das, S. A portrayal of E3 ubiquitin ligases and deubiquitylases in cancer. *Int. J. Cancer* **2013**, *133*, 2759–2768.
143. Wang, Y.; Hu, L.; Wang, J.; Li, X.; Sahengbieke, S.; Wu, J.; Lai, M. HMGA2 promotes intestinal tumorigenesis by facilitating MDM2-mediated ubiquitination and degradation of p53. *J. Pathol.* **2018**, *246*, 508–518.
144. Shen, T.H.; Lin, H.K.; Scaglioni, P.P.; Yung, T.M.; Pandolfi, P.P. The Mechanisms of PML-Nuclear Body Formation. *Mol. Cell* **2006**.
145. Lallemand-Breitenbach, V.; Jeanne, M.; Benhenda, S.; Nasr, R.; Lei, M.; Peres, L.; Zhou, J.; Raught, B.; de Thé, H. Arsenic degrades PML or PML-RAR α through a SUMO-

- triggered RNF4/ ubiquitin-mediated pathway. *Nat. Cell Biol.* **2008**.
146. Tatham, M.H.; Geoffroy, M.C.; Shen, L.; Plechanovova, A.; Hattersley, N.; Jaffray, E.G.; Palvimo, J.J.; Hay, R.T. RNF4 is a poly-SUMO-specific E3 ubiquitin ligase required for arsenic-induced PML degradation. *Nat. Cell Biol.* **2008**.
 147. Hands, K.J.; Cuchet-Lourenco, D.; Everett, R.D.; Hay, R.T. PML isoforms in response to arsenic: High-resolution analysis of PML body structure and degradation. *J. Cell Sci.* **2014**.
 148. Nagane, M.; Huang, H.J.S.; Cavenee, W.K. The potential of TRAIL for cancer chemotherapy. *Apoptosis* **2001**.
 149. Suzuki, H.I.; Yamagata, K.; Sugimoto, K.; Iwamoto, T.; Kato, S.; Miyazono, K. Modulation of microRNA processing by p53. *Nature* **2009**, *460*, 529–533.
 150. Waldman, T.; Kinzler, K.W.; Vogelstein, B. p21 Is Necessary for the p53-mediated G1 Arrest in Human Cancer Cells. *Cancer Res.* **1995**.
 151. Kischkel, F.C.; Lawrence, D.A.; Chuntharapai, A.; Schow, P.; Kim, K.J.; Ashkenazi, A. Apo2L/TRAIL-dependent recruitment of endogenous FADD and caspase-8 to death receptors 4 and 5. *Immunity* **2000**.
 152. Sprick, M.R.; Weigand, M.A.; Rieser, E.; Rauch, C.T.; Juo, P.; Blenis, J.; Krammer, P.H.; Walczak, H. FADD/MORT1 and caspase-8 are recruited to TRAIL receptors 1 and 2 and are essential for apoptosis mediated by TRAIL receptor 2. *Immunity* **2000**.
 153. Müller, I.; Strozyk, E.; Schindler, S.; Beissert, S.; Oo, H.Z.; Sauter, T.; Lucarelli, P.; Raeth, S.; Hausser, A.; Al Nakouzi, N.; et al. Cancer Cells Employ Nuclear Caspase-8 to Overcome the p53-Dependent G2/M Checkpoint through Cleavage of USP28. *Mol. Cell* **2020**, *77*, 970-984.e7.
 154. Kuribayashi, K.; Krigsfeld, G.; Wang, W.; Xu, J.; Mayes, P.A.; Dicker, D.T.; Wu, G.S.; El-Deiry, W.S.; Gen, S.W.; El-Deiry, W.S. TNFSF10 (TRAIL), a p53 target gene that mediates p53-dependent cell death. *Cancer Biol. Ther.* **2008**, *7*, 2034–8.
 155. Carl G. Maki, Jon M. Huijbregtse, P.M.H. *PROTEASOME INHIBITION AFFECTS p53*; 1996;
 156. Chao, T.; Zhou, X.; Cao, B.; Liao, P.; Liu, H.; Chen, Y.; Park, H.-W.; Zeng, S.X.; Lu, H. ARTICLE Pleckstrin homology domain-containing protein PHLDB3 supports cancer growth via a negative feedback loop involving p53. **2016**.
 157. Higashitsuji, H.; Higashitsuji, H.; Itoh, K.; Sakurai, T.; Nagao, T.; Sumitomo, H.; Masuda,

- T.; Dawson, S.; Shimada, Y.; Mayer, R.J.; et al. The oncoprotein gankyrin binds to MDM2/HDM2, enhancing ubiquitylation and degradation of p53. *Cancer Cell* **2005**, *8*, 75–87.
158. Sui, G.; Affar, E.B.; Shi, Y.; Brignone, C.; Wall, N.R.; Yin, P.; Donohoe, M.; Luke, M.P.; Calvo, D.; Grossman, S.R.; et al. *Yin Yang 1 Is a Negative Regulator of p53 YY1 in vivo, we ablated YY1 in cultured cells using both homologous recombination-based gene knockout and RNA-mediated interference (RNAi) (Fire et al These studies have led to the discovery of a previously;* 2004; Vol. 117;.
159. Wu, H.; Pomeroy, S.L.; Ferreira, M.; Teider, N.; Mariani, J.; Nakayama, K.I.; Hatakeyama, S.; Tron, V.A.; Saltibus, L.F.; Spyrapoulos, L.; et al. UBE4B promotes Hdm2-mediated degradation of the tumor suppressor p53. *Nat. Med.* **2011**, *17*, 347–355.
160. Syed, A.; Tainer, J.A. The MRE11-RAD50-NBS1 Complex Conducts the Orchestration of Damage Signaling and Outcomes to Stress in DNA Replication and Repair. *Annu. Rev. Biochem.* 2018, *87*, 263–294.
161. Banin, S.; Moyal, L.; Shieh, S.Y.; Taya, Y.; Anderson, C.W.; Chessa, L.; Smorodinsky, N.I.; Prives, C.; Reiss, Y.; Shiloh, Y.; et al. Enhanced phosphorylation of p53 by ATM in response to DNA damage. *Science (80-.)*. **1998**, *281*, 1674–1677.
162. Shieh, S.Y.; Ikeda, M.; Taya, Y.; Prives, C. DNA damage-induced phosphorylation of p53 alleviates inhibition by MDM2. *Cell* **1997**.
163. Wu, J.; Wang, Y.; Xu, X.; Cao, H.; Sahengbieke, S.; Sheng, H.; Huang, Q.; Lai, M. Transcriptional activation of FN1 and IL11 by HMGA2 promotes the malignant behavior of colorectal cancer. *Carcinogenesis* **2016**.
164. Wang, X.; Liu, X.; Li, A.Y.J.; Chen, L.; Lai, L.; Lin, H.H.; Hu, S.; Yao, L.; Peng, J.; Loera, S.; et al. Overexpression of HMGA2 promotes metastasis and impacts survival of colorectal cancers. *Clin. Cancer Res.* **2011**.
165. Frasca, F.; Rustighi, A.; Malaguarnera, R.; Altamura, S.; Vigneri, P.; Del Sal, G.; Giancotti, V.; Pezzino, V.; Vigneri, R.; Manfioletti, G. HMGA1 inhibits the function of p53 family members in thyroid cancer cells. *Cancer Res.* **2006**, *66*, 2980–2989.
166. Kriehoff-Henning, E.; Hofmann, T.G. Role of nuclear bodies in apoptosis signalling. *Biochim. Biophys. Acta - Mol. Cell Res.* 2008.
167. Matt, S.; Hofmann, T.G. Crosstalk between p53 modifiers at PML bodies. *Mol. Cell. Oncol.* **2018**.

168. Möller, A.; Sirma, H.; Hofmann, T.G.; Rueffer, S.; Klimczak, E.; Dröge, W.; Will, H.; Schmitz, M.L. PML is required for homeodomain-interacting protein kinase 2 (HIPK2)-mediated p53 phosphorylation and cell cycle arrest but is dispensable for the formation of HIPK domains. *Cancer Res.* **2003**.
169. Bernardi, R.; Scaglioni, P.P.; Bergmann, S.; Horn, H.F.; Vousden, K.H.; Pandolfi, P.P. PML regulates p53 stability by sequestering Mdm2 to the nucleolus. *Nat. Cell Biol.* **2004**.
170. Yang, Q.; Liao, L.; Deng, X.; Chen, R.; Gray, N.S.; Yates, J.R.; Lee, J.D. BMK1 is involved in the regulation of p53 through disrupting the PML-MDM2 interaction. *Oncogene* **2013**.
171. Wan, J.; Block, S.; Scribano, C.M.; Thiry, R.; Esbona, K.; Audhya, A.; Weaver, B.A. Mad1 destabilizes p53 by preventing PML from sequestering MDM2.
172. Nisole, S.; Stoye, J.P.; Saïb, A. TRIM family proteins: Retroviral restriction and antiviral defence. *Nat. Rev. Microbiol.* 2005.
173. Varadaraj, A.; Dovey, C.L.; Laredj, L.; Ferguson, B.; Alexander, C.E.; Lubben, N.; Wylie, A.H.; Rich, T. Evidence for the receipt of DNA damage stimuli by PML nuclear domains. *J. Pathol.* **2007**.

List of Figures

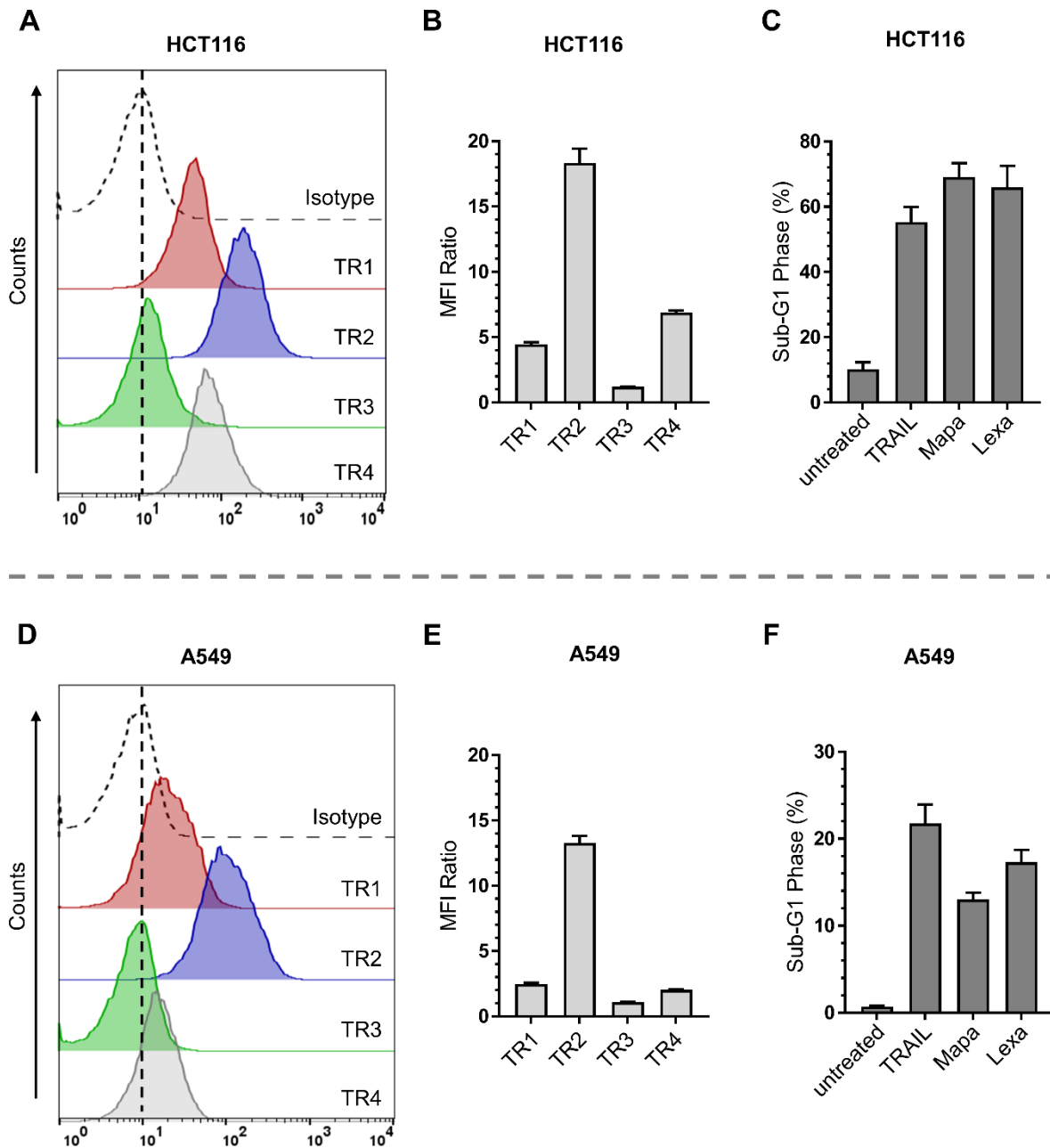
Figure 1: The TRAIL-TRAIL-Receptor System.....	2
Figure 2: TRAIL-mediated apoptotic signaling.	5
Figure 3: TRAIL-induced non-canonical signaling and functions of nuclear TRAIL-R2.....	7
Figure 4: The domain organization of p53.	10
Figure 5: The p53-mediated cellular responses and its regulation by MDM2.....	13
Figure 6: Regulation of p53 by MDM2, HAUSP and USP10.....	14
Figure 7: Determination of TRAIL-R levels in A549 and HCT116 wild type and TRAIL-R2 silenced cells.	42
Figure 8: 5-FU treatment leads to increased p53 and TRAIL-R2 protein levels.	43
Figure 9: TRAIL-R2 co-localizes and interacts with p53 in the nucleus of A549 cells.	45
Figure 10: TRAIL-R2 affects the expression of p53 and its targets.	47
Figure 11: TRAIL-R2 decreases the protein level of p53.	48
Figure 12: TRAIL-R2 impacts p53 levels independent of caspases.....	49
Figure 13: TRAIL-R2 affects p53 TRAIL-independent.	50
Figure 14: TRAIL-R2 affects p53 protein stability.....	52
Figure 15: TRAIL-R2 decreases p53 levels via ubiquitin-proteasome-dependent degradation.	53
Figure 16: MDM2 impacts the TRAIL-R2-mediated p53 destabilization.....	54
Figure 17: MDM2, p53 and TRAIL-R2 co-localize in the nucleus of A549 cells, but MDM2 does not co-precipitate with TRAIL-R2.	57
Figure 18: USP10 co-localizes with TRAIL-R2 and p53 in the cytosol and nucleus.	59
Figure 19: USP10 interacts with p53 and TRAIL-R2 in A549 cells and is located to a higher extent in the nucleus of TRAIL-R2 KO cells than WT cells.	61
Figure 20: SiRNA-mediated knockdown of USP10 does not affect the increased p53 stability in A549 TRAIL-R2 KO cells.	62
Figure 21: TRAIL-R2 affects p53 protein stability independent of deubiquitinating enzymes in A549 cells.....	64
Figure 22: TRAIL-R2 overexpression upregulates HMGA2 levels.....	65
Figure 23: SiRNA-mediated knockdown of HMGA2 does not affect increased p53 stability in A549 TRAIL-R2 KO cells.....	66
Figure 24: TRAIL-R2 co-localizes and interacts with PML in the nucleus of A549 cells.....	67
Figure 25: TRAIL-R2-mediated decrease of p53 stability depends on PML.....	68
Figure 26: TRAIL-R2 is a negative regulator of p53.	77

Supplementary Figure 1: Expression of TRAIL-Rs at the cell surface and sensitivity to TRAIL-R-mediated cell death of HCT116 and A549 cells.....97

List of Tables

Table 1: Master Mix composition per sample for qPCR from ChIP DNA templates.....	38
Table 2: Thermal cycling conditions for qPCR reaction using SYBR Green.....	38
Table 3: Master Mix composition per sample for qPCR from cDNA templates.....	40
Table 4: Thermal cycling conditions for qPCR using TaqMan assays.	40

Supplementary Data

**Supplementary Figure 1: Expression of TRAIL-Rs at the cell surface and determination of cell viability.**

For analysis of cell surface expression of TRAIL-Rs, **(A, B)** HCT116 cells and **(D, E)** A549 cells were stained with APC-conjugated receptor-specific antibodies and the stainings were measured by flow cytometry. Corresponding APC-conjugated isotype controls were used to validate staining specificity. Shown are representative histograms for TRAIL-Rs stainings in **(A)** HCT116 and **(D)** A549 cells. **(B, E)** Bar charts show mean values \pm SD of median fluorescence intensity (MFI) ratios (TRAIL-R/ Isotype) from three independent experiments of TRAIL-R stainings. For determination of cell viability **(C)** HCT116 cells and **(F)** A549 cells were stimulated either with TRAIL (100 ng/ml), Mapatumumab (10 μ g/ml) or Lexatumumab (10 μ g/ml) for 24 h and DNA-fragmentation assay was performed. Results are shown \pm SD of two to three biological replicates (n = 2–3). TRAIL-Rs, TRAIL receptors; TR1, TRAIL-R1; TR2, TRAIL-R2; TR3, TRAIL-R3; TR4, TRAIL-R4; Mapa, Mapatumumab agonistic TRAIL-R1 antibody; Lexa, Lexatumumab agonistic TRAIL-R2 antibody. (published data [141]).

Declaration on oath

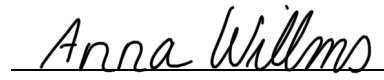
Hiermit versichere ich, Anna Willms (geboren am 15.10.1991 in Aurich), an Eides statt, dass ich die vorliegende wissenschaftliche Abhandlung mit dem Titel:

„TRAIL-Receptor 2 as a novel regulator of tumor suppressor protein p53“

nach den Regeln guter wissenschaftlicher Praxis eigenständig verfasst und keine anderen als die angegebenen Hilfsmittel und Quellen benutzt habe. Dabei habe ich keine Hilfe, außer der wissenschaftlichen Beratung durch meine Doktormutter Prof. Dr. Anna Trauzold und durch die namentlich erwähnten Kooperationspartner in Anspruch genommen. Weder wurde diese Arbeit bisher im Rahmen eines Prüfungsverfahrens vorgelegt, noch wurde ein akademischer Grad entzogen.

Teile dieser Arbeit sind bereits veröffentlicht in Willms *et al.*, Plos One (2019) oder sind Bestandteil eines Manuskripts, das bereits bei einem Journal für die Veröffentlichung eingereicht wurde.

Kiel, 20.04.2021


Anna Willms

Acknowledgements

Ein besonderes Wort des Dankes möchte ich an meine Doktormutter Prof. Dr. Anna Trauzold richten, für die Möglichkeit meine Doktorarbeit in ihrer Arbeitsgruppe anfertigen zu können. Danke für die Unterstützung, die wertvollen Anregungen und Ratschläge. Für das mir entgegengebrachte Vertrauen in meine Person und meine Arbeit möchte ich herzlich Danke sagen. Ich habe die sehr persönliche, aber auch produktive Arbeitsatmosphäre immer geschätzt!

Prof. Dr. Thomas Roeder danke ich für die Übernahme des Zweitgutachtens.

Prof. Dr. Heiner Schäfer danke ich für die konstruktiven Diskussionen, die Anregungen und die Unterstützung bei der Ausarbeitung der PML Thematik. Für die Unterstützung bei den LSM Aufnahmen möchte ich mich bei Dr. Jürgen Fritsch bedanken.

Ein ganz besonderer Dank geht an die lieben Kollegen aus der AG Trauzold und dem gesamten Institut für Experimentelle Tumorforschung. Der offene und freundliche Umgang miteinander, sowie die Hilfsbereitschaft in vielerlei Hinsicht haben dazu beigetragen, dass ich immer gerne ins Institut gekommen bin. Danke für die familiäre Atmosphäre, den Zusammenhalt, die fröhlichen Pausen und die vielen sportlichen und geselligen Momente. Auf die gemeinsame Zeit, werde ich sicherlich immer wieder gerne zurückblicken. Ein herzliches Dankeschön geht an dieser Stelle vor allem an Prof. Dr. Susanne Sebens, der besonders daran gelegen ist, dass sich alle Mitarbeiter im Institut wohl fühlen und fit durch den gemeinsamen Arbeitstag gehen. Besonders danken möchte ich auch Gökhan Alp für die tatkräftige technische Unterstützung, Tim Krichel für seine Unterstützung als Masterstudent und Kirsten Meinhardt für die Hilfe bei organisatorischen Belangen. Besonders hervorheben möchte ich außerdem Doaa Tawfik, Alshaimaa Adawy, Jule Mischke, Ufuk Mert, Johannes Angermann, Sofie Emilie Hagelund, Anna-Christina Rambow, Insa Aschenbach, Elisabeth Scharff, Carmina Markwardt, Lisa Marie Phillipp, Tina Daunke, Silje Beckinger und Dagmar Leisner, die mich alle ein Stück auf dem Weg meiner Promotion begleitet haben und mich sowohl beruflich als auch privat inspiriert haben.

Ein ganz besonders großes Dankeschön geht an Sascha Rahn für die Unterstützung in jeglicher Weise. Danke, dass du immer für mich da warst und an mich geglaubt hast!

Meiner Familie danke ich von ganzem Herzen für den Rückhalt. Danke, dass ihr mich auf diesem Weg unterstützend begleitet habt, ohne euch hätte ich es nicht so weit geschafft. Ihr seid wundervoll!